8-2016

Influence of stormwater control measures on watershed hydrology and biogeochemical cycling

Colin D. Bell
Purdue University

Graduate School Form
30 Updated 12/26/2015

PURDUE UNIVERSITY
GRADUATE SCHOOL
Thesis/Dissertation Acceptance

This is to certify that the thesis/dissertation prepared

By Colin Bell

Entitled
INFLUENCE OF STORMWATER CONTROL MEASURES ON WATERSHED HYDROLOGY AND BIOGEOCHEMICAL CYCLING

For the degree of Doctor of Philosophy

Is approved by the final examining committee:

Dr. Sara McMillan
Chair

Dr. Bernard Engel

Dr. Christina Tague

Dr. Jane Frankenberger

To the best of my knowledge and as understood by the student in the Thesis/Dissertation Agreement, Publication Delay, and Certification Disclaimer (Graduate School Form 32), this thesis/dissertation adheres to the provisions of Purdue University's "Policy of Integrity in Research" and the use of copyright material.

Approved by Major Professor(s): Dr. Sara McMillan

Approved by: Dr. Bernard Engel 7/25/2016

Head of the Departmental Graduate Program Date

INFLUENCE OF STORMWATER CONTROL MEASURES ON WATERSHED HYDROLOGY AND BIOGEOCHEMICAL CYCLING

A Dissertation

Submitted to the Faculty

of

Purdue University

by

Colin D Bell

In Partial Fulfillment of the

Requirements for the Degree

of

Doctor of Philosophy

August 2016

Purdue University

West Lafayette, Indiana

For all those who have been rained on

ACKNOWLEDGEMENTS

I must start by thanking Dr. Sara McMillan, my advisor, mentor, and friend. She has taught me so much about the science and the salesmanship that this job requires. She has repeatedly reminded me of the value of our research, even when results were not "as hypothesized" or when the ISCO distributor arms jammed. She has always been there to help me navigate the tough decisions demanded by the science, my career, and life. She has worked tirelessly to keep the lights on, and even harder to keep my bank account in the black – despite my habit of sabotaging this.

I would also like to the Dr. Naomi Tague, Dr. Anne Jefferson, and Dr. Sandra Clinton for all of the advice they have given me over the past five years. I would never have been able to produce this document without the time, knowledge, and inspiration that you all have so generously shared with me. I wish you all continued success in the years to come, and I hope your individual success is grown, in part, from future collaboration between us.

I am indebted to the rest of my PhD committee, Dr. Bernie Engle and Dr. Jane Frankenberger, for their excellent criticisms, comments, ideas, and questions that helped evolve this document. There are countless other teachers, including Dr. Ted Endreny, Dr. Craig Allan, and Dr. Jim Bowen, and who have helped me on my journey.

Janet Choate and Dr. Brian Miles were instrumental for enabling me to contribute what I could to RHESSys.

Acknowledgement – both in the forms of thanks and praise – is due to the folks at Charlotte-Mecklenburg Stormwater Services. Thanks for the equipment, expertise and data they shared with me. Praise for the impressively thorough and inspired job they do monitoring, reporting, and protecting waterways around the city of Charlotte, NC.

So many students and friends in Charlotte helped me collect, analyze, and digest data along the way. This list includes (but is not limited to) Alea Tuttle, Erin Looper, Mackenzie Osypian, Rebeca Tinnel, Dr. Viajaya Gagrani, Josh Davis, Brittany Marvel, Kendra Branch, Charles Safrit, Chris Jordan, Perry Isner, and Xueying Wang. Many others, not on the payroll, have also given me help in the field including, first-and-foremost, Jan Kofsky and, to a much lesser extent, Kyle Russell. Although they missed out on data collection, I'd also like to thank the graduate students at Purdue. There are too many to name so I will refer to them collectively as "Knights."

Finally, I have to thank my family for instilling in me a small fraction of their own character, which I was able to call on while producing this document. My father's critical thinking, perspective, and obstinacy. My mother's motivation and leadership. My sister's idealism and enthusiasm. Thanks also to all those named Bell, Maune, Fote, Spears, and Mulderink for the lifetime of support.

Speaking of support – I must truly, finally, acknowledge the National Science Foundation and the Purdue University Bilsland Dissertation Fellowship for funding this work.

TABLE OF CONTENTS

Page

Page

Page

Page

Page

LIST OF TABLES

Table Page

LIST OF FIGURES

Figure Page

Figure Page

Figure Page

Figure Page

Figure Page

Figure Page

ABSTRACT

Bell, Colin D. Ph.D, Purdue University, August 2016. Influence of Stormwater Control Measures on Watershed Hydrology and Biogeochemical Cycling. Major Professor: Sara McMillan.

Urban development replaces vegetation with impervious surfaces and natural drainage channels with pipe networks that quicken flow paths and alter hydrologic regimes. Additionally, the import of food, application of fertilizer to lawns and gardens, and heightened atmospheric deposition increases nutrient availability in urban landscapes. These excess nutrients are ultimately routed to streams through the pipe networks before it can be processed by the vegetation and microorganisms of the landscape. This combination of physical and chemical disturbances impacts stream ecosystems and degrades their ability to perform valuable services such as removal of nutrients, degradation of pollutants, and provision of recreational and aesthetic value. Stormwater control measures (SCMs) are a management strategy that can mitigate these impacts urbanization, ultimately preserving those valuable stream ecosystems.

While the effects of urban development and individual SCMs on water quantity and quality have been well documented independently, studies examining the cumulative influence of SCMs on water quantity and nitrogen cycling throughout entire developed watersheds are lacking. First, this work addresses this gap in knowledge by

empirically relating hydrologic regimes at sixteen urban watersheds in Charlotte, NC, USA to a series of metrics that describe the extent of urban development and mitigation with SCMs. Next, water quality data were collected at four of the sixteen sites to determine how SCMs affect stream nutrient and carbon concentrations during storms, and how the extent and distribution of urban development modulates the effects of SCMs. Because of the limited ability for monitoring approaches to capture variability along a continuum of development and mitigation, a modeling approach was used to further understand the role of SCMs on hydrology and water quality. A new model was developed, calibrated, validated, and used to assess uncertainty of the hydrologic and ecological processes that occur in SCMs. Finally, these SCM routines were incorporated into an existing spatially-distributed watershed model to test how varying levels of impervious surface connectivity to SCMs changed hydrologic and water quality regimes in a watershed in Charlotte, NC.

The results of the study indicate that the degree of urbanization, as measured by a watershed metric total imperviousness, controlled hydrologic behavior at the storm event time scale across the 16 sites monitored. There is evidence that SCMs are able to effect the hydrologic record flashiness at an annual time scale by temporarily storing runoff and extending hydrograph recession. An analysis of water quality data indicates that SCMs are able to reduce N, phosphorous and dissolved organic carbon concentrations in the stream in watersheds with a homogeneous urban land use. However, in newly developing watersheds (e.g., suburban), the presence of SCMs coincides with the addition of urban impervious surfaces and SCMs are not sufficient to return water quality

to pre-development conditions, as reflected in increased in nutrient concentrations. To understand how SCMs are able to affect nutrient concentrations along a continuum of development and mitigation intensity, we explored a hydrologic and water quality model of SCMs. Through calibration, the model was able to match the distribution of outflow water and both nitrate and ammonium concentrations of a single SCM monitored in Charlotte, NC. SCM inorganic N removal and retention increased with temperature and SCM water depth. When the SCM routines were used at the watershed scale, results showed that increased mitigation of urban impervious surfaces with SCMs led to proportional reductions in total runoff volumes, and annual loads of both nitrate and ammonium.

These results have implications for watershed managers looking to protect stream ecosystems through the use of SCMs. Treating urban impervious areas with SCMs can reduce hydrologic record flashiness, which is correlated to stream invertebrate health. Mitigating impervious surfaces with SCMs may be able to reduce nitrogen loads by both reducing total water yield and reducing in-stream N concentrations, although the change in concentrations is likely to be dependent on climatic forcing, the distribution of land use, and design of the SCM. Finally, a management strategy as simple as planting trees may also produce similar reductions in runoff and loads, as results showed lower runoff volumes and lower N concentrations in watersheds with greater tree coverage.

CHAPTER 1. INTRODUCTION

1.1 Background

Roads and buildings of urban environments facilitate economic activity in cities, but also have a profound effect on the water cycle. This infrastructure, and the storm sewers that protect it from flooding, shorten hydrological flow paths causing more frequent and intense flooding (Leopold, 1968). These high-energy storm pulses lead to stream bank erosion and subsequent degradation of stream ecosystem health (Paul and Meyer, 2001). Additionally, the concentration of people in these areas leads to an increased supply of both nitrogen (N) from imported food, fertilizer and automobile activity, (Bernhardt et al., 2008), and phosphorous (P) from food, fertilizer and detergents (La Valle, 1975; Waschbusch et al., 1994). The hydrologically efficient flow paths that carry these nutrients from the watershed to the stream limit the terrestrial ecosystem's ability to retain and remove the nutrients, leading to elevated concentrations in urban streams. Stream ecosystems are degraded by the erosive flows and high concentrations, and therefore lose their ability to provide valuable ecosystem services such as improving water quality for downstream lakes and estuaries, and promoting of recreational and aesthetic value. Stormwater control measures (SCMs) are one strategy for mitigating the impacts of urbanization on hydrologic regimes by attenuating storm volumes, reducing peak discharges and promoting evaporation (Roesner et al., 2001). Additionally, the

aquatic environments created by SCMs can improve water quality through vegetative uptake of N and P, microbial removal of N, and P burial through settling of sediments and organic matter with sorbed P (Kulzer, 1989; Comings et al., 2000; Hsieh and Davis, 2005). However, the ability of SCMs to restore natural hydrologic regimes and stream ecosystem function depends on both the extent of implementation within the watershed and the degree of impact from urbanization (Roesner et al., 2001; Hur et al., 2008; Roy et al., 2008; NRC, 2009; Burns et al., 2012).

From a bird's eye view, urban development appears as rectangular rooftops and parking lots connected with a lattice of roads and sidewalks. These types of land coverage are collectively referred to as impervious surfaces because precipitation falling on these areas does not infiltrate into underground soil storage zones. As reviewed by Paul and Meyer (2001), the impervious surfaces of the urban environment increase peak discharge, bankfull discharge, and runoff ratio at the event and annual time scales. The lag time between rainfall and runoff has also been shown to shorten with increasing urbanization. In a review of urban streams in the U.S. Southeast, O'Driscoll et al. (2010) demonstrated that these hydrologic changes alter channel geomorphology, reduce the ability of streams to retain and remove nutrients, and decrease the abundance of intolerant macroinvertebrate taxa.

In addition to altered physical hydrological regimes, urban areas have more nutrients exported by the waterways that drain them. In two surveys of N exported by the large rivers throughout the globe, both Peierls et al. (1991) and Howarth et al. (1996) found a strong correlation with N flux and population density, although water treatment

technologies in developed countries can reduce the strength of this correlation. The cause for this elevated N is twofold. First, N loads are increased from imported food and fertilizer and localized atmospheric deposition is accelerated by automobile exhaust (Bernhardt et al., 2008). Second, as urbanization increases, shortened flow paths reduce the time that N is retained in the watershed, limiting the potential for biological processing and removal. Of particular importance is the short circuiting of runoff around the riparian zone, which can remove a disproportionate fraction of N relative to its area within the watershed when groundwater flowpaths are maintained (Groffman et al., 2002; Taylor et al., 2005, Duncan et al., 2013). As with N, positive relationships have been found between urbanization and P export attributed to increased loading from fertilizer, food, and detergents (Smart et al., 1985; Walker Jr, 1985; Winter and Duthie, 2000; Hatt et al., 2004; Duan et al., 2012, La Valle, 1975; Waschbusch et al., 1994).

A common solution to alleviate hydrologic impacts and elevated nutrient loading to stream ecosystems from impervious surfaces is through the use of SCMs. SCMs take many forms of design (e.g. wet ponds, dry ponds, wetlands, bioretention areas) but all use depression storage to receive, retain, and then slowly release water to the drainage network. SCMs are typically designed so that the peak of the outflow hydrograph for a particular design storm (e.g., a 10-yr return interval, 6-hour duration) matches the peak hydrograph for the same watershed without any urban development. This process of water attenuation, shown in Figure 1-1, reduces peak flows and increases the time between precipitation and stormflow generation (Horner et al., 2001; Villarreal et al., 2004; Hood et al., 2007).

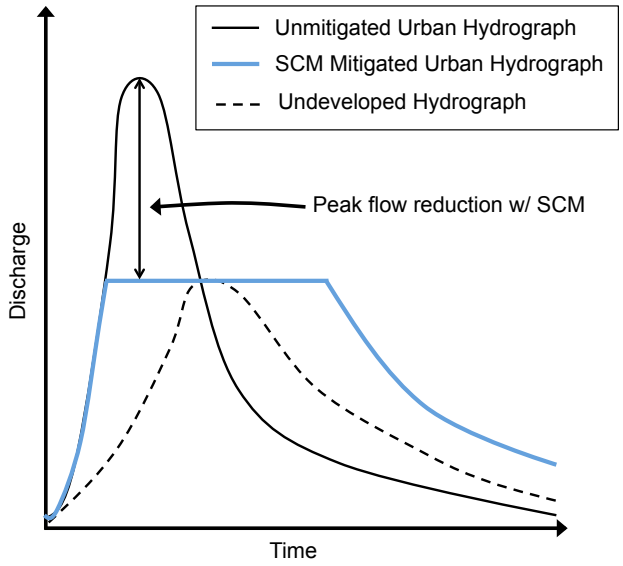

Figure 1-1: Example of design objectives of SCMs for managing peak flows

SCMs are also dynamic ecosystems, and as such can also impact water quality of urban runoff. SCMs are hosts for plant, algal, and microbial communities that assimilate, store, release, and transform N, P and carbon (C). Additionally, physical processes such as settling and burial can effectively remove N, P and C from the water column. SCMs have been demonstrated to reduce outflow concentrations of N, P and C relative to inflow concentrations, although performance varies with the type, design, and age of SCM (Mallin et al., 2002; Hunt et al., 2008; Collins et al., 2010; Geosyntec Consultants and Wright Water Engineers, 2012; Kearney et al., 2013; Koch et al., 2014).

1.2 Research Objectives

As shown, there is abundant literature documenting the relationship between urban development and hydrologic and water quality impacts to streams. Also, several monitoring studies have demonstrated the ability of individual SCMs to remove nutrients

from stormwater inflow. However, few studies have explicitly linked urban development and subsequent SCM mitigation at the watershed scale. Therefore, the purpose of this research is to characterize the relationship between varying degrees of both urban development and mitigation with SCMs on urban hydrologic regimes and nutrient cycling at the watershed scale. Also, this work uses both monitoring and modeling approaches to identify the form and direction of these relationships so that managers can select watersheds likely to produce the greatest benefits from the addition of SCMs (Figure 1-2).

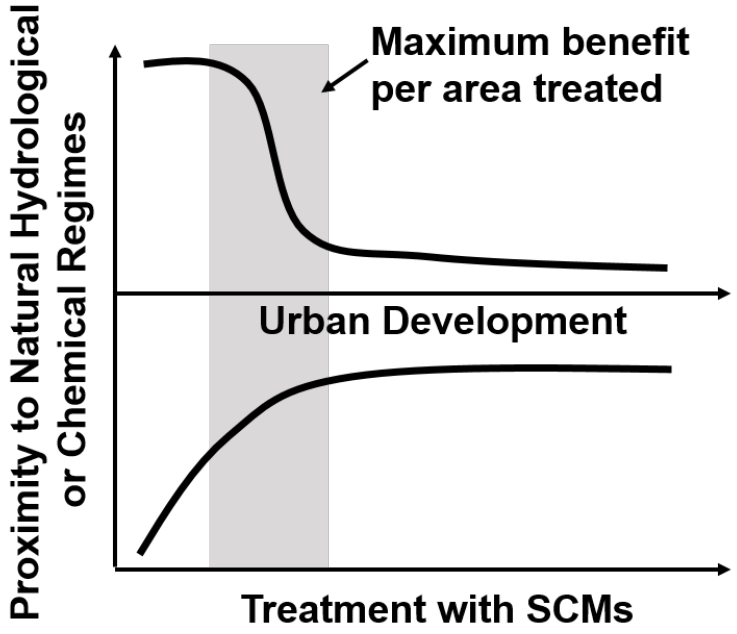

Figure 1-2: Hypothetical response of hydrologic and nitrogen cycling variables to changing amount of urban development and mitigation with SCMs. The highlighted area identifies a hypothetical threshold behavior which has the potential to maximize benefits to stream ecosystems with minimum changes to watershed development and mitigation.

1.2.1 Objective 1

Empirically relate hydrologic regimes at 16 urban streams to metrics that describe the condition of urban development, urban surface connectivity to the stream network, and mitigation with SCMs.

1.2.2 Objective 2

Use high resolution water quality data at four urban watersheds to determine how SCMs affect stream concentrations of N, P, and dissolved organic carbon (DOC) and quantify how the type, extent, and arrangement of urban development modulates their effects.

1.2.3 Objective 3

Develop, calibrate, validate, and quantify uncertainty of a hydro-ecological model of hydrology, algae growth, and N cycling in SCMs and test the ability of SCMs to remove inorganic N under varying environmental and design scenarios.

1.2.4 Objective 4

Integrate the newly developed SCM model into a spatially-explicit, process-based watershed model to characterize how hydrology and water quality change as function of urban impervious surfaces connectivity.

1.3 Hypothesis

Hydrologic and water quality indicators of urban stream behavior will become more damaging as the extent of urban impervious surfaces within watershed increases, but

increasing connectivity of these surfaces to SCMs will ameliorate this intensity of this relationship.

1.4 Document Outline

This document is divided into six chapters. This first chapter is an introduction that provides a background on the threat the urbanization poses to stream ecosystems, discusses how implementation of SCMs can mitigate this threat, identifies a gap in research linking urbanization and SCMs at the watershed scale, and outlines research objectives to fill that gap. Chapters two through six detail independent experiments aimed at addressing the four research objectives of the dissertation, sequentially. Each of these four chapters is written as a journal manuscript as they all have been or will soon be submitted for peer-review publication. The sixth and final chapter summarizes the results from the four experiments, discusses the management implications of those findings, and provides recommendations for future research.

1.5 References

Bernhardt, E.S., Band, L.E., Walsh, C.J., Berke, P.E., 2008. Understanding, managing, and minimizing urban impacts on surface water nitrogen loading. Ann NY Acad Sci, 1134(1): 61-96.

Burns, M.J., Fletcher, T.D., Walsh, C.J., Ladson, A.R., Hatt, B.E., 2012. Hydrologic shortcomings of conventional urban stormwater management and opportunities for reform. Landscape and Urban Planning, 105(3): 230-240.

Collins, K.A. et al., 2010. Opportunities and challenges for managing nitrogen in urban stormwater: A review and synthesis. Ecol Eng, 36(11): 1507-1519.

Comings, K., Booth, D., Horner, R., 2000. Storm Water Pollutant Removal by Two Wet Ponds in Bellevue, Washington. J Environ Eng-ASCE, 126(4): 321-330.

Duan, S., Kaushal, S.S., Groffman, P.M., Band, L.E., Belt, K.T., 2012. Phosphorus export across an urban to rural gradient in the Chesapeake Bay watershed. J Geophys Res-Biogeo, 117(G1): G01025.

Duncan, J.M., Groffman, P.M., Band, L.E., 2013. Towards closing the watershed nitrogen budget: Spatial and temporal scaling of denitrification. J Geophys Res-Biogeo, 118(3): 1105-1119.

Geosyntec Consultants, I., Wright Water Engineers, I., 2012. International Stormwater Best Management Practices (BMP) Database Pollutant Category Summary Statistical Addendum: TSS, Bacteria, Nutrients, and Metals.

Groffman, P.M. et al., 2002. Soil Nitrogen Cycle Processes in Urban Riparian Zones. Env Sci Tech, 36(21): 4547-4552.

Hatt, B.E., Fletcher, T.D., Walsh, C.J., Taylor, S.L., 2004. The Influence of Urban Density and Drainage Infrastructure on the Concentrations and Loads of Pollutants in Small Streams. Environ Manage, 34(1): 112-124.

Hood, M.J., Clausen, J.C., Warner, G.S., 2007. Comparison of Stormwater Lag Times for Low Impact and Traditional Residential Development. J Am Water Resour As, 43(4): 1036-1046.

Horner, R., Lim, H., Burges, S., 2001. Hydrologic monitoring of the Seattle ultra-urban stormwater management projects. Water Resources Series, Technical Report no. 170.

Howarth, R.W. et al., 1996. Regional nitrogen budgets and riverine N & P fluxes for the drainages to the North Atlantic Ocean: Natural and human influences. In: Howarth, R. (Ed.), Nitrogen Cycling in the North Atlantic Ocean and its Watersheds. Springer Netherlands, pp. 75-139.

Hsieh, C., Davis, A., 2005. Evaluation and Optimization of Bioretention Media for Treatment of Urban Storm Water Runoff. J Environ Eng-ASCE, 131(11): 1521-1531.

Hunt, W., Smith, J., Jadlocki, S., Hathaway, J., Eubanks, P., 2008. Pollutant Removal and Peak Flow Mitigation by a Bioretention Cell in Urban Charlotte, N.C. J Environ Eng-ASCE, 134(5): 403-408.

Hur, J. et al., 2008. Does current management of storm water runoff adequately protect water resources in developing catchments? Journal of Soil and Water Conservation, 63(2): 77-90.

Kearney, M.A., Zhu, W., Graney, J., 2013. Inorganic nitrogen dynamics in an urban constructed wetland under base-flow and storm-flow conditions. Ecol Eng, 60: 183-191.

Koch, B.J., Febria, C.M., Gevrey, M., Wainger, L.A., Palmer, M.A., 2014. Nitrogen Removal by Stormwater Management Structures: A Data Synthesis. J Am Water Resour As, 50(6): 1594-1607.

Kulzer, L., 1989. Considerations for the use of wet ponds for water quality enhancement. Office of Water Quality, Municipality of Metropolitan Seattle.

La Valle, P.D., 1975. Domestic sources of stream phosphates in urban streams. Water Res, 9(10): 913-915.

Leopold, L.B., 1968. Hydrology for urban land planning: A guidebook on the hydrologic effects of urban land use. USGS Circular 554.

Mallin, M.A., Ensign, S.H., Wheeler, T.L., Mayes, D.B., 2002. Pollutant Removal Efficacy of Three Wet Detention Ponds. J. Environ. Qual., 31(2): 654-660.

NRC, 2009. Urban stormwater management in the United States. National Academies Press, Washington D. C.

O'Driscoll, M., Clinton, S., Jefferson, A., Manda, A., McMillan, S., 2010. Urbanization effects on watershed hydrology and in-stream processes in the Southern United States. Water, 2(3): 605-648.

Paul, M.J., Meyer, J.L., 2001. Streams in the urban landscape. Urban Ecology: 207-231.

Peierls, B.L., Caraco, N.F., Pace, M.L., Cole, J.J., 1991. Human influence on river nitrogen. Nature, 350(6317): 386-387.

Roesner, L., Bledsoe, B., Brashear, R., 2001. Are best-management-practice criteria really environmentally friendly? Journal of Water Resources Planning and Management, 127(3): 150-154.

Roy, A. et al., 2008. Impediments and Solutions to Sustainable, Watershed-Scale Urban Stormwater Management: Lessons from Australia and the United States. Environ Manage, 42(2): 344-359.

Smart, M.M., Jones, J.R., Sebaugh, J.L., 1985. Stream-Watershed Relations in the Missouri Ozark Plateau Province1. J. Environ. Qual., 14(1): 77-82.

Taylor, G.D., Fletcher, T.D., Wong, T.H.F., Breen, P.F., Duncan, H.P., 2005. Nitrogen composition in urban runoff—implications for stormwater management. Water Res, 39(10): 1982-1989.

Villarreal, E.L., Semadeni-Davies, A., Bengtsson, L., 2004. Inner city stormwater control using a combination of best management practices. Ecol Eng, 22(4–5): 279-298.

Walker Jr, W., 1985. Urban nonpoint source impacts on a surface water supply.

Waschbusch, R., Selbig, W., Bannerman, R., 1994. Sources of phosphorus in stormwater and street dirt from two urban residential basins in Madison. Wisconsin, 95: 1999.

Winter, J.G., Duthie, H.C., 2000. Export coefficient modeling to asses phosphorus loading in an urban watershed. J Am Water Resour As, 36(5): 1053-1061.

CHAPTER 2. HYDROLOGIC RESPONSE TO STORMWATER CONTROL MEASURES IN URBAN WATERSHEDS

2.1 Abstract

Stormwater control measures (SCMs) are designed to mitigate deleterious effects of urbanization on river networks, but our ability to predict the cumulative effect of multiple SCMs at watershed scales is limited. The most widely used metric to quantify impacts of urban development, total imperviousness (TI), does not contain information about the extent of stormwater control. We analyzed the discharge records of 16 urban watersheds in Charlotte, NC spanning a range of TI (4.1 to 54%) and area mitigated with SCMs (1.3 to 89%). We then tested multiple watershed metrics that quantify the degree of urban impact and SCM mitigation to determine which best predicted hydrologic response across sites. At the event time scale, linear models showed TI to be the best predictor of both peak unit discharge and rainfall-runoff ratios across a range of storm sizes. TI was also a strong driver of both a watershed's capacity to buffer small (e.g., 1-10 mm) rain events, and the relationship between peak discharge and precipitation once that buffering capacity is exceeded. Metrics containing information about SCMs did not appear as primary predictors of event hydrologic response, suggesting that the level of SCM mitigation in many urban watersheds is insufficient to influence hydrologic response. Over annual timescales, impervious surfaces unmitigated by SCMs and tree coverage

were best correlated with streamflow flashiness and water yield, respectively. The shift in controls from the event scale to the annual scale has important implications for water resource management, suggesting that overall limitation of watershed imperviousness rather than partial mitigation by SCMs may be necessary to alleviate the hydrologic impacts of urbanization.

2.2 Introduction

Urbanization alters the response of river networks to hydrometeorological drivers, causing more frequent and intense floods (Leopold, 1968). This new flood regime causes more stream bank erosion, destroys habitat, and subsequently degrades stream ecosystem health (Paul and Meyer, 2001). Runoff generated during storm events is quickly concentrated in pipes and stream networks by stormwater drainage systems, which produce elevated peak flows and cause flooding and infrastructure damage. Additionally, urbanization can lead to rising or falling baseflow, which affects stream ecosystems by changing temperatures and nutrient cycling (Bhaskar et al., 2016). Stormwater control measures (SCMs) mitigate the impacts of urbanization by attenuating storm volumes, reducing peak discharges, accelerating groundwater recharge, and promoting evaporation (Roesner et al., 2001; Hamel et al., 2015). However, the capacity for SCMs to restore natural hydrologic regimes and stream ecosystem functions depends on both the extent of implementation within the watershed and the degree of impact from urbanization (Roesner et al., 2001; Hur et al., 2008; NRC, 2008; Roy et al., 2008; Burns et al., 2012).

Total imperviousness (TI), which is the fraction of the watershed area covered by an impervious surface, has often been used as a way to quantify the degree of urbanization.

It is both integrative and easily measurable (Arnold and Gibbons, 1996). While the form of the relationship between stream degradation and TI is uncertain (e.g., linear or having a threshold after which degradation begins), it is well established that stream degradation does increase with TI (Schueler, 1995; May et al., 1997; Booth et al., 2002). As reviewed by Paul and Meyer (2001), TI increases runoff magnitude manifested as peak discharge, bankfull discharge, and runoff ratio at both event and annual time scales. The lag time between rainfall and runoff generation has also been shown to shorten with increasing TI (Espey et al., 1966; Leopold, 1968). In a review of urban streams in the U.S. Southeast, O'Driscoll et al. (2010) demonstrated that these hydrologic changes have cascading effects on stream ecosystems by altering channel geomorphology, reducing the ability of streams to retain and remove nutrients, and decreasing the abundance of intolerant macroinvertebrate taxa.

One criticism of TI as a metric for predicting stream response is that not all impervious surfaces are directly connected to drainage networks through surface conveyance channels or pipes. An example of a disconnected impervious surface is the rooftop of a building that is surrounded by vegetation on all sides. Effective imperviousness (EI) accounts for this important nuance in impervious surface connectivity and is defined as the portion of the watershed covered by impervious surfaces directly connected to the drainage network (Alley et al., 1980; Alley and Veenhuis, 1983; Shuster et al., 2005; Walsh et al., 2005). As with TI, EI is an integrative measure characterizing urbanization, however it is not as easily quantified because it requires information on the connectivity of impervious surfaces.

SCMs are designed to produce hydrographs that mimic pre-development conditions, therefore impervious surfaces mitigated by SCMs are assumed to be disconnected from the streams when computing EI (Walsh et al., 2005). SCMs take many forms (e.g. wet ponds, dry ponds, bioretention areas), but are generally hydrologically connected elements within the landscape that temporarily store and release water to the drainage network at a slower rate determined by the size and design of the SCM and its outlet structure. This process of water attenuation reduces peak flows, and increases lag times between precipitation and stormflow volumes (Horner et al., 2001; Villarreal et al., 2004; Hood et al., 2007; Jarden et al., 2015). However, the water balance of urban watersheds is often still perturbed, because of water importation and decreased evapotranspiration, unless the SCMs include a significant water harvest or reuse component (Askarizadeh et al., 2015).

Accurately quantifying EI for large areas is time consuming and requires knowledge of roof downspout connections and pipe networks (Lee and Heaney, 2003). Therefore, simply distinguishing unmitigated impervious areas from mitigated ones may be a simple way to derive a watershed metric similar to EI. Here were propose an additional metric: unmitigated imperviousness (UI), which is the fraction of total watershed area occupied by impervious surfaces that are not mitigated by SCMs. The ratio of UI/TI, then, is the percentage of impervious area that is unmitigated by SCMs. This ratio is analogous to the directly connected impervious areas fraction (often abbreviated DC, DCI or DCIA) used in other studies (Lee and Heaney, 2003; Walsh et al., 2005; Walsh and Kunapo, 2009; Shields and Tague, 2014).

Because UI and EI contain additional information about connectivity and the role of SCMs, they may explain the difference in hydrologic response to rainfall between sites better than TI. However, neither contains information about treated pervious areas. Inclusion of the treated pervious areas is important, particularly in residential urban and suburban environments, where lawns occupy on average 23% of the area (Robbins and Birkenholtz, 2003). During construction, lawns are compacted which reduces infiltration and contributes to excess runoff (Pitt et al., 2008). Hence, treating surface runoff from these pervious, but potentially runoff-yielding areas may mitigate peak flows. Therefore, quantifying the mitigated area (MA) of the watershed may prove to be useful for characterizing the benefits of treated pervious and impervious areas.

We hypothesized that if stormwater management is affecting urban hydrology, then metrics that include both urbanization and SCM mitigation will explain variation in hydrologic response variables across sites better than those that quantify either urbanization or SCM mitigation alone. Specifically, we predicted that MA, which accounts for potential storage of runoff from pervious and impervious surfaces in SCMs, would be most closely correlated with runoff volume. Also, we predicted that UI would best explain variation in peak discharge and record flashiness because it enumerates the potential for impervious surface runoff to bypass SCMs and flow efficiently to the stream. In addition, water resource managers seeking to limit the impacts of urbanization can use the metrics that best explain hydrologic response to SCM mitigation in a planning and policy development.

2.3 Site Descriptions

We examined 16 watersheds with SCMs in the Charlotte, North Carolina (35° 13' 36.9" N, 80° 50' 35.9" W) metropolitan region in the Piedmont physiographic province (Figure 2-1). Between 1971 and 2000, Charlotte's mean annual precipitation was 1105 mm and was distributed evenly across months. Over the same time period, the average daily temperature was 16.4°C annually, and 5.4°C and 26.8°C for the months of January and July respectively (State Climate Office of North Carolina, 2013).

Of the 16 sites selected for hydrological analysis, streamflow was recorded at 12 of them by the United States Geologic Survey (USGS) (Table 2-1). These twelve sites had drainage areas ranging from 2.5 km^2 to 32.9 km^2 and were selected to span a range of urban development and SCM density. Little Sugar Creek drains Charlotte's city center and serves as an upper bound on urban development intensity in the city. Only 14% of the Reedy Creek watershed is developed (Table 2-1), and it was included as a control against any effects that watershed size may have on the results at Little Sugar Creek.

In addition to the 12 USGS sites, we included 4 smaller streams that were gaged as part of a larger study of the impacts of SCMs on multiple ecosystem services. Two of these four watersheds, UP1 (1.4 km^2) and UL1 (1.5 km^2), were adjacent to one another and are subwatersheds of Edward's Branch and Campbell Creek, respectively. The other two, SP1 (1.0 km^2) and SL1 (0.15 km^2), were drained by a tributary to Beaverdam Creek (BD4), which flowed into Beaverdam Creek downstream of a USGS gage used in this study. Changes to the hydrology and water quality during urbanization and contributions

Table 2-1: Extent of urban development and SCM mitigation for the 16 analyzed watersheds.

USGS ID	Site Name	Drainage Area (km^2)	Total Impervious Area (TI) [%]	Effective Impervious Area (EI) [%]	Untreated Impervious Area (UI) [%]	Unmitigated Impervious Fraction (UI/TI) [%]	Mitigated Area (MA) [%]	SCM Density [/ km^2]	Tree Coverage [%]
--	SL1	0.15	24	0.2	0.48	2.0	89	20.4	16
--	SP1	1.01	14	5.4	7.4	53	16	2.0	49
--	UL1	1.44	43	28	41	95	16	3.5	41
--	UP1	1.45	27	7.7	12	44	48	3.4	59
214643820	Edwards Branch	2.51	43	--	29	67	28	2.0	45
214645080	Briar Creek Trib.	3.11	32	--	31	97	1.3	0.96	56
2146470	Little Hope Creek	6.81	42	--	39	93	5.5	1.5	50
214297160	Beaverdam Creek	9.62	8.6	--	6.9	80	4.0	1.2	66
214266080	Gar Creek	9.79	4.1	--	4.0	98	1.3	0.10	67
214642825	Briar Creek	13.4	34	--	31	91	5.8	2.2	40
2142914	Gum Branch	13.9	23	--	20	87	10	1.9	50
2146315	Taggart Creek	14.0	37	--	30	81	12	2.9	46
2146562	Campbell Creek	14.7	37	--	29	78	17	2.6	49
2146211	Irwin Creek	15.4	32	--	27	84	9.0	2.1	47
2146409	Little Sugar Creek	31.5	54	--	52	96	3.2	1.5	36
212430293	Reedy Creek	32.8	12	--	11	92	2.9	0.73	61

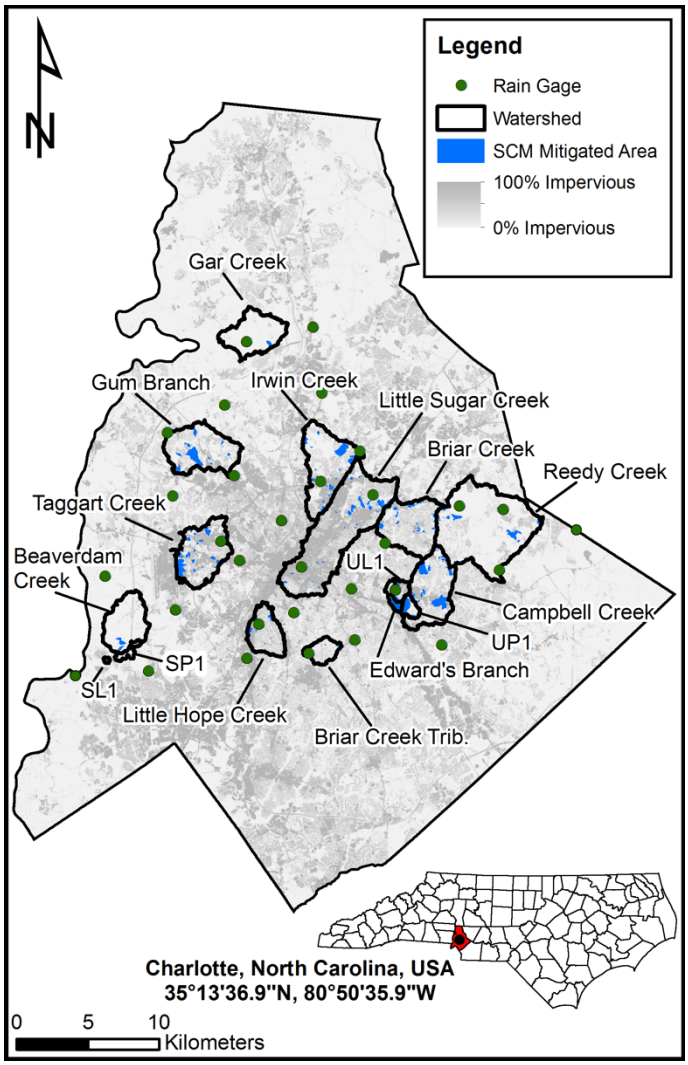

Figure 2-1: Map of 16 watersheds analyzed in the Charlotte, NC region. The dense cluster of impervious area in the southern portion of the Little Sugar Creek watershed is the city center.

highly treated sites because they are smaller than watersheds typically gaged by the USGS. Also, EI can be estimated at this scale with a few simplifying assumptions, but is not practical for larger watersheds with complex engineered drainage networks. This allows us to use these sites to test the ability of other metrics to serve as a proxy for EI.

Drainage areas were calculated using the Hydrology Toolbox in ArcGIS (ESRI, Redlands, CA, USA) with a 6.1 m (20 ft) digital elevation model (DEM). For the all sites, spatial

data from the City of Charlotte identifying the location of underground pipe networks was burned into the DEM prior to automatic delineation. For the highly treated sites, we manually adjusted watershed boundaries to incorporate additional knowledge of the underground storm sewer networks from field visits, aerial imagery and stormwater pipe network data. These manual adjustments were made at the small, highly treated sites because misidentification of watershed area there could produce large relative errors when calculating metrics such as TI, EI, UI and MA.

TI was determined from two spatial datasets: the first is a remote sensing land cover map developed for the year 2012 by Mecklenburg County, and the second is a vector shapefile of impervious surfaces used for stormwater taxation developed by the City of Charlotte. Tree coverage was also derived from the Mecklenburg County land coverage map.

The location and extent of SCMs and corresponding drainage areas were taken from a database compiled by the City of Charlotte Division of Storm Water Services, accessed upon its first release in July 2015. This dataset was created from records kept by the City of Charlotte's Division of Land Management in compliance with the city's post-construction stormwater ordinances. The dataset is also linked to spatial data outlining the drainage area that each SCM mitigates, which was determined using a combination of high-resolution topographic data and site designs provided by developers in accordance with the post-construction ordinance. In addition to the City's database, we used aerial photos available via Google Earth (Google Inc., 2015) dating from 1993 to 2012 to identify any SCMs in the watersheds missing from the database. We manually delineated

drainage basins and calculated drainage area for these additional SCMs using pipe network data, aerial photos, and elevation data.

Only SCMs designed to add storage were included when determining SCM mitigated area, while conveyance SCMs (e.g. swales) were left out. A number of in-line ponds existed in Charlotte, but were not considered SCMs unless they were included in the City's pond rehabilitation program, which retrofits ponds with either an outlet weir, littoral zone vegetation, or both to provide water quantity and quality benefits. We used the spatial datasets of SCM mitigated area and TI to compute UI and UI/TI at all 16 sites.

We estimated EI at the highly treated sites only using the following simplifying assumptions: (1) all impervious surfaces within an SCM drainage area were considered to be not effective; (2) all hydrologically remote, disconnected impervious surfaces were considered to be not effective; (3) 100% of roads and parallel sidewalks drained by pipe networks leading directly to a stream were considered effective; (4) single-family residential rooftops with driveways tangent to an unmitigated road were assumed to be 50% connected on lots ≤ ¼ acre and 33% connected on lots > ¼ acre, but the driveways were assumed 100% effective at both parcel classifications; and (5) other larger, multi-family residential and commercial buildings and associated parking lots were considered 80% connected. These assumptions were based on field observations and aerial photographs, and applying these assumptions produced land use specific EI estimates comparable to those of Alley and Veenhuis (1983) for 19 urban watersheds in Denver, CO, USA.

2.4 Data and Analysis

2.4.1 Data Sources

At the highly treated sites, a period of approximately one year (2011-2012) was used for hydrologic analysis. The period was slightly different for each site, running from 6/21/11 to 5/1/12 at UP1, 6/20/11 to 6/20/12 at UL1, 9/27/11 to 9/27/12 at SP1 and 8/18/11 to 8/18/12 at SL1. These time periods were chosen to include dates of stormwater quality sampling done as part of a companion study. At the USGS sites, the 2012 water year was selected for analysis, as it is the water year that corresponds best with the records selected at the highly treated sites. Data from Charlotte Douglas Airport (station ID: KCLT, downloaded from http://www.ncdc.noaa.gov/cdo-web/) indicated that the 960 mm of water fell during the 2012 water year, which was the 25th percentile of total annual precipitation on the station's 72-year record.

For the USGS sites, approved instantaneous discharge data, measured at 15-minute intervals, were downloaded from the USGS National Water Information System (http://nc.water.usgs.gov/char/streamflow.html). At the highly treated sites, we recorded stream stage at 10-minute intervals using a 730 Bubbler Module Sensor attached to an ISCO autosampler (Teledyne Technologies Inc., Thousand Oaks, CA, USA). We developed stage-discharge relationships for each site using a HEC-RAS (US Army Corps of Engineers) hydraulic model built from cross sectional geometry data collected at approximately 1.5 m longitudinal intervals. The modeled Manning's roughness coefficient for the channel banks was calibrated to match four to five high storm flow observations collected using velocity-area and dilution gaging methods (USGS, 1982).

For calibrating Manning's roughness in the channel at low flows, the total unit stormflow volume contributed from flows less than the 90th percentile discharge value was calibrated to be within ± 10% of the observed annual unit discharge from nearby gages over the same period. The USGS gage at Edward's Branch was used for calibration of low flows at UL1 and UP1, since the watersheds are adjacent and have similar land use and stormwater infrastructure. The USGS Edward's Branch gage was located 0.4 km downstream from UL1. For the two suburban sites, the record for low-flow calibration was compiled from a capacitance water level record combined with a stage-discharge rating curve by Gagrani et al. (2014) for the BD4 watershed.

We used 5-minute precipitation data from 31 rain gages in the USGS National Water Information System (NWIS) (http://nc.water.usgs.gov/char/raingage.html) to construct composite precipitation records for each watershed using the Thiessen method (Thiessen, 1911) (Figure 2-1). The number of gages used to create the area-weighted composite record at a given site ranged from 1 to 8.

2.4.2 Hydrologic Variable Considered

To characterize the hydrologic response, we first developed a procedure to identify individual storm events. We modified the constant line separation method developed by Hewlett and Hibbert (1967) to separate stormflow from baseflow and to define the end of a hydrologic event (Figure 2-2). This method was originally applied in forested watersheds to separate stormflow from baseflow, but because response times are considerably faster in urban streams, we decreased the slope of the separation line to $3.3x10^{-5}$ m^3 s^{-1} km^{-2} hr^{-1} based on observations of a subset of individual events at each site.

We defined the initiation of an event as the time of the first positive hydrograph slope during a 60-minute period that exceeded the slope of the hydrograph separation line. We determined the end of the event as the time when the separation line intersected the hydrograph. Of all hydrologic events identified, we retained only events in which total precipitation (PPT_E) exceeded 2.54 mm (0.1 in) for analysis. While other hydrograph separation methods using digital filters exist (Lyne and Hollick, 1979; Eckhardt, 2005), these methods are not designed to determine the start and end of individual storm events at a sub-daily time step.

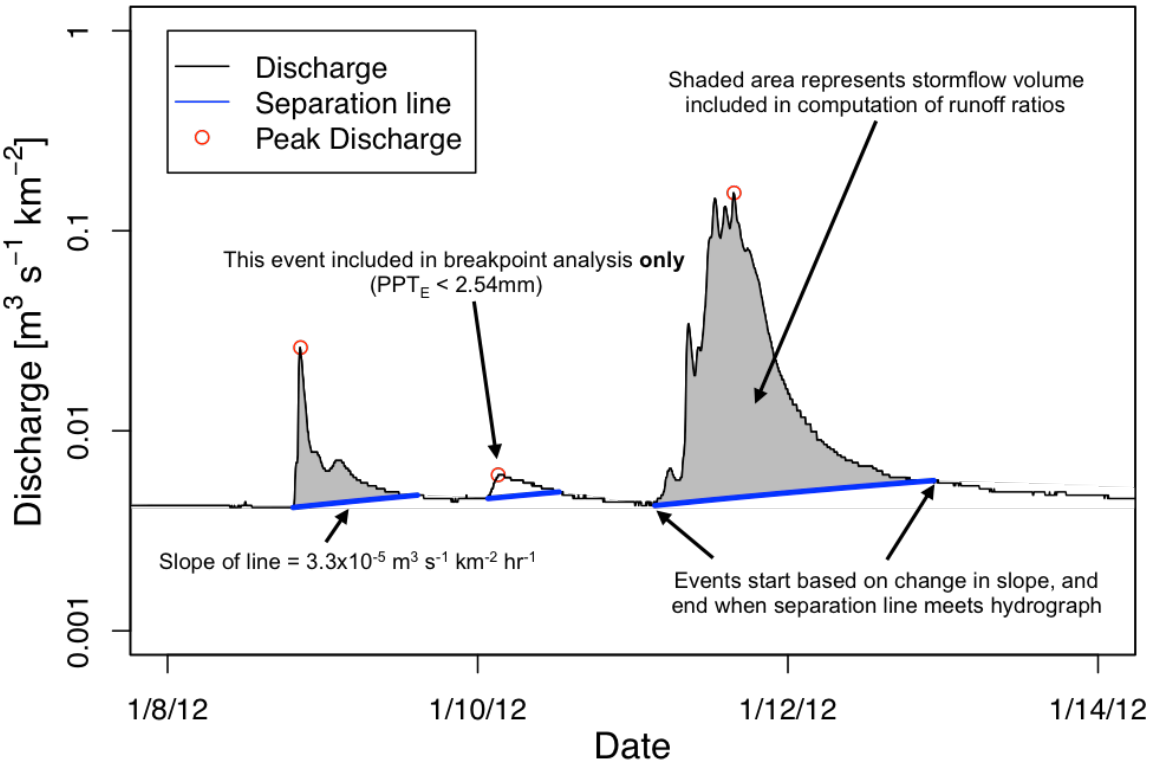

Figure 2-2: Example of modification to Hewlett and Hibbert (1967) constant line separation method used to define the beginning and end of storm events storm events, and to separate stormflow from baseflow for runoff ratio calculation. Example shown is for the first hydrological events of the 2012 calendar year at Little Sugar Creek

Using the discharge and precipitation data, we derived several metrics of event-scale hydrologic response. First we calculated the rainfall-runoff ratio as shown in Eq. 1.1:

$$Runoff\ Ratio = \frac{V/A}{PPT_E} \quad \text{(Eq. 1.1)}$$

where V is the total stormflow volume [L^3] above the separation line (Figure 2-2), A is the watershed area [L^2], and PPT_E is the total event precipitation [L]. PPT_E was the sum of all rain falling during the defined hydrologic event and any rain that had fallen 1.5 h prior to the event. Using this 1.5 h time window, pre-event precipitation accounted for <10% of total event rainfall for 75% of events analyzed.

We defined peak discharge as the largest instantaneous discharge value during the hydrologic event and normalized it to watershed area to allow for comparisons across sites. We calculated a "response rate" using the slope of a log-transformed linear model of peak discharge vs. maximum 60-minute precipitation intensity (I_{60}). This precipitation metric was chosen over PPT_E and the maximum 15-minute precipitation intensity as it produced the highest R^2 values at 9 of the 16 sites. We also estimated the amount of storage within the watershed as the threshold of precipitation above which streamflow responds more rapidly to rainfall (Loperfido et al., 2014). We calculated this as the breakpoint in slope of piecewise linear models between peak discharge and total precipitation using the "segmented" package in R (R Core Team, 2013). For computation of these breakpoints only, precipitation events with PPT_E less than 2.54 mm were also included.

In addition to these event-specific metrics, we computed two metrics to describe hydrologic behavior over longer timescales. We computed the annual water yield ratio as the slope of the regression line fit between cumulative daily flow depth and cumulative daily precipitation. Additionally, we calculated the percent of time the instantaneous discharge was above the mean value to characterize flashiness, a metric that can be used to describe the regime of hydrologic disturbances to stream ecosystems and is also tied to ecosystem biological integrity (Booth et al., 2004; Cassin et al., 2005; Burns et al., 2015).

2.4.3 Statistical Analysis

We used the software R (R Core Team, 2013) to perform all statistical analyses and all results reported as significant are within 95% confidence unless otherwise indicated. To determine trends across sites, we fit both linear and log-transformed linear models through the hydrologic response variables using the eight watershed metrics (Table 2-2). The watershed metric producing a univariate model with the highest performance determined by R^2 was deemed the primary control on hydrologic behavior across sites. To further characterize potential secondary controls, we performed a correlation analysis between the residuals of the linear models and the each of the remaining watershed metrics. All correlations were quantified using the Pearson product-moment correlation coefficient (R).

We computed 6 percentiles (10^{th}, 30^{th}, 50^{th}, 70^{th}, 90^{th} and 99^{th}) for peak discharge and runoff ratio at all 16 sites. We then performed the linear modeling procedure outlined above on all these percentile values (6 models per variable, each with n=16) to characterize the primary and secondary control across the entire range of event scale

Table 2-2: Separated into three sections by horizontal bars. The top section contains the abbreviations and computation methods of the metrics used to characterize the extent of urban development and SCM mitigation in the 16 watersheds. The middle section contains abbreviations and descriptions of the precipitation metrics used in the hydrologic analysis. The bottom section lists the hydrologic variables chosen to characterize each site's hydrologic regime at the event and annual time scales.

Abbreviation/Name	Metric	Unit
Watershed Characteristics		
Area	Total watershed area	km^2
TI	Total imperviousness (total impervious area / total area)	%
UI	Unmitigated imperviousness [(TI – Mitigated impervious area) / total area]	%
EI	Effective imperviousness (directly connected impervious area/ total area)	%
UI/TI	Fraction of impervious area unmitigated (UI/TI)	%
MA	Mitigated Area (SCM mitigated area / total area)	%
SCM Density	(Total number of SCMs in the watershed / total area)	SCMs km^{-2}
Tree Coverage	Fraction of watershed covered by trees (forested area / total area)	%
Precipitation Magnitude and Intensity		
PPT_E	Total event precipitation	mm
I_{15}	Maximum fifteen-minute precipitation intensity	mm hr^{-1}
I_{60}	Maximum sixty-minute precipitation intensity	mm hr^{-1}
Storm Event Hydrologic Variables		
Runoff ratio	Fraction of rainfall runoff during an event (quick-flow runoff volume / PPT_E)	unitless
Peak discharge	Maximum instantaneous unit discharge during each event	m^3 km^{-2} s^{-1}
Peak Flow Response to Precipitation		
Peak response rate	Slope of linear model between the logarithm of peak discharge vs. I_{60}	m^3 km^{-2} s^{-1} / mm hr^{-1}
Breakpoint	PPT_E value where there is a break in slope between peak discharge and PPT_E	mm
Annual Hydrologic Variables		
Water yield	Annual fraction of precipitation leaving watershed as streamflow	mm/mm
Time above mean	Percentage of time discharge was above mean annual discharge	%

observations, rather than just characterizing the mean or median. Performing this analysis across the distribution of hydrologic variables allowed us to identify which watershed factors controlled hydrologic response under varying antecedent moisture, temperature, and precipitation characteristics, which contribute to the variability within each site.

2.5 Results

2.5.1 Watershed Metrics

All of the watersheds metrics considered characterized either the intensity of urbanization, SCM mitigation or both (Table 2-1), and several of them correlated with each other (Table 2-3). The level of urbanization, quantified by TI, spanned from 4% to 51%. Mitigated Area (MA) ranged from 1.3 to 89%, but only three sites (all from the highly treated sites group) had MA values > 20%. EI, computed at only the 4 highly treated sites, ranged from 0.2% at SL1 to 41% at UL1. UI ranged from 0.48% to 52%. UI was very strongly correlated with EI (Table 2-3), which indicates that it can serve as a suitable replacement for EI if SCMs are assumed to convert effective impervious areas into non-

Table 2-3: Correlation matrix of 8 site metrics considered in this analysis. Values in the table are Pearson's product moment correlation coefficient (R). EI correlations are only for the four highly treated sites, while the rest are for all 16 sites.

	Area	TI	UI	EI*	MA	Tree Coverage	SCM Density	UI/TI
Area	1.00	0.07	0.27	0.64	-0.48	0.12	-0.34	0.49
TI	0.07	1.00	0.91	0.87	-0.01	-0.51	-0.01	0.18
UI	0.27	0.91	1.00	1.00	-0.41	-0.23	-0.34	0.56
EI*	0.64	0.87	1.00	1.00	-0.65	0.24	-0.51	0.93
MA	-0.48	-0.01	-0.41	-0.65	1.00	-0.63	0.91	-0.94
Tree Coverage	0.12	-0.51	-0.23	0.24	-0.63	1.00	-0.76	0.52
SCM Density	-0.34	-0.01	-0.34	-0.51	0.91	-0.76	1.00	-0.82
UI/TI	0.49	0.18	0.56	0.93	-0.94	0.52	-0.82	1.00

effective ones. UI and TI were also strongly correlated, and UI averaged 77% of TI. TI and tree coverage were moderately negatively correlated.

2.5.2 Runoff Ratios

For the analysis period, across 16 sites, we identified a total of 737 hydrologic events with precipitation ≥2.54 mm. Of the eight watershed metrics, TI was the best predictor of the 10-90th percentile runoff ratios, and runoff ratios increased with increasing TI (Figure 2-3a, Table 2-4). No significant relationship was produced for 99th percentile storms, which were highly variable. Additionally, the coefficient of variation of runoff ratios decreased with increasing TI (R^2=0.57, $p<0.001$). Significant linear models were also identified for the 30th-90th percentile runoff ratios using UI as the independent variable, and for the 10th-90th percentiles using tree coverage fraction. Runoff ratios increased with increasing UI and decreased with increasing tree cover. These models had lower explanatory power (R^2) than the TI models. No significant relationships were identified for any runoff ratio percentile versus MA, SCM density or UI/TI.

Table 2-4: Best linear models for predicting the 10th, 30th, 50th, 70th, 90th and 99th percentile rainfall-runoff ratios and peak unit discharge (log-transformed) using only a single site metric. Only significant models ($p<0.05$) with the highest R^2 are reported. This table describes the linear models shown in Figures 2-2(a) and 3(a).

Percentile	Rainfall-runoff ratio			Peak unit discharge		
	Metric	R^2	Slope	Metric	R^2	Slope
10	TI	0.76	0.32	TI	0.76	7.8
30	TI	0.75	0.41	TI	0.83	7.8
50	TI	0.74	0.47	TI	0.87	8.1
70	TI	0.72	0.51	TI	0.82	7.3
90	TI	0.43	0.43	TI	0.63	5.8
99	--	--	--	TI	0.45	5.6

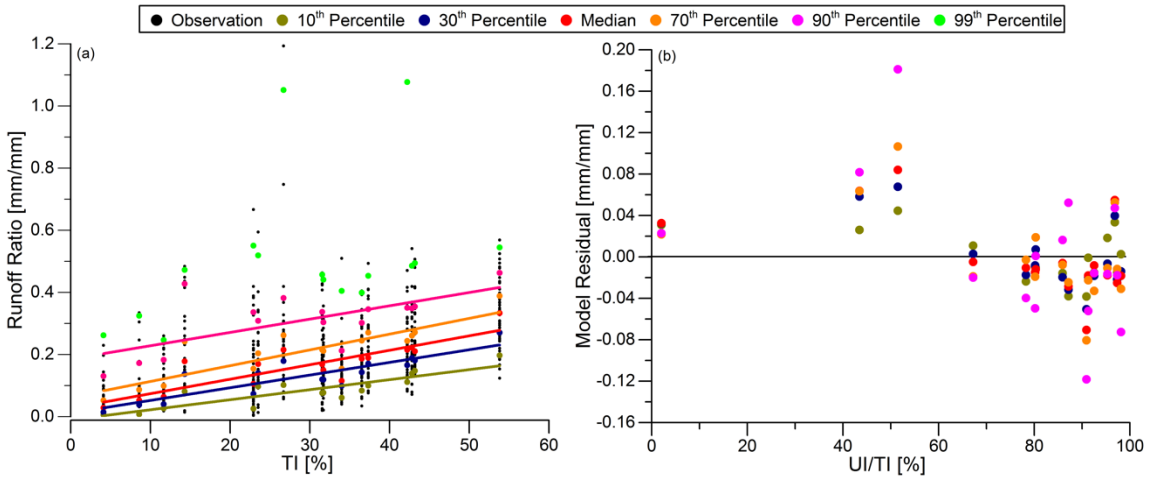

Figure 2-3: Panel (a) plots all observations of event rainfall-runoff ratios vs. TI. The solid lines represent significant linear relationships at selected percentiles, indicated by the color in the legend. Panel (b) shows the residuals of each of the linear models in (a) vs. the percentage of unmitigated impervious area. Generally, sites with less mitigated imperviousness have a higher runoff ratio, after discounting the effect of total TI.

To identify secondary controls on the 10-90th percentile runoff ratios, we correlated the residuals of the runoff ratio-TI models with the remaining site metrics. Residuals were most strongly correlated with the ratio of UI/TI (i.e., the percentage of impervious area that was unmitigated by SCMs). All correlations were negative ($-0.46 \leq R \leq -0.63$), which indicated that sites with a higher ratio of unmitigated imperviousness to total imperviousness had higher runoff ratios (Figure 2-3b).

2.5.3 Peak Discharge

Across all events and watersheds, simple linear regression models show peak discharge to be most strongly predicted by TI at all percentiles (Figure 2-4a, Table 2-4). In addition, significant models with lower explanatory power (R^2) were identified for UI (10th – 70th percentiles) and tree coverage (10th – 90th percentiles).

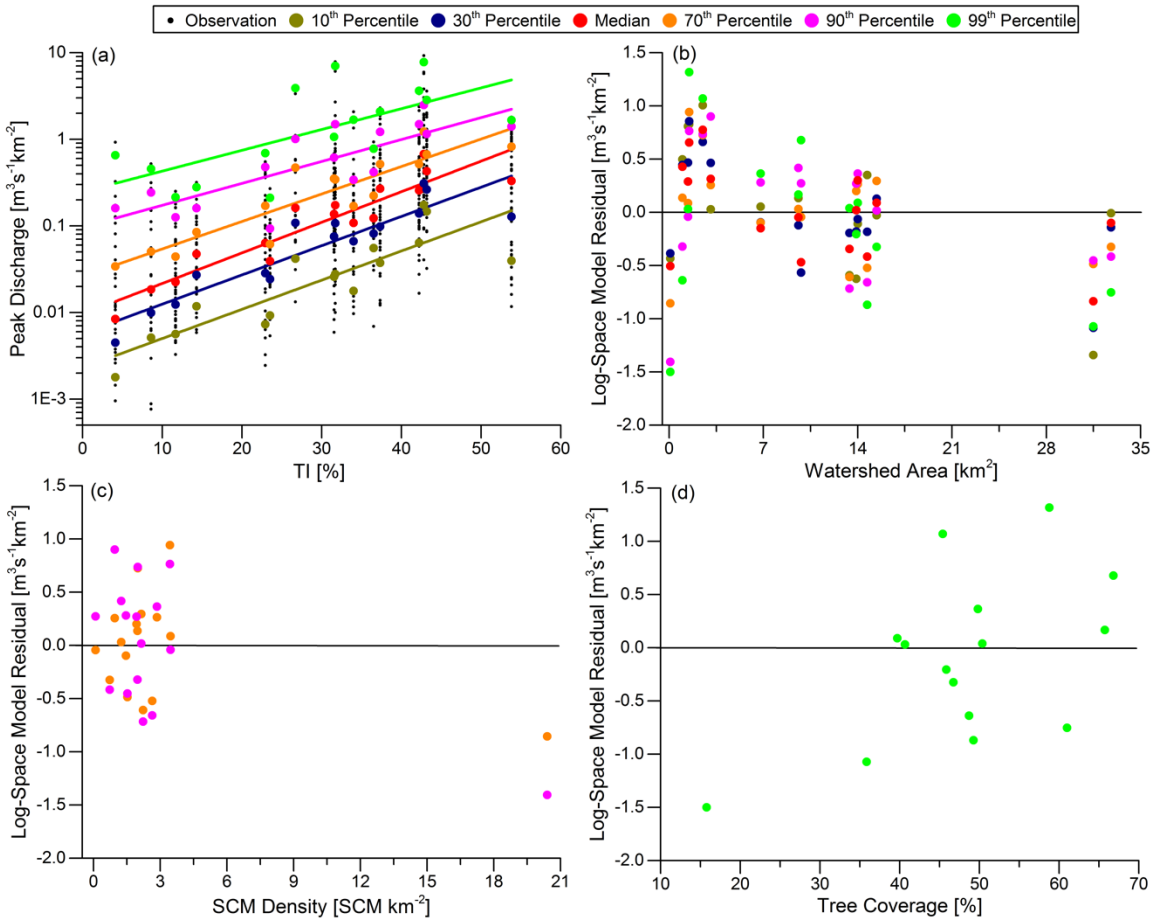

Figure 2-4: Panel (a) plots all observations of event peak unit discharge vs. TI. The solid lines are significant linear relationships at selected percentiles, indicated by the color in the legend. Panel (b) shows the residuals of all of the linear models in (a) vs. watershed area. The residuals of the 10th-50th percentiles were most strongly correlated to watershed area. Generally, the residuals decrease as watershed area increases, however the smallest sites deviate from this trend. Panel (c) shows the residuals of the 70th and 90th percentile linear model vs. SCM density, as this produced strongest correlation, although it was heavily leveraged by one site. Panel (d) shows the residuals of the 99th percentile model vs. tree cover, which produced the strongest correlation.

Correlation with the residuals of the peak discharge-TI models identified multiple secondary controls, changing with event size. Watershed area was identified as the strongest secondary control for smaller peak flows (10th-50th percentiles, $R < -0.53$, shown in Figure 2-4b). Larger peak flows (70th and 90th percentiles) were inversely correlated to SCM density (R=-0.414 and -0.594, respectively, Figure 2-4c), and the 99th

percentile was best correlated to the tree coverage (R=0.556, Figure 2-4d). However, the correlations for the 70^{th}-90^{th} percentiles were strongly leveraged by one point.

Despite the shifting secondary control, when plotted against watershed area, the peak flow-TI residuals for all percentiles generally declined as area increased (Figure 2-4b). This indicated that as watershed size shifted from small to large, the TI model shifted from under-predicting to over-predicting peak discharge. However, below 2 km^2, the trend was reversed, potentially due to the high level of SCM mitigation at the small, highly treated sites.

2.5.4 Peak Discharge Response to Precipitation Across Sites

Two record-long metrics were used to characterize the form of the relationship between peak discharge and precipitation characteristics. First, we defined the discharge response rate as the slope of the linear model of peak discharge (log-transformed) and I_{60}. This site-specific variable ranged from 0.59 at Gar Creek to 1.65 at Briar Creek Trib. As with the event scale metrics, the primary site factor that best predicted this variable across sites was TI (R^2=0.54, p=0.001, Figure 2-5). Significant, but weaker linear models were also observed between the response rate and UI.

The second metric describing the relationship between rainfall and peak discharge was the breakpoint in the slope of a linear model of peak unit discharge and PPT_E. Examples of this break in slope are shown for sites at the opposite ends of the urbanization spectrum. Figure 2-6a shows that Gar Creek, with 4% TI, had a flatter slope between 0

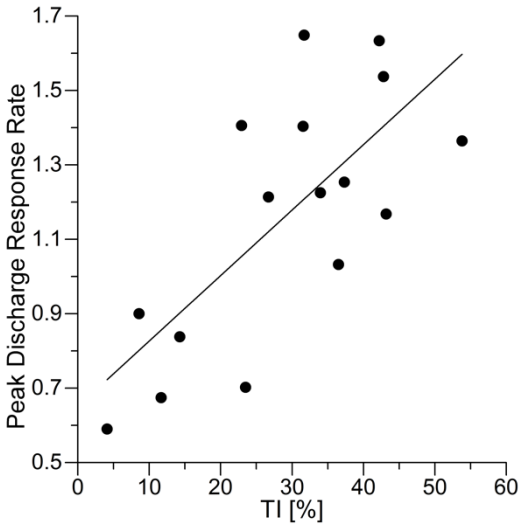

Figure 2-5: Peak discharge response rate vs. TI. This value was computed as the slope of a linear model constructed between peak discharge and maximum 60-minute rainfall intensity at each site. This plot shows that the sensitivity of peak discharge to equivalent forcing from precipitation increases as TI increases ($R^2 = 0.53$ $p = 0.001$).

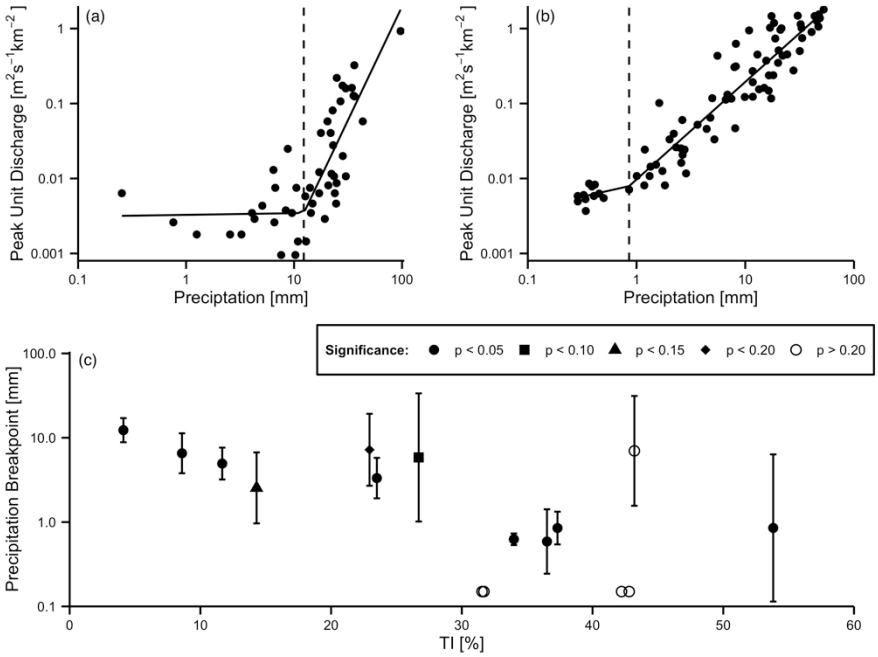

Figure 2-6: Panels (a) and (b) give examples of breaks in the slope of log-transformed peak discharge vs. log-transformed PPT_E at the lowest TI site, Gar Creek (a), and highest TI site, Little Sugar Creek (b). The dashed, vertical lines run through the breakpoints for clarity. Panel (c) shows that as TI increases, the breakpoints decrease indicating a more sensitive response to rainfall and therefore a loss in watershed storage. Different symbols are used to show different levels of statistical significance, and sites with $p > 0.20$ are plotted as open circles near the x-axis to indicate no change in slope, and therefore no storage. The point for UL1 is left hollow despite being significant ($\alpha < 0.15$) because the slope decreases at this breakpoint at this site, rather than increases.

and 12 mm of rain, above which the stream responded at a higher rate. Little Sugar Creek, with 54% TI, shifted at precipitation levels as low as 1 mm (Figure 2-6b). Our data showed that with increasing TI, runoff generation and streamflow response occurred during smaller rain events (Figure 2-6c). There was a downward trend in the breakpoint as TI increased. Determining the primary site metric controlling the breakpoints across site was difficult, as a number of sites did not exhibit a significant breakpoint (Figure 2-6c). Using subsets of the data based on breakpoint significance, TI consistently showed the strongest correlation with the breakpoint.

2.5.5 Annual Metrics

Two annual hydrologic metrics (water yield and time above mean) were also computed. Of all eight site metrics tested, water yield was most strongly correlated tree coverage (R^2=0.53, p=0.002) (Figure 2-7a). TI and UI also produced significant linear models, but with poorer performance.

The second annual metric considered was the fraction of time the hydrologic record spent above the mean discharge. This metric is an indication of flashiness with low values representing rapid watershed response (e.g., higher peaks and shorter duration). The time above mean ranged from 7.1% at Edwards Branch to 31% at SP1. UI was the best predictor of time above mean across all sites (Figure 2-7b, R^2=0.60, p=0.005), and TI also produced a significant, but less explanatory model. In search of secondary controls, no watershed metrics were strongly correlated ($|R| < 0.45$) with the primary model residuals.

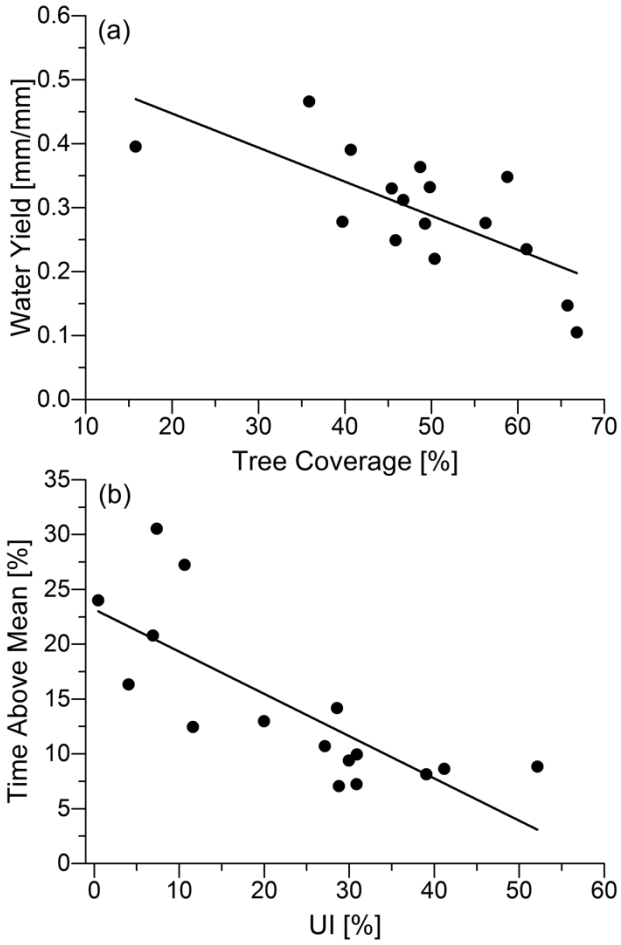

Figure 2-7: (a) Annual water yield fraction decreased with increased tree coverage ($R^2 = 0.52$, $p = 0.002$), and (b) time above mean decreased with increased UI ($R^2 = 0.60$, $p < 0.001$).

2.6 Discussion

2.6.1 Total imperviousness controls event scale response

At the event scale, TI was the dominant control on a range of hydrologic response metrics at 16 sites in Charlotte, NC that spanned a range of imperviousness and mitigation by SCMs. Regression analysis demonstrated that TI was best of a suite of spatially integrated, watershed-scale metrics at describing the variance of storm event runoff ratios. Additionally, a watershed's ability to store small rain events, quantified by a breakpoint

in slope between total precipitation and peak discharge, was also tied best to TI. These results are in alignment with other hydrologic effects of urbanization, including a loss of watershed recharge and storage (Booth 2002) and decreased evaporation and transpiration with loss of vegetation (Grimmond and Oke, 1999). Lower storage capacity would lead to more frequent flooding events, and therefore alter disturbance regimes in stream ecosystems. Additionally, TI had the strongest statistical control on both the distributions of peak discharge across sites and the rate of response of peak discharge to rainfall once initial storage (i.e., breakpoint) had been exceeded. These results add to an increasing body of evidence of urbanization, measured by TI, causing increased surface runoff and drainage efficiency (Shuster et al 2005). This is also demonstrated by the negative correlation (R=-0.75) between TI and each site's coefficient of variation of runoff ratios.

Other metrics like UI and tree coverage fraction frequently produced significant linear regression relationships at our study sites, but the strength of these was consistently less than those produced by using TI. Many studies have shown the relationship between hydrologic response and TI (see reviews by Arnold and Gibbons, 1996 and Shuster et al., 2005). However, modeling studies that considered both TI and EI (EI is assumed to be analogous to UI if SCMs operate as designed), found EI to be either a better metric than TI or an important control when modeling hydrologic response to rainfall (Lee and Heaney, 2003; Guo, 2008; Dewals et al., 2012; Shields and Tague, 2014). In the watersheds in our study, TI best explained event scale hydrology across sites, indicating

that TI is the single best metric for quantifying impacts of urban development on storm runoff delivered to streams.

2.6.2 Secondary controls on event scale hydrology

An analysis of residuals of the linear models between event hydrologic variables and TI was performed to identify secondary watershed controls. Analogous to the fraction of directly connected impervious surfaces (e.g., Shuster et al., 2005; Walsh et al., 2005; Shields and Tague, 2014), UI/TI was the dominant secondary control of runoff ratios. In our 16 watersheds, the correlation between the residuals and UI/TI was negative, so that for a given TI, runoff ratios decrease as the proportion of untreated impervious increases. Counterintuitively, this suggests that as a higher percentage of TI is treated by SCMs (i.e., UI/TI decreases), runoff ratios actually increase for given a level TI. We postulate that this effect is a result of different ages and styles of infrastructure within the SCM catchments than in areas with untreated imperviousness. In areas with high density of SCMs, development is likely newer, with less secondary permeability of pavement (Wiles and Sharp, 2008) and fewer joints and breaks in drainage pipes. Areas with SCMs may also be more likely to have a higher density of drainage pipes and curb and gutter systems, than in areas without SCMs, where informal drainage (e.g., roads without curbs) may be more prevalent (Walsh et al., 2012). Together or separately, these differences result in greater drainage efficiency of stormwater runoff to SCMs in newer developments, producing the higher runoff ratios observed in this study. The presence of a SCM may even spur greater connectivity of impervious surfaces because of the perception that the SCM will mitigate the effects of the runoff.

Although peak discharge did not have a consistent, dominant secondary control across the percentiles considered, watershed area was the most prevalent. The trend, as shown in Figure 2-4b was that as watershed area increases, the residuals decrease (i.e., peak discharge for a given TI decreases as area increases). This finding is consistent with peak attenuation due to channel and floodplain storage during flood routing (Bedient et al., 2002). It may also be attributable to non-uniform rainfall (both spatially and temporally) in larger watersheds, where isolated convective thunderstorms may produce high rain intensities in a small area while the rest of the watershed receives little or no precipitation. This finding contrasts that of Galster et al. (2006) who observed a positive linear relationship between peak unit discharge and area. Galster et al. (2006) tracked a single event downstream within the channel network and attributed the observed relationship to downstream increases in TI, which does, however, agree with our findings of TI as a primary control. Despite our observed trend of decreasing peak unit discharge residuals with increasing area, in the smallest watersheds (<2 km^2) with the highest SCM treatment, the residuals are negative compared to positive residuals in slightly larger watersheds (2-5 km^2) with lower SCM treatment. The effects of flood routing and spatial variation in rainfall should be small over this range of scales, so the difference between the highly treated and less treated watersheds implies that SCM mitigation may be a tertiary control on peak discharges across sites.

2.6.3 Tree coverage and SCM mitigation predict annual hydrologic response

While processes associated with impervious coverage were found to dominate the hydrology at the event scale, at the annual scale, tree coverage and stormwater mitigation

of impervious surfaces have a larger impact. The water yield fraction across sites was best explained by tree coverage, as a linear relationship showed lower water yield as tree coverage increased (Figure 2-7a). An urban forest canopy can increase transpiration, interception and subsequent evaporation (Nowak and Dwyer, 2007). This is inconsistent with the finding for runoff ratios at the event time scale, which were best explained by TI. TI is approximately the complement of total vegetation (i.e., total vegetation coverage = tree coverage + lawn coverage ≈ 1 – TI). At the event time scale, fresh rainfall is available for transpiration by both shallow-rooted lawns and deep-rooted trees, so TI may best represent plant access to water for transpiration. However, at longer time scales, tree coverage may better represent vegetative effects on hydrology than TI because trees have deeper rooting systems than grasses that allow them to transpire groundwater between rain events when the water table is lowered. The increased transpiration of urban trees compared to urban grasses was demonstrated by Shields and Tague (2014), where simulations of suburban and urban residential neighborhoods in semiarid Santa Barbara, California showed live oak consistently transpired more water per unit vegetated area than local grasses.

We characterized stream flashiness as the fraction of time the hydrologic record spent above its mean discharge. Low values of this metric occur if the flow distribution is skewed up towards fewer, larger events and this is indication of the intensification of the hydrologic response to precipitation. A previous study demonstrated that increased urbanization, as measured by TI, lead to decreases in the time spent above the mean (Booth et al., 2004). In this study, a similar relationship between the time above mean

and TI existed, but UI, the fraction of watershed area covered by impervious surfaces not mitigated by SCMs, was a stronger predictor. We attribute this to SCM design, which both delays the release of stored runoff from impervious surfaces and can promote local infiltration and groundwater recharge (Roesner et al., 2001; CMSWS, 2013). Localized infiltration in SCMs can lead to increased baseflow, which causes hydrologic records to spend more time above the mean discharge (Hamel et al., 2013; Bhaskar et al., 2016). However, a vast majority of the SCMs in this study were retention ponds and wetlands which designed with liners to limit infiltration (CMSWS, 2013). Therefore, we attribute this result to attenuation of surface water in SCMs rather than elevated infiltration. Jefferson et al. (2015) used isotopic hydrograph separation to show that SCMs surface outflow contributes disproportionately high amounts of runoff to streamflow during hydrograph recession relative to their drainage area. Our results, in combination with the goals of SCM design and observations of Jefferson et al. (2015), explain why UI, which implicitly incorporates SCM mitigated impervious surfaces, outperforms TI at predicting stream flashiness because SCMs temporarily retain surface runoff. Together, results of annual hydrologic variables indicate that management strategies like tree planting and mitigating impervious areas can reduce total water runoff and decrease hydrologic record flashiness.

2.6.4 Why was our hypotheses wrong? Highlighting topics for further research

We hypothesized that metrics incorporating both the extent of urban impact and mitigation with stormwater control measures (i.e., UI and MA), would better predict hydrologic variables than those quantifying urbanization or SCM mitigation alone. This

hypothesis implied that SCMs are affecting storm event runoff. However, at the event-scale, TI produced the strongest relationships. We propose four possible explanations for these unexpected results: (1) the signal produced by the distribution of SCM mitigation was insufficient to overcome the signal from imperviousness, (2) these metrics do not incorporate necessary information on spatial arrangement of both impervious surfaces and SCMs, (3) TI is actually a better predictor than EI of the suite of hydrologic behaviors studied here and (4) SCMs are unable to reverse the connection between urban surfaces and streams formed by storm drainage pipes (i.e., some mitigated impervious surfaces are still effective). These possible explanations highlight needs for future research.

The sixteen sites span a range of urbanization and SCM mitigation that reflects current practices in Charlotte, NC. The population of Charlotte grew by 14% between 2007 and 2014 (United States Census Bureau, downloaded at: http://factfinder.census.gov/), and this growth has coincided with urban development under stormwater post-construction ordinances implemented in 2007. This extensive, regulated development makes Charlotte a city with a relatively high level of SCM mitigation. However, while the range of mitigated area at the sites considered in this study is broad, it is skewed toward sites with less mitigation, which may not be sufficient to compensate for the impacts of urbanization at the watershed scale.

To investigate the sensitivity of our analyses to the influence of including a single very small, highly mitigated watershed (SL1), we repeated the analysis without SL1. This analysis showed that TI was still the best predictor of the distributions of runoff ratios

and peak discharges, the breakpoint in slopes of the relationship of peak discharge vs. PPT_E, and discharge response rates. Similarly, tree coverage remained the best predictor of total water yield. The only result that changed was that TI slightly outperformed UI (R^2 = 0.58 and 0.54, respectively) at predicting the time above mean. Since the results were mostly unchanged, we assert that these 15 sites may not have enough SCM mitigation to override the signal of urbanization. This is similar to results from studies in Cincinnati, OH on the effects of implementing rain gardens and rain barrels, which are more distributed forms of stormwater management. The authors found that partial mitigation (which reduced EI by ~9%) made small, but detectable changes to hydrology, however, these changes were not enough to effect stream biota (Shuster and Rhea, 2013; Roy et al., 2014).

Secondly, while one of the strengths of the metrics we chose is that they are easily computed and readily incorporated into policy, their simplicity renders them blind to spatial arrangement. Our analysis was not able to address proximity of impervious surfaces to one another or to the watershed outlet. In a modeling study, Corbett et al. (1997) found that although clustering impervious surfaces did not change event-scale rainfall-runoff ratios compared to scenarios with distributed impervious surfaces, it did increase peak flows. Other modeling study showed that runoff volumes increased (Zhang and Shuster, 2014) and peak discharge decreased (Yang et al., 2011) as the average hydrologic distance between impervious areas and the outlet decreased. These studies highlight complexity of the interaction between impervious area distribution and stormwater hydrology. Similar information is lacking with regard to the location of

SCMs that could also have significant effects on runoff timing and volume. At four sites in the Mid-Atlantic United States, Loperfido et al. (2014) showed that many small, distributed SCMs increased baseflow, increased precipitation-peak discharge breakpoints, and decreased extreme event runoff volumes more than a site with larger, more centralized SCMs. This shows that metrics like TI, UI, and MA may be missing important information about the spatial arrangement of both urban surfaces and SCMs.

Our hypotheses may also have been incorrect because one of two assumptions made in our theoretical framework was invalid. The first assumption was that EI is a better predictor of urban event scale hydrologic response than TI because it accounts for both impervious surfaces and their connectivity. There is a strong theoretical basis for EI as a predictor of urban hydrologic response (Shuster et al., 2005), and numerous modeling (Lee and Heaney, 2003; Guo, 2008; Dewals et al., 2012; Shields and Tague, 2014) and ecological studies (Walsh et al., 2005; Walsh and Kunapo, 2009) have demonstrated the importance of including connectivity. However, no empirical studies known to the authors have actually demonstrated the predictive power of EI with respect to hydrologic response.

The second assumption is that because SCMs are designed to replicate the hydrology in an undeveloped watershed (i.e., meet pre-development conditions), mitigated impervious surfaces are no longer directly connected and therefore not effective (suggested by Walsh et al. (2005)). However, this assertion requires that SCM design standards address all of the changes to flow regimes from urbanization, which some argue is not the case in practice (e.g., Burns et al., 2012; Askarizadeh et al., 2015). Additionally, the

performance of a SCM may vary based on SCM type, design approach, age or a combination of these factors. For example, in-line ponds may provide flow control and water quality benefits for smaller events, but larger events or events in wet antecedent conditions pass through with little retention. Because these ponds are directly on the stream network, they typically mitigate much larger areas than those closer to the ridgeline. This is further complicated because policies that specify SCM design, and therefore performance, vary both across political districts and in the same district through time. If in-line ponds or other SCMs underperform, this will lead to a misrepresentation of metrics like MA, UI and EI. The opposite effect may also be true: in-line ponds that we have ignored from our analysis, along with SCM approaches that provide small amounts of storage such as swales and infiltration trenches, may be affecting the hydrological signal. A potential improvement to these problems is to base the metrics of SCM mitigation on their performance or quality. However, quantifying "quality" in the face of varying design standards and watersheds is challenging. Indeed, this variability of performance is demonstrated by the wide range of volume reduction reported by the International Stormwater Best Management Practice Database (Geosyntec Consultants and Wright Water Engineers, 2011). Finally, it is possible that the effects of a fully functioning SCM on local hydrology do not translate to the watershed scale where multiple SCMs influence streamflow at different times.

2.7 Conclusions and Implications

The purpose of this study was to test whether or not watershed metrics characterizing both urban development and mitigation with SCM were better able to explain variation in

hydrology across sites than those quantifying urbanization or mitigation alone. We analyzed hydrologic regimes for 16 urban watersheds with stormwater control measures in Charlotte, NC. Total imperviousness, a metric characterizing only urbanization with no information about SCMs, was the best predictor of storm event hydrologic variables including rainfall runoff ratios, peak discharge, the ability of watersheds to buffer small rain events, and the rate of response between peak discharge and precipitation once that buffering capacity has been exceeded. Watershed metrics that included SCM mitigation were only found to be secondary or tertiary controls on hydrologic behavior at the event scale. These data indicate that SCMs implemented at the levels observed are not significantly affecting event hydrology at the watershed scale.

Annual hydrologic behavior, however, was best correlated to metrics other than TI. The total water yield was best related to the fraction of tree coverage, potentially because trees can transpire deeper groundwater between rain events. The time the discharge record spent above mean, a measurement of streamflow flashiness, was best related to unmitigated impervious area, indicating that SCMs may affect baseflow recession at time scales longer than a single event, as defined in this study.

Despite intense efforts to mitigate stormwater runoff through SCMs in newly developed areas and opportunistically through retrofits in older developments, our analysis demonstrates that these investments have not paid off in terms of storm event scale hydrologic response at the watershed scale. Therefore, unless different results are produced by future empirical studies either at sites with a broader range of SCM mitigation (e.g., 20-80%) or that incorporate SCM performance, TI is the watershed

metric that policy makers should use to manage watersheds to mitigate impacts to streams. Tree planting may be a desirable management strategy for reducing total runoff, while SCM mitigation of impervious surfaces is a strategy that may reduce hydrologic flashiness on longer time scales by extending baseflow recession.

2.8 References

Allan, C.J., Diemer, J.A., Gagrani, V., 2013. Beaverdam Creek Watershed Monitoring Report 2005-2012, Charlotte, NC.

Alley, W., Veenhuis, J., 1983. Effective Impervious Area in Urban Runoff Modeling. J. Hydraul. Eng.-ASCE, 109(2): 313-319.

Alley, W.M., Schaake, J.C., Dawdy, D.R., 1980. Parametric-deterministic urban watershed model. J. Hydr. Eng. Div.-ASCE, 106(5): 679-690.

Arnold, C.L., Gibbons, C.J., 1996. Impervious surface coverage: the emergence of a key environmental indicator. J. Am. Plann. Assoc., 62(2): 243-258.

Askarizadeh, A. et al., 2015. From Rain Tanks to Catchments: Use of Low-Impact Development To Address Hydrologic Symptoms of the Urban Stream Syndrome. Envir. Sci. Tech. Lib., 49(19): 11264-11280.

Bedient, P.B., Huber, W.C., Vieux, B.E., 2002. Hydrology and floodplain analysis. Prentice-Hall, Inc., NJ.

Bhaskar, A.S. et al., 2016. Will it rise or will it fall? Managing the complex effects of urbanization on base flow. Freshwater Science, 35(1): 293-310.

Booth, D.B., Hartley, D., Jackson, R., 2002. Forest cover, impervious-surface area, and the mitigation of stormwater impacts. J. Am. Water Resour. Assoc. (JAWRA), 38(3): 835-845.

Booth, D.B. et al., 2004. Reviving urban streams: Land use, hydrology, biology, and human behavior. J. Am. Water Resour. Assoc. (JAWRA), 40(5): 1351-1364.

Burns, M.J., Fletcher, T.D., Walsh, C.J., Ladson, A.R., Hatt, B.E., 2012. Hydrologic shortcomings of conventional urban stormwater management and opportunities for reform. Landsc. Urban Plan., 105(3): 230-240.

Burns, M.J., Walsh, C.J., Fletcher, T.D., Ladson, A.R., Hatt, B.E., 2015. A landscape measure of urban stormwater runoff effects is a better predictor of stream condition than a suite of hydrologic factors. Ecohydrology, 8(1): 160-171.

Cassin, J. et al., 2005. Development of hydrological and biological indicators o flow alteration in Puget Sound Lowland streams. King County DNRP, Seattle, WA.

CMSWS, C.-M.S.W.S., 2013. Charlotte-Mecklenburg BMP Design Manual (Revised Edition).

Corbett, C.W., Wahl, M., Porter, D.E., Edwards, D., Moise, C., 1997. Nonpoint source runoff modeling A comparison of a forested watershed and an urban watershed on the South Carolina coast. J. Exp. Mar. Biol. Ecol., 213(1): 133-149.

Dewals, B.J., Archambeau, P., Khuat Duy, B., Erpicum, S., Pirotton, M., 2012. Semi-Explicit Modelling of Watersheds with Urban Drainage Systems. Eng. Appl. Comp. Fluid, 6(1): 46-57.

Eckhardt, K., 2005. How to construct recursive digital filters for baseflow separation. Hydrolog. Process., 19(2): 507-515.

Espey, W.H., Morgan, C.W., Masch, F.D., 1966. A study of some effects of urbanization on storm runoff from a small watershed. Texas University at Austin, Center for Research in Water Resources.

Gagrani, V., Diemer, J.A., Karl, J.J., Allan, C.J., 2014. Assessing the hydrologic and water quality benefits of a network of stormwater control measures in a SE U.S. Piedmont watershed. J. Am. Water Resour. Assoc. (JAWRA), 50(1): 128-142.

Galster, J.C. et al., 2006. Effects of urbanization on watershed hydrology: The scaling of discharge with drainage area. Geology, 34(9): 713-716.

Geosyntec Consultants, I., Wright Water Engineers, I., 2011. International Stormwater Best Management Practices (BMP) Database Technical Summary: Volume Reduction.

Google, I., 2015. Google Earth, Mountain View, CA.

Grimmond, C., Oke, T., 1999. Evapotranspiration rates in urban areas. Int. Assoc. Hydrolog. Sci. (IAHS), 259: 235-244.

Guo, J., 2008. Volume-Based Imperviousness for Storm Water Designs. J. Irrig. Drain. E.-ASCE, 134(2): 193-196.

Hamel, P., Daly, E., Fletcher, T.D., 2013. Source-control stormwater management for mitigating the impacts of urbanisation on baseflow: A review. J Hydrol, 485: 201-211.

Hood, M.J., Clausen, J.C., Warner, G.S., 2007. Comparison of Stormwater Lag Times for Low Impact and Traditional Residential Development. J. Am. Water Resour. Assoc. (JAWRA), 43(4): 1036-1046.

Horner, R., Lim, H., Burges, S., 2001. Hydrologic monitoring of the Seattle ultra-urban stormwater management projects. Water Resources Series, Technical Report no. 170.

Hur, J. et al., 2008. Does current management of storm water runoff adequately protect water resources in developing catchments? J. Soil and Water Conserv., 63(2): 77-90.

Jarden, K.M., Jefferson, A.J., Grieser, J.M., 2015. Assessing the effects of catchment-scale urban green infrastructure retrofits on hydrograph characteristics. Hydrolog. Process. (In Press).

Jefferson, A., Bell, C.D., Clinton, S., McMillan, S., 2015. Application of isotope hydrograph separation to understand contributions of stormwater control measures to urban headwater streams. Hydrolog. Process. (In Press).

Lee, J.G., Heaney, J.P., 2003. Estimation of Urban Imperviousness and its Impacts on Storm Water Systems. J. Water Res. Pl.-ASCE, 129(5): 419-426.

Leopold, L.B., 1968. Hydrology for urban land planning: A guidebook on the hydrologic effects of urban land use. USGS Circular 554.

Loperfido, J.V., Noe, G.B., Jarnagin, S.T., Hogan, D.M., 2014. Effects of distributed and centralized stormwater best management practices and land cover on urban stream hydrology at the catchment scale. J. Hydrol., 519, Part C(0): 2584-2595.

Lyne, V., Hollick, M., 1979. Stochastic time-variable rainfall-runoff modelling, Institute of Engineers Australia National Conference, pp. 89-93.

May, C.W., Horner, R.R., Karr, J.R., Mar, B.W., Welch, E.B., 1997. Effects of urbanization on small streams in the Puget Sound ecoregion. Watershed Prot. Tech., 2(4): 483-494.

Nowak, D., Dwyer, J., 2007. Understanding the Benefits and Costs of Urban Forest Ecosystems. In: Kuser, J. (Ed.), Urban and Community Forestry in the Northeast. Springer Netherlands, pp. 25-46.

NRC, 2008. Urban stormwater management in the United States. National Academies Press, Washington D. C.

O'Driscoll, M., Clinton, S., Jefferson, A., Manda, A., McMillan, S., 2010. Urbanization effects on watershed hydrology and in-stream processes in the Southern United States. Water, 2(3): 605-648.

Paul, M.J., Meyer, J.L., 2001. Streams in the urban landscape. Urban Ecol.: 207-231.

Pitt, R., Chen, S., Clark, S., Swenson, J., Ong, C., 2008. Compaction's Impacts on Urban Storm-Water Infiltration. J. Irrig. Drain. E.-ASCE, 134(5): 652-658.

R Core Team, 2013. R: A language and environment for statistical computing. R Foundation for Statistical Computing, Vienna, Austria.

Robbins, P., Birkenholtz, T., 2003. Turfgrass revolution: measuring the expansion of the American lawn. Land Use Policy, 20(2): 181-194.

Roesner, L., Bledsoe, B., Brashear, R., 2001. Are best-management-practice criteria really environmentally friendly? J. Water Res. Pl.-ASCE, 127(3): 150-154.

Roy, A.H. et al., 2014. How Much Is Enough? Minimal Responses of Water Quality and Stream Biota to Partial Retrofit Stormwater Management in a Suburban Neighborhood. PLoS ONE, 9(1): e85011.

Roy, A.H. et al., 2008. Impediments and solutions to sustainable, watershed-scale urban stormwater management: Lessons from Australia and the United States. Environ. Manage., 42(2): 344-359.

Schueler, T.R., 1995. The importance of imperviousness. Watershed Prot. Tech., 1(3): 100-111.

Shields, C., Tague, C., 2014. Ecohydrology in semiarid urban ecosystems: Modeling the relationship between connected impervious area and ecosystem productivity. Water Resour. Res., 51(1):302-319

Shuster, W., Rhea, L., 2013. Catchment-scale hydrologic implications of parcel-level stormwater management (Ohio USA). J. Hydrol., 485: 177-187.

Shuster, W.D., Bonta, J., Thurston, H., Warnemuende, E., Smith, D.R., 2005. Impacts of impervious surface on watershed hydrology: A review. Urban Water J., 2(4): 263-275.

State Climate Office of North Carolina, 2013. CRONOS.

Thiessen, A.H., 1911. Precipitation averages For large areas. Monthly Weather Review, 39(7): 1082-1089.

United States Census Bureau, 2015. American Fact Finer, downloaded at: http://factfinder.census.gov/

USGS, 1982. Measurement and computation of streamflow: Volume 1. Measurement of stage and discharge. US Geological Survey water supply paper, 2175: 1-284.

Villarreal, E.L., Semadeni-Davies, A., Bengtsson, L., 2004. Inner city stormwater control using a combination of best management practices. Ecol.Eng., 22(4–5): 279-298.

Walsh, C.J., Fletcher, T.D., Burns, M.J., 2012. Urban Stormwater Runoff: A New Class of Environmental Flow Problem. PLoS ONE, 7(9): e45814.

Walsh, C.J., Fletcher, T.D., Ladson, A.R., 2005. Stream restoration in urban catchments through redesigning stormwater systems: looking to the catchment to save the stream. J. N. Am. Benthol. Soc., 24(3): 690-705.

Walsh, C.J., Kunapo, J., 2009. The importance of upland flow paths in determining urban effects on stream ecosystems. J. N. Am. Benthol. Soc., 28(4): 977-990.

Wiles, T.J., Sharp, J.M., 2008. The Secondary Permeability of Impervious Cover. Environ. Eng. Geosci., 14(4): 251-265.

Yang, G.X., Bowling, L.C., Cherkauer, K.A., Pijanowski, B.C., 2011. The impact of urban development on hydrologic regime from catchment to basin scales. Landsc. Urban Plan., 103(2): 237-247

Zhang, Y., Shuster, W., 2014. Impacts of Spatial Distribution of Impervious Areas on Runoff Response of Hillslope Catchments: Simulation Study. J. Hydraul. Eng.-ASCE, 19(6): 1089-1100.

CHAPTER 3. STORMWATER CONTROL MEASURES CHANGE URBAN STREAM NUTRIENT AND CARBON CONCENTRATIONS

3.1 Abstract

The urbanization of watersheds increases nutrient loading and lowers residence times for processing of reactive solutes (i.e., nitrate (NO_x-N), total dissolved nitrogen (TDN), orthophosphate (PO_4-P) and dissolved organic carbon (DOC)), which leads to increased concentrations and export of those solutes. Stormwater control measures (SCMs) mitigate these impacts of urbanization, and therefore have the potential to improve stream water quality. Our goal was to characterize the effects of SCMs on in-stream solute during storm events, focusing on two urban and two suburban watersheds in Charlotte, NC. We measured solute concentrations in outflow from a SCM in each watershed and in the receiving stream immediately downstream of the stream-SCM confluence during baseflow and 47 storms from 2011-2012. Average concentrations during stormflow were generally greater than baseflow, indicating that storms are important times of solute export. Watershed land use was an important control on export of nitrogen and phosphorus, as event mean concentrations of TDN and NO_x-N were higher at sites with less forest coverage and event mean concentrations of PO_4-P were higher at the suburban sites, possibly due to more fertilizer application. In the two urban sites, lower solute concentrations in SCM outflow decreased in-stream concentrations below the stream-

SCM confluence. However, SCM outflow in the suburban watersheds increased in-stream concentrations, because the addition of SCMs coincided with additional impervious area. Taken together, these results suggest SCMs have the potential to improve water quality by decreasing solute concentrations from urban runoff, but the type, location, and extent of urban development in the watershed may influence the degree to which this occurs.

3.1.1 Introduction

The connection between urban development and increased nutrient and carbon export is well documented (e.g., Paul and Meyer 2001), but the role of stormwater management in mediating solute export at the watershed scale is not as well understood (Koch et al. 2015). Urban impervious surfaces and storm sewers increase hydrologic efficiency which causes more runoff to quickly reach streams (Leopold 1968). When these hydrologic changes are combined with the greater loading of solutes to urban watersheds, total mass export of those solutes increases. These chemical disturbances damage downstream stream and lake ecosystems (O'Driscoll et al. 2010), and therefore erode the value of the services they provide (Brauman et al. 2007). Stormwater management often sets the goal of re-establishing the hydrological and biogeochemical processes that characterize undeveloped watersheds (CMSWS 2013). Specifically, stormwater control measures (SCMs), including detention ponds, wetlands and rain gardens, are designed to increase water retention in watersheds, thereby decreasing total runoff and nutrient and carbon export (Gagrani et al. 2014; Hale et al. 2015). In this paper, we seek to identify whether

SCMs alter stream water chemistry during storm events, and to determine how confounding environmental factors such as land use, seasonality, and SCM design affect these changes.

Urbanization elevates export of nitrogen (N), phosphorous (P) and dissolved organic carbon (DOC) from watersheds. Loading of N into urban areas is increased by importing food and fertilizer and accelerated atmospheric deposition from automobile exhaust (Bernhardt et al. 2008). However, the efficient hydrologic flowpaths that transport N across urban areas reduce retention time, limiting the potential for biological processing and removal. Of particular importance is the short circuiting of runoff past the riparian zone (Groffman et al. 2002; Taylor et al. 2005), which can remove a disproportionate fraction of nitrogen relative to its area within the watershed (Duncan et al. 2013). P export is also positively correlated to urbanization (Duan et al. 2012; Hatt et al. 2004; Smart et al. 1985; Walker Jr 1985; Winter and Duthie 2000), and is attributed to increased loading from fertilizer, food, and detergents (La Valle 1975; Waschbusch et al. 1994). Mass export of DOC also increases with urbanization, which is related to increased carbon concentrations in water due to leaching from older organic material and the presence of wastewater treatment plants and urban open areas (Aitkenhead-Peterson et al. 2009; Sickman et al. 2007; Walsh et al. 2005). Even if stream concentrations do not change, the excess runoff volume from urban watersheds alone leads to greater DOC mass export, which can accelerate respiration processes downstream (Hale et al. 2015; Petrone 2010; Vidon et al. 2009).

The increased solute export changes caused by urbanization can be compounded during storm events. In some cases, storm events account for a temporally disproportionate amount of nutrient and carbon mass leaving urban watersheds, which is attributed to increased water runoff, increased transport from watershed sources (i.e., concentration effect), or a combination of the two (Hook and Yeakley 2005; Poor and McDonnell 2007; Shields et al. 2008). However, other urban watersheds have shown either that storm events do not account for a majority of export, or that concentrations decrease or remain static during storms (i.e., dilution effect) (Groffman et al. 2004; Hook and Yeakley 2005; Lewis and Grimm 2007; Taylor et al. 2005). These dynamics are often site specific and depend upon multiple factors including, development patterns, land use history, topography and climate. Because SCMs are only engaged during storms, it is important to establish whether or not storms account for a majority of mass export, in order to understand whether SCMs can have a meaningful impact on stream water quality.

SCMs can reduce nutrient export in two ways, first by reducing total runoff volume and second by enhancing removal and retention processes within the SCM. SCMs are local depressions on the landscape that first collect and retain urban surface runoff, and then slowly release the water. SCMs reduce peak flows in the stream by delaying runoff and promoting infiltration during storm events, and reduce total runoff volume by allowing for evapotranspiration between events (Roesner et al. 2001).

In addition to hydrologic benefits of SCMs, accelerated biological activity, coupled with the physical settling process, can further reduce outlet concentrations of N, P and C

relative to inlet concentrations (Collins et al. 2010; Geosyntec Consultants and Wright Water Engineers 2012; Hunt et al. 2008; Kearney et al. 2013; Koch et al. 2014; Mallin et al. 2002). Plants and algal biomass assimilate dissolved nutrients and later release them in organic forms during senescence. Microbial communities also play an important role in altering water chemistry via denitrification and respiration, which convert dissolved N and C to gaseous forms. Physical processes within SCMs also change water quality, particularly sedimentation of P sorbed to particulate organic material and suspended sediments (Boström et al. 1988). Additionally, if the sediments and organic material are routinely dredged from SCMs or permanently buried, P is effectively removed (Walker 1987). Collectively, these processes enable SCMs to reduce concentrations of nutrients and carbon in outflow water relative to inflow.

The effectiveness of these removal and retention processes is determined through SCM design, which is largely focused on water residence time (Passeport et al. 2013). While many other design factors such as aerial footprint, geometry, and vegetation type affect SCM performance (Mallin et al. 2002), the simplest way to compartmentalize a continuum of SCM designs is by the depth of water maintained during dry periods, referred to as the permanent pool. This variable has been shown to be important for predicting removal and retention of nitrogen (Koch et al. 2014). Non-existent or shallow permanent pools create an ecosystem similar to a natural wetland. Wetland SCMs have distinct dry and wet periods, which allows for both aerobic and anaerobic biogeochemical processes (Collins et al. 2010). Additionally, shallow pooled water means wetland vegetation can populate a larger portion of the SCM's footprint (Collins et al. 2010).

SCMs with deeper permanent pools mimic natural pond ecosystems. In these "wet pond" SCMs, deeper water causes longer mean residence times of water and solutes, which is better suited to settle sediments and organic material out of the water column to the bottom sediments (Toet et al. 1990). Additionally, the deeper water leads to anaerobic conditions in the bottom sediments facilitating NO_3-N removal via denitrification. Algal assimilation dominates in the surface waters while wetland vegetation along the perimeter (i.e., littoral shelf) allows for additional nutrient uptake (Perniel et al. 1998).

While there is much literature on the nutrient retention and removal of individual SCMs, considerably less is known about the effects of stormwater management at the watershed scale. Many studies have demonstrated the importance of water volume reduction, which acts to reduce nutrient and C export (e.g., Bedan and Clausen (2009); Hale et al. (2015); Selbig and Bannerman (2008)). Retention and delayed release of the storm pulse also has potential for altering the timing of nutrient pulses to receiving stream networks (Jefferson et al. 2015). Recent studies have indicated that inclusion of SCMs can reduce in-stream concentrations of some solutes (Gagrani et al. 2014; Hale et al. 2015), but considerable uncertainty remains regarding local and watershed scale controls on these dynamics.

We link knowledge of urban hydrology and biogeochemical export at the watershed scale with that of SCM biogeochemical processes at a more localized scale by identifying the cumulative influence of SCMs on urban stream nutrient and DOC export. Specifically, we address three questions. First, are storm events times of elevated export due to increased runoff, increased concentrations, or both? If so, this would indicate that SCMs

have the potential for influencing biogeochemistry at a crucial time. Second, does water flowing out of an SCM into the stream change the concentrations of nutrients and DOC in the stream itself? And finally, what are the controls (e.g., seasonality, SCM type, land use) on the magnitude and direction of these stream concentration changes? This knowledge could help inform management decisions seeking to minimize nutrient export by minimizing concentrations of runoff.

3.2 Site Descriptions

We examined nutrient export from two suburban and two urban watersheds with SCMs near Charlotte, NC (35° 13' 36.9" N, 80° 50' 35.9" W). Charlotte's average annual precipitation is 1105 mm. Daily average temperatures for the months of January and July were 5.4°C and 26.8°C, respectively, between 1950-2000 at the meteorological station at Charlotte-Douglas Airport (KCLT) (State Climate Office of North Carolina 2013).

We classified two pairs of the four watersheds as having either urban (U) or suburban (S) land use. The differences between these land use categories were based on proximity to the city center and age of residential development. The outlet of each watershed was a short distance downstream of an SCM that was monitored for stream water quality; one wet pond (P) and one wetland (L) were in each of the development categories (Figure 3-1). The two urban sites were adjacent to one another other and the two suburban sites were in the same residential development. Approximately 12 miles separated the two pairs of watersheds. The four watersheds were also the subject of a companion study of

hydrologic response to precipitation on gradients of urbanization and SCM mitigation (Bell et al. In review).

We computed a number of metrics including total impervious area (TI), effective impervious area (EI), fraction of watershed area that is SCM-mitigated area (MA), and total vegetative coverage (Table 3-1). Table 3-1 also contains the TI of the subwatershed of the monitored in each of the four watersheds. We calculated drainage areas using the Hydrology Toolbox in ArcGIS (ESRI, Redlands, CA, USA) with a 6.1 m (20 ft) digital elevation model (DEM). We manually adjusted watershed boundaries to incorporate additional knowledge of the underground storm sewer networks from field visits, aerial imagery, and stormwater pipe network data. Impervious areas and vegetation coverage estimates came from a remotely sensed land cover map developed for the year 2012 by Mecklenburg County (Mecklenburg County GIS 2013).

The 145 ha urban wet pond watershed (UP1) has 27% TI, with dense commercial buildings in the upper portion of the watershed, and medium-density residential land uses in the middle and lower watershed (Figure 3-1a). There is forest coverage in the middle part of watershed, as well as a preserved riparian corridor. UP1 has three SCMs, including one inline wet pond in the upper watershed, a restored wetland, and a wet pond SCM near the watershed outlet. Together, these three SCMs treat 56% of the impervious area.

The UL1 watershed is the most heavily urbanization and least mitigated of the four sites. It is adjacent to UP1 and has impervious area distributed similarly: dense, commercial

Table 3-1: Extent of urban development and SCM mitigation for the 4 monitored watersheds

Site Name	Land Use Class	Monitored SCM Class	Drainage Area (ha)	Total Imperviousness (TI) [%]	Effective Imperviousness (EI) [%]	Mitigated Area (MA) [%]	Total Vegetation [%]	TI of SCM Subwatershed [%]
SL1	Suburban	Wetland	15	24	0.2	89	64	23
SP1	Suburban	Wet pond	111	14	5.4	16	83	30
UL1	Urban	Wetland	144	43	28	16	57	42[a]
UP1	Urban	Wet Pond	145	27	7.7	48	73	32

[a]Due to sampling constraints at UL1, instead of the monitored SCM, this table contains data describing the entire upstream right branch (US-R) as it is heavily influenced by SCMs compare to the upstream left branch (US-L) – see Figure 3-1

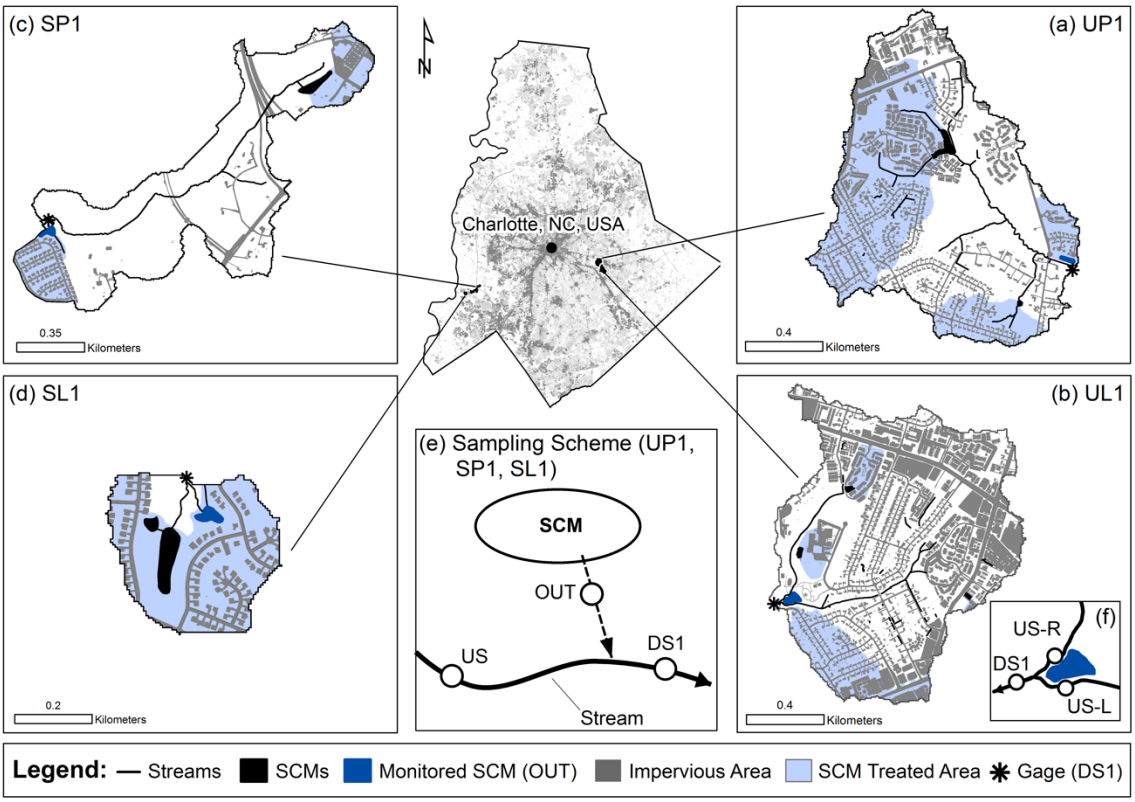

Figure 3-1: The locations of the four monitored watersheds near Charlotte, NC, USA. The inset maps of UP1 (a), UL1 (b), SP1 (c) and SL1 (d) show the location of impervious surfaces, SCMs, the areas mitigated by the SCMs, and the surface drainage networks. Inset (e) is a representative diagram of the sampling locations around the SCM-stream confluence. OUT is outflow from the SCM, US is stream water upstream of the confluence, and downstream 1 (DS1) is a mixture of OUT and US. Sampling following the scheme outlined in inset (e) was not possible at UL1, so instead we sampled at two tributaries, shown in inset (f). Due to a pipe routing stormwater underneath the US-L branch and into the monitored wetland, US-R was stream water heavily influenced by SCMs, while US-L was stream water less influenced by SCMs

development in the headwaters and 1950's residential areas throughout the remainder (Figure 3-1b). There are four SCMs in this watershed: a dry pond mitigating runoff from mixed residential and commercial land, a wet pond that mitigates runoff from an elementary school, a rain garden mitigating runoff from a single parking lot, and finally the monitored wetland just upstream of the outlet. Collectively, the four SCMs treat 16% of the watershed.

The two suburban watersheds, one with a monitored wet pond SCM (SP1) and one a wetland (SL1), are located in an actively urbanizing portion of the Beaverdam Creek watershed southwest of Charlotte (Figures 3-1c and 3-1d respectively). Impervious cover in the suburban watershed comprises a shopping center and freeway interchange in the upper watershed and medium density residential impervious areas in the lower watershed. Both clusters of impervious area are treated by one wet pond each. At the time of the study, the area between these two clusters was a hardwood forest, a few decades old.

At 15 ha, the SL1 watershed is considerably smaller than the others, and 24% of it is covered by residential impervious surfaces. The watershed contains three SCMs: a large in-line pond, a dry pond, and a wetland with no permanent pool that drains to the stream just above the monitored location. The in-line pond pre-dated the residential development, and receives overland flow and piped stormflow from 55% of the watershed. It was retrofitted with an outflow structure for flow control, however, water levels in the pond seldom reached levels high enough for the outlet structure to become activated. Instead, water seeped through the dam and contributed a low but constant flow to the stream during both storm and baseflow conditions.

3.3 Data and Analysis

3.3.1 Monitoring Framework

3.3.1.1 Hydrology

We monitored streamflow and water quality for a period of approximately one year (2011-2012). The range of dates monitored at each site varied: 6/21/11 to 5/1/12 at UP1, 6/20/11 to 6/20/12 at UL1, 9/27/11 to 9/27/12 at SP1 and 8/18/11 to 8/18/12 at SL1. We chose the monitoring windows based on quality of hydrologic data and to coincide with a maximum amount of stormwater quality samples. A 730 Bubbler Module Sensor attached to an ISCO autosampler (Teledyne Technologies Inc., Thousand Oaks, CA, USA) measured stream stage at 10-minute intervals at each of the four sites. We developed a stage-discharge relationship using a calibrated HEC-RAS (US Army Corps of Engineers) hydraulic model (see Bell et al. (In review) for details).

To describe historical precipitation data for the Charlotte area, we used data downloaded precipitation data from the National Oceanic and Atmospheric Administration's meteorological station at Charlotte-Douglas Airport (KCLT). However, the sub-daily rainfall patterns varied substantially between watersheds, particularly between the urban and suburban pairs. We therefore used Theissen polygons to generate a sub daily rainfall record at each watershed using data from the United States Geological Survey's Charlotte-Mecklenburg Network of rain gages (data downloaded from: http://nc.water.usgs.gov/char/rainfall.html).

3.3.1.2 Water Quality

We collected discrete water samples by hand and using ISCO autosamplers, in order to characterize patterns in nutrient and carbon concentrations during storm events. We configured the ISCO samplers to collect stream water from the center of the channel downstream of the confluence of the SCM and the stream, denoted as cross section DS1. DS1 was also the location of the hydrologic gage and considered the watershed outlet (Figure 3-1e). ISCO samplers began sampling once stream stage rose by 5-10% of the pre-event stage, after which the sampler pumped 800 mL of stream water into bottles every 15 minutes for two hours. After these first 8 samples were collected, the ISCO collected samples every 2 hours for up to 32 hours to characterize the hydrograph recession.

We also collected grab samples before, during, and after the storm at two other locations (Figure 3-1e): the ephemeral channel that transported water from the outlet of SCM to the stream (OUT); and within the stream, just upstream of the SCM-stream confluence (US). These sampling locations acted as end-members for the water sampled at DS1, which is inferred to represent a mixture of the two end-members. The general sampling configuration (Figure 3-1e) was not possible at UL1, as the SCM outlet pipe became inundated during storm events, rendering sampling from the outlet culvert impossible. Instead, we sampled water from the upstream left (US-L) and upstream right (US-R) tributaries. Three of the four SCMs in UL1 drain to US-R, while the US-L watershed has only a rain garden. The monitored wetland captures stormwater runoff from a residential

area adjacent to US-L; however, a siphon inflow structure runs underneath the US-L tributary and outflow water from wetland drains to the US-R tributary (Figure 3-1b). As a result, these two branches have the same land use, but very different levels of SCM mitigation, which allowed us to use the US-R and US-L end members in place of OUT and US, respectively.

To complement grab samples, we installed passive siphon samplers (Diehl 2008) at the US location of all four sites, and at the SCM outlets at all sites but UL1. These samplers act as first flush bottles because they fill on the rising limb, but do not allow for the exchange of water between and the bottle and stream once filled. The temporal density of all sample types (ISCO, passive siphon, and grab) varied between events, and the minimum number of total samples collected for each storm analyzed was 7 per site.

We collected ISCO samples upon conclusion of each rain event, returned them to the lab in coolers, and filtered them using pre-ashed 0.7 µm Whatman® glass fiber filters. We stored one sample aliquot in the refrigerator until analyzed for concentrations of TDN (mg-N L^{-1}) and DOC (mg-C L^{-1}) on Shiamadzu TNM-1 and TOV-V analyzers (Shiamadzu Corp., Kyoto, Japan). We stored two sample aliquots frozen in the dark until thawed for analysis of NO_x-N and PO_4-P (as mg-N L^{-1} and mg-P L^{-1}, respectively) on a Lachat QuikChem 8500 Series 2 - FIA Automated Ion Analyzer (Hach Company, Loveland, CO, USA) using the cadmium reduction method for NO_x-N (QuikChem Method 10-107-04-1-A; detection limit 0.016 mg NO_x-N L^{-1}) and the ascorbic acid

method for PO_4-P (QuikChem Method 10-115-01-1-Q; detection limit 0.01 mg PO_4-P L^{-1}) (APHA et al. 2005).

3.3.2 Data Analysis

3.3.2.1 Monthly export estimates

We calculated total mass export for all solutes during two 28 day intensively sampled periods in October (10/7/11-11/5/11) and February (2/1/12-3/1/12). We determined export by linearly interpolating all measured concentration values, multiplying concentrations by stormflow volume, and dividing the cumulative sum by watershed area. We sampled all storm events at all sites during this period, except for one storm event at UL1 occurring on 10/11/11 and 10/12/11. For this missing event, we computed the average event mean concentration (EMC, the methods of computation are described in the following section) for each of the constituents for all other events through the entire monitoring period. We then assigned this average EMC as the concentration throughout the duration of the missing event. To account for uncertainty, we also calculated export using both the maximum and minimum observed EMCs from all other events as the concentration during the missing event, thus we generated a maximum, mean and minimum export estimate.

3.3.2.2 Event-scale chemical export magnitude and timing

During each storm, we calculated the peak concentration (C_{MAX}) and the flow-weighted event mean concentration (EMC) for each of the four solutes sampled at DS1. For 11 out

of 48 events considered, we took a grab sample at DS1 72 hr prior to the rain event. When this pre-event grab sample was not taken, we assumed the concentration at the time of hydrograph rise was equal to the mean of all samples taken while stream flow was below the 80^{th} percentile of mean daily flow for the entire record. For computation of the water quality variables, we defined the inception of each event based on the first period of a positive slope that resulted in hydrograph above antecedent conditions for at least 3 hr. The event's conclusion was the time when the last water quality sample had been taken. The length of the events was therefore sensitive to the sampling procedure. On average, storm sampling continued until the hydrograph receded to 13% of the peak discharge, and sampling continued until the hydrograph receded until <20% of the peak discharge for 69% of the storms. If water quality sampling persisted across multiple, distinct hydrograph pulses during which the hydrograph receded to ~20% of the peak discharge, we separated the pulses into individual events (i.e., two or more values of C_{MAX} and EMC were determined).

To compare the timing of each solute exported through the rain event, we computed a first flush coefficient (b), calculated as the slope of a linear model between log-transformed mass export fraction and the log-transformed volume export fraction. Bertrand-Krajewski et al. (1998) explored this coefficient in depth, but generally as b decreases from 1 to 0, the export pattern displays a more positive gap in which the cumulative mass fraction leads the cumulative volume fraction. This phenomenon is commonly referred to as the "first flush." As b increases from 1 to infinity, the reverse is true: the cumulative volume fraction leads the cumulative mass fraction. We computed

these three variables (EMC, C_{MAX}, and b) for each solute for each storm and used the variables to compare magnitude and timing of solute export across sites.

We used the software R (R Core Team 2013) to perform all statistical analysis. One-way analyses of variance (ANOVAs) with site as the grouping factor determined if the means of the three variables were significantly different among sites. For all tests we determined significance when $p<0.05$. All ANOVA analyses employed a Bonferroni p-value adjustment for uneven sample sizes, and were complimented with a Tukey's honestly significant difference (Tukey-HSD) post-hoc comparison test. Where necessary, we transformed the data prior to the ANOVAs to ensure normality.

3.3.2.3 SCM Influence on water chemistry

To determine the influence of SCMs on stream chemistry through time, we analyzed hydro-chemographs of water from the three cross-sections around the SCM-stream confluence. Time series rainfall data from the Charlotte-Mecklenburg Network rain gages supplemented this hydro-chemograph analysis. For brevity, the data shown here are for only two successive hydrologic events occurring in the month of August. These August events contained either the highest (UP1 and UL1), fourth highest (SL1), or fifth highest (SP1) recorded discharges at each site. The events chosen were representative of chemograph behavior during other sampled events. While all events occurred in first week of the month of August, the data shown for the urban sites is from the year 2011 and the suburban sites from 2012. Although they occur in different years, showing events from the same time of year from all sites minimizes variability due to seasonality.

Finally, we also chose to show these August storms because they had relatively dense temporal sampling at US and OUT or US-R end members. Paired sample t-tests ($p<0.05$) determined if the differences in concentrations of samples take synchronously (within 2 hr) at OUT and DS1 were significantly different than 0. We chose to compare OUT to DS1 rather than to US because the number of sample pairs was higher, and results were comparable for both DS1 and US. Values greater than 0 indicated that the SCM increased DS1 solute concentrations in the stream on average, while values less than 0 indicated that the SCM decreased concentrations on average. For UL1, we used the difference between concentrations at US-R and DS1 in place of OUT and DS1, as water in the US-R cross-section included outflow from the three large SCMs in the watershed.

Using the entire period of record, we compared synchronous (within 2 hr) samples from SL-OUT and SP-OUT using paired sampled t-tests ($p<0.05$) to isolate the effects of SCM type. Because the suburban SCMs are within ~730 m of each other and had identical land use in their contributing areas, we assumed that export per unit area to the SCMs is equal. This isolates SCM type as the dominant difference between the two sets of samples. Only the suburban sites were chosen for the analysis of SCM type because we were unable to sample directly from the SCM outlet at UL1, and comparing UP1 to SP1 would introduce variability associated with different land use and meteorological forcing.

3.4 Results

3.4.1 Monthly export estimates

We quantified the total export of four solutes at each site during October 2011 and February 2012 (Figure 3-2). Additionally, we separated this export into storm and baseflow fractions, and computed a mean concentration for each flow condition by dividing the total export by the total volume. During October, which received 77 mm of rainfall, 38-72% of the runoff volume occurred during storms. Greater than 50% of the mass for all solutes at all sites was also exported during storm events. In February, less rainfall (33 mm) led to smaller and less frequent storms with 28-50% of the runoff volume delivered during storms. Despite higher concentrations during February storm periods, greater solute export occurred during baseflow conditions at the two urban sites. Export at the suburban sites was more variable. At SP1, baseflow periods also accounted for more mass export than storm periods for all solutes except NO_x-N, however storm events accounted for more than half of the export of all four solutes at SL1.

We calculated the average monthly concentration during baseflow and stormflow during the months of October and February for each solute (Figure 3-2). To compare baseflow and stormflow concentrations, we used the minimum concentration estimate at UL1 in October to be conservative. Mean storm condition concentrations were higher than baseflow with a few exceptions, which did not occur at a consistent site or for a single solute.

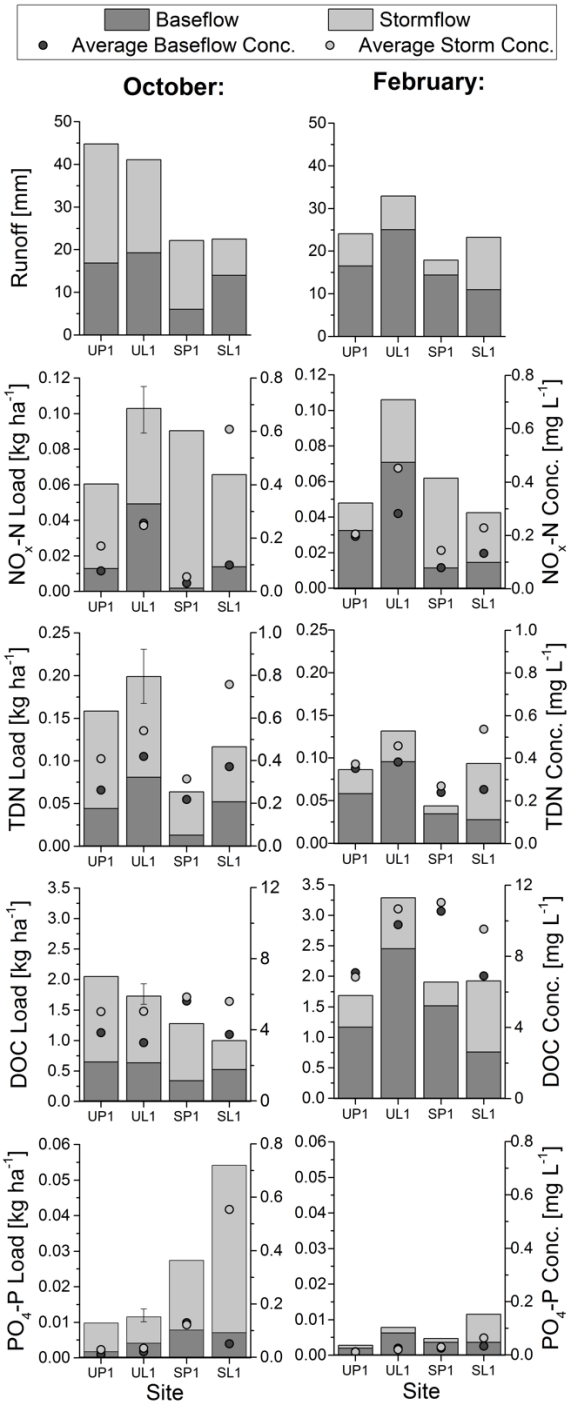

Figure 3-2: Total water runoff (top row) and solute export (rows 2-5) for the months of October and February. Mass export (left y-axis) is shown as bars and average concentration (right y-axis) is shown as points of each subplot. Samples were separated into stormflow and baseflow time periods following the method of Bell et al. (In review). Error bars on the October storm export at UL1 represent a maximum and minimum estimate given a storm occurring on October 11-12, 2011 was unsampled

Stormflow concentration of the two nitrogen species generally decreased in order of SL1, UL1, UP1 to SP1 (Figure 3-2). DOC concentrations were strongly affected by seasonal differences, with average baseflow and storm concentrations higher in February than October at all sites (Figure 3-2). These higher concentrations lead to a greater mass export of DOC during February despite lower streamflow volume. To a lesser extent, seasonality also influenced PO_4-P concentrations, as the average storm concentrations were higher in October compared to February at all sites (Figure 3-2).

Table 3-2: Summary of minimum, mean, and maximum values of two water quality variables, C_{MAX} and b, for NOx-N, TDN, and DOC at each site. Significant differences ($p<0.05$) in mean values between sites are indicated by unique letters in the "ANOVA Group" column.

Solute	Site	C_{MAX}				b			
		Min.	Mean	Max.	ANOVA Group	Min.	Mean	Max.	ANOVA Group
NO_x-N	UP1	0.16	0.32	0.55	a	0.86	1.1	1.7	a
	UL1	0.33	0.65	1.2	b	0.90	1.1	1.2	a
	SP1	0.067	0.30	0.56	a	0.90	1.1	1.3	a
	SL1	0.36	0.75	1.1	b	0.87	1.1	1.3	a
TDN	UP1	0.45	0.71	1.1	a	0.88	1.0	1.1	a
	UL1	0.67	1.2	2.4	b	0.93	1.1	1.1	a
	SP1	0.43	0.68	1.1	a	0.95	1.0	1.1	a
	SL1	0.88	1.4	2.5	b	0.92	1.1	1.3	a
DOC	UP1	4.0	8.0	22	a	0.97	1.0	1.2	a
	UL1	5.6	10	17	a	0.93	1.1	1.2	a
	SP1	7.2	12	19	a	0.77	1.0	1.1	a
	SL1	5.2	10	20	a	0.92	1.0	1.1	a

3.4.2 Storm event solute export magnitude and timing

Using the entire period of record (48 storms), we tested for differences in concentration among sites by comparing EMC and C_{MAX}, and for differences in timing by comparing the flushing coefficient b. UL1 and SL1 had significantly higher EMCs compared to UP1 and SP1 for both NO_x-N and TDN (Figure 3-3). Results were similar for tests performed

on the distributions of C_{MAX} (Table 3-2). We found no significant differences in mean values of b for either N species, and the average b values for both N species were between 1.0 and 1.1 at all sites (Table 3-2). For DOC, we saw no significant difference in the means of EMC, $C_{MAX,}$ or b among any sites (Figure 3-3, Table 3-2).

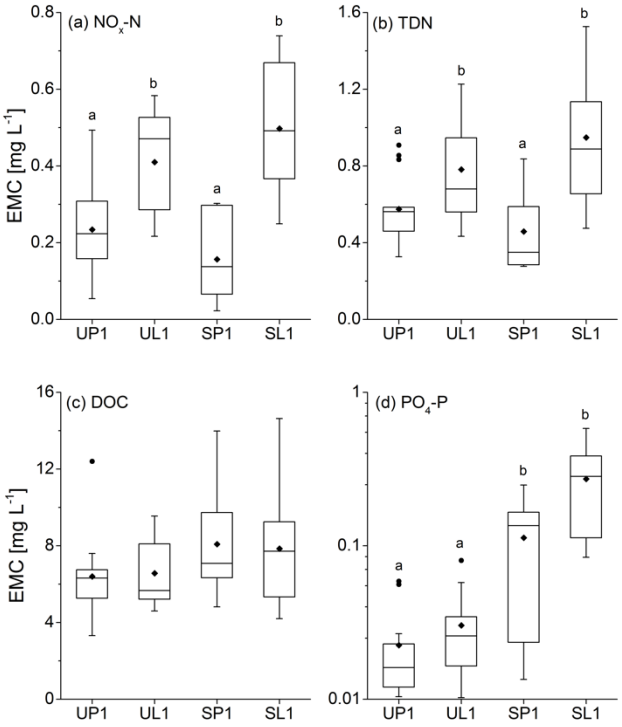

Figure 3-3: Boxplots of EMC for NO_x-N (a), TDN (b), DOC (c), and PO_4-P (d) at all four sites. The mean value is plotted as a diamond. Different letters above the boxplots in each panel indicate significant differences between sites (ANOVA, $p<0.05$). No significant differences were found between any pairs of sites for DOC. Number of storms at each site was 13 at UP1, 17 at UL1, 7 at SP1 and 11 at SL1

Because the differences among sites in NO_x-N and TDN followed similar patterns, we created exploratory plots of NO_x-N vs. TDN for all individual samples, with the points coded by environmental factors such as discharge at time of measurement, two-day antecedent rainfall, time to peak discharge (if during an event), and season. We found clear seasonal groupings at the sites with lower N concentrations (UP1 and SP1),

compared to the higher N sites (UL1 and SL1) (Figure 3-4). The other factors considered did not display any groupings.

Generally, PO_4-P concentrations during storms were higher at the two suburban sites compared to the two urban sites. One-way ANOVAs with site as the primary factor

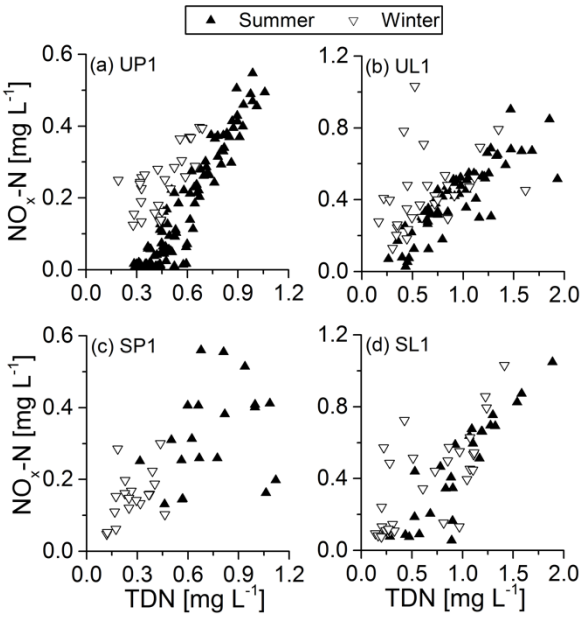

Figure 3-4: Plots of NO_x-N vs. TDN coded by season at UP1 (a), UL1 (b), SP1 (c) and SL1 (d). The low nitrogen sites (UP1 and SP1) show a clear grouping by season while the higher nitrogen sites (UL1 and SL1) do not. Only points occurring during summer (6/21 - 9/21) and winter (12/21 - 3/21) are shown for clarity

revealed significant differences in the means of observed EMC (Figure 3-3). Tukey-HSD tests of C_{MAX} showed the same significant differences between urban and suburban sites, but also detected that C_{MAX} at SL1 was significantly higher than at SP1 (Figure 3-5a). For b, SL1 was significantly higher than the other three sites (Figure 3-5b). As b increases from 1 to infinity, the water volume fraction is exported faster relative to the

PO_4-P mass fraction. Therefore, the PO_4-P export relative to water export was significantly delayed at SL1 compared to the other three sites.

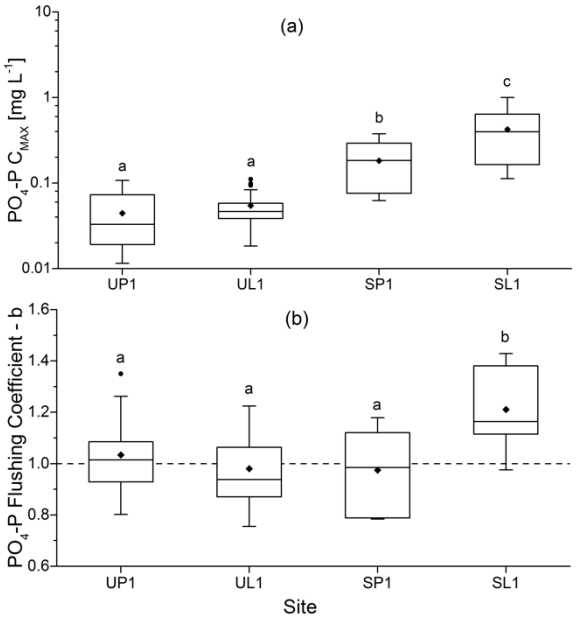

Figure 3-5: Boxplots of C_{MAX} (a) and the b flushing coefficient (b) of PO_4 at each site, with the mean value plotted as a diamond. Note that C_{MAX} is plotted on a log scale in (a). Values greater than 1 in (b) indicate that the fraction of water exported during the storm leads the mass fraction, while values less than one indicate the opposite. Different letters above the boxplots in each panel indicate significant differences between sites (ANOVA, $p<0.05$). Number of storms at each site was 13 at UP1, 17 at UL1, 7 at SP1 and 11 at SL1

3.4.3 Storm event dynamics

We compared solute export patterns during storm events, coupled with end member grabs, to identify when different sources of solutes entered the stream. Here, we present data from two large, back-to-back storms in the month of August that have water quality data with a high temporal resolution and demonstrated chemograph pattern representative of those observed for the other storms (not shown).

3.4.3.1 UP1

The first of the August events selected for hydro-chemograph analysis at UP1 had a peak discharge of 5.8 $m^3 s^{-1} km^{-2}$, which was the largest observed discharge value during the monitored period (Figure 3-6), and was followed by an event occurring approximately 1.25 d later on 8/6/11 with a peak discharge of 0.30 $m^3 s^{-1} km^{-2}$. For NO_x-N and TDN, the 8/5/11 rain event also had the largest observed EMC and C_{MAX} values during the monitoring period. The 8/6/11 rain event, while much smaller, produced the second largest EMC and C_{MAX} values. Generally, NO_x-N and TDN concentrations increased during hydrograph rise, peaked shortly after hydrograph peak, and receded more slowly than they rose after the flood peak (Figure 3-6b and c). SCM outlet (OUT) concentrations of both N species were lower than DS1 during hydrograph rise on 8/5/11, but increased through the storm, possibly elevating above DS1 concentrations during the recession between storms.

DOC export patterns for this event were more variable than N (Figure 3-6d). At DS1, DOC concentrations increased during hydrograph rise, peaked shortly after peak discharge and remained elevated during hydrograph recession. Two pulses in DOC concentration punctuated the general trend during recession of the 8/6/11 event, which also corresponded to elevated concentrations of TDN. DOC concentrations at OUT were near or below DS1 concentrations for all 3 samples, and were lowest shortly after peak flow, when they were 67% of DS1 concentrations.

PO_4-P chemographs mirrored those of the N species with one difference: both the 8/5/11 and 8/6/11 rain events show very high concentrations during the first sample taken on hydrograph rise (Figure 3-6e), which could be evidence for near-stream sources of PO_4-P

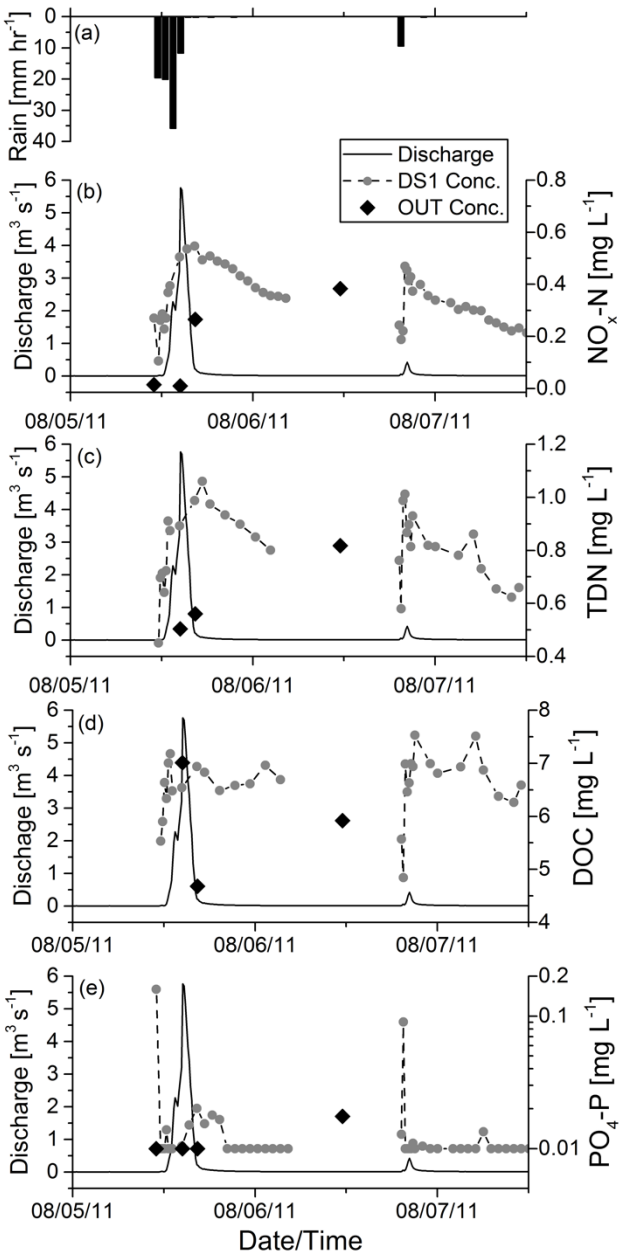

Figure 3-6: Rainfall (a) and resulting hydrograph and chemographs of NO_x-N (b), TDN (c), DOC (d) and PO_4-P (e) at UP1 for two August storms

at UP1. After this initial rise, both events show an elevation in concentration after peak discharge. PO_4-P patterns of OUT water also mirror those of the N species, as they are low at the onset of the event and enrich during the hydrologic event as the SCM releases new urban runoff.

3.4.3.2 UL1

At UL1, the first of two hydrologic events, occurring on 8/5/11, was also the largest observed storm event during the period of record with a peak discharge of 3.6 $m^3 s^{-1} km^{-2}$ (Figure 3-7). Although nearly adjacent to UP1, the hydrology of the 8/5/11 event was slightly more complicated with two distinct pulses of water, possibly reflecting the dynamics of the two stream branches that join at the watershed outlet. Export patterns of NO_x-N and TDN both showed concentrations that increased during hydrograph rise and decreased during hydrograph recession during the first pulse (Figures 3-7b and c). However, during the second, larger discharge pulse, concentrations increased during hydrograph recession. NO_x-N concentrations during this event were negatively correlated ($r = -0.58$) to discharge, which could indicate a dilution effect. DOC concentrations mirrored those of TDN during the first event (Figure 3-7d).

The 8/6/11 event was similar to other events sampled (not shown) in that NO_x-N increased during hydrograph rise, peaked slightly after, and receded to pre-event levels. Concentrations of PO_4-P remained below detection (0.01 mg-P/L) during both flood pulses (Figure 3-7e). However, during hydrograph recession on 8/5/11, PO_4-P

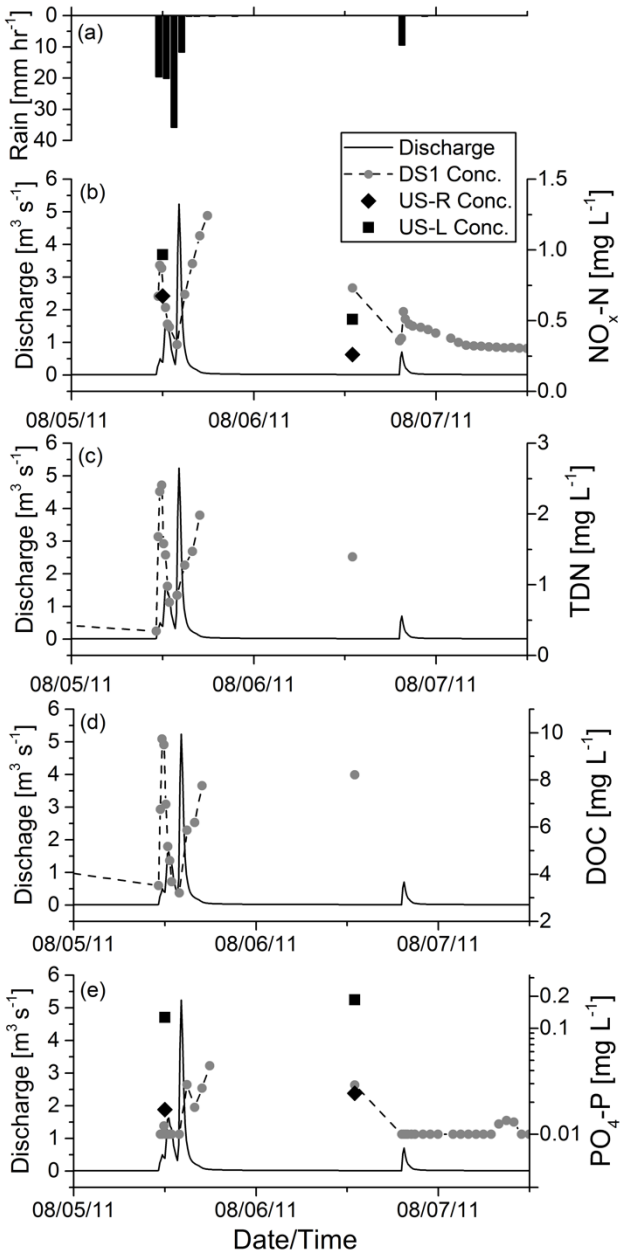

Figure 3-7: Rainfall (a) and resulting hydrograph and chemographs of NO_x-N (b), TDN (c), DOC (d) and PO_4-P (e) at UL1 for two August storms. DOC and TDN samples were not processed for the 8/6/11 event because the analyzer was temporarily out of service

concentrations rose and remained elevated until the onset of the next rain event on 8/6/11. Again, concentrations remained below detection until after the discharge peak.

Paired samples from US-R (with SCMs) and US-L (without SCMs) were collected during rise of the 8/5/11 event and approximately 7 hr before the start of the 8/6/11 event. NO_x-N concentrations at US-R (SCM-influenced) were lower than US-L, whereas the opposite was observed for PO_4-P. The first of two paired samples bracketed DS1 NO_x-N concentrations during hydrograph rise, but measured concentrations between the 8/5/11 and 8/6/11 events were lower than observed in-stream values, which suggests that the SCM may be a source of NO_x-N during hydrograph recession. PO_4-P concentrations were higher at US-L than US-R and DS1.

3.4.3.3 SP1

At the two suburban sites, we plotted a single event with two unique hydrograph pulses occurring on 8/6/12 and 8/7/12. At SP1, the second discharge peak of 0.15 $m^3 s^{-1} km^{-2}$ was the larger of the two, and was the 5th largest hydrologic event observed during the study period (Figure 3-8). We observed similar patterns for all four solutes: concentrations rose during both discharge pulses, peaked at or near peak discharge, then receded during hydrograph recession. In all cases, the peak concentration was higher during the first pulse than the second, and the difference in peak concentrations was greater for NO_x-N (Figure 3-8b) and TDN (Figure 3-8c) than for DOC (Figure 3-8d) and PO_4-P (Figure 3-8e). This could indicate that the N sources had been exhausted by the time of the second storm pulse.

Paired concentrations of the OUT and US end member concentrations were more similar on the rise of the first hydrograph pulse than they were on the recession of the second.

Both of the recession pairs had higher concentrations at OUT than at US, and the end member concentrations typically bounded the DS1 concentrations.

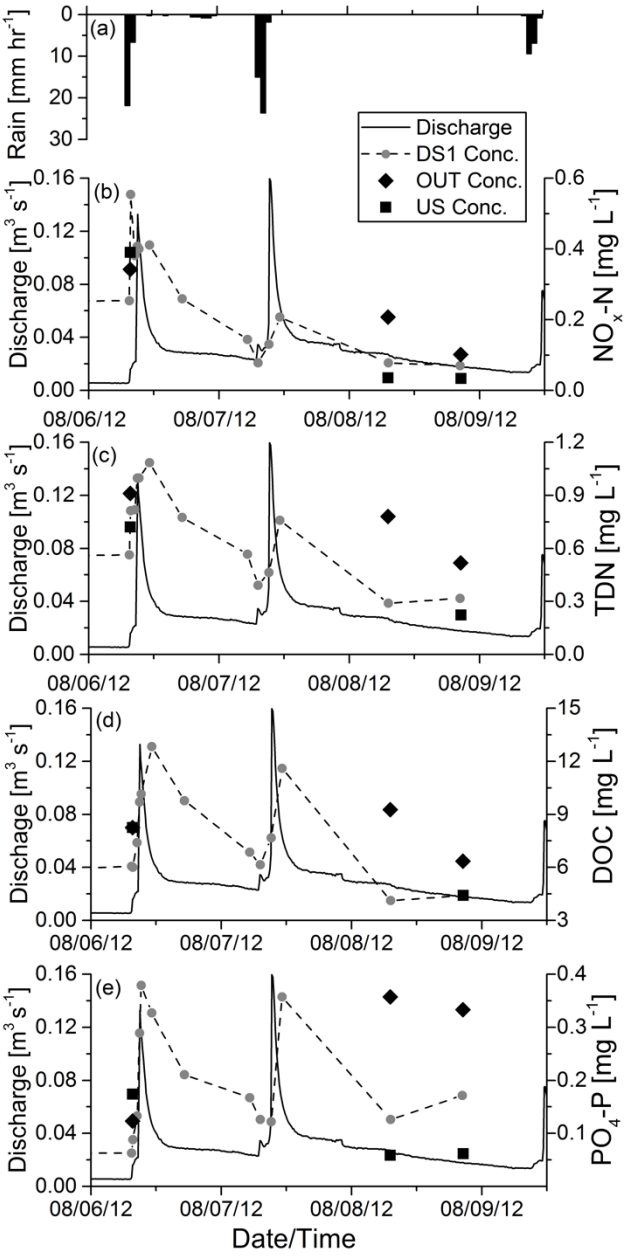

Figure 3-8: Rainfall (a) and resulting hydrograph and chemographs of NO_x-N (b), TDN (c), DOC (d) and PO_4-P (e) at SP1 for one August storm with two peaks

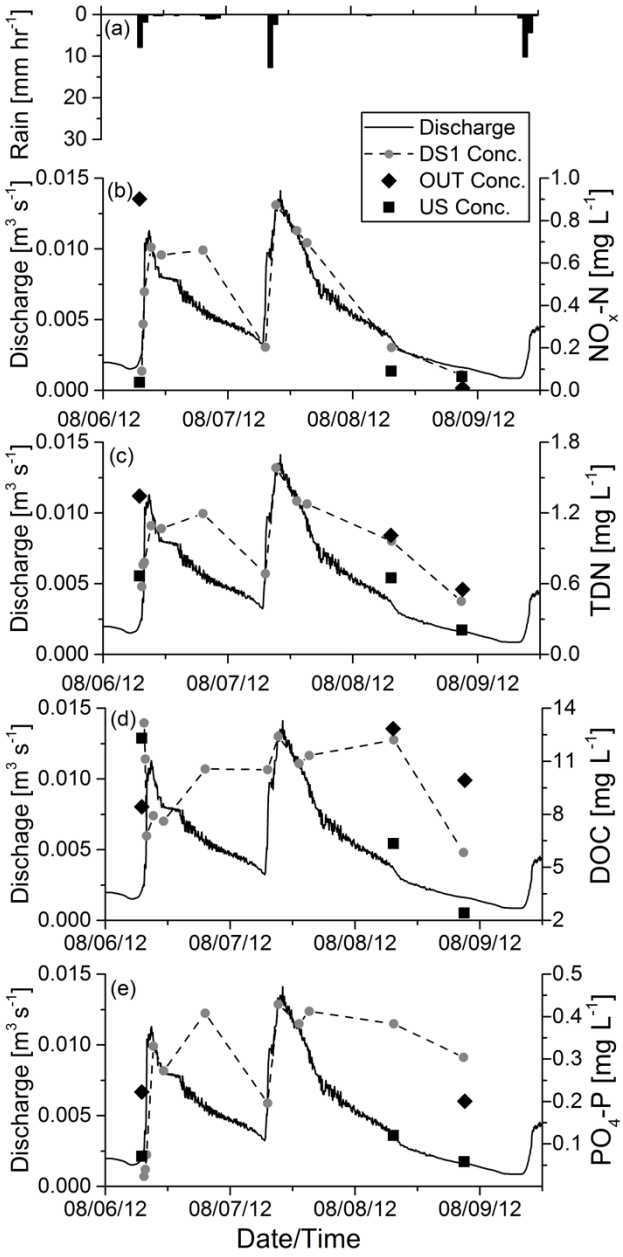

Figure 3-9: Rainfall (a) and resulting hydrograph and chemographs of NO_x-N (b), TDN (c), DOC (d) and PO_4-P (e) at SL1 for one August storm with two peaks.

3.4.3.4 SL1

At SL1, the same rain event as at SP1 was plotted. At SL1, this event also produced two distinct peaks. The second discharge peak of 0.093 $m^3\ s^{-1}\ km^{-2}$ was again the higher of

the two pulses, and was the 4th highest discharge observed (Figure 3-9). As with SP1, all four solutes behaved similarly. First, concentrations increased during rise of the first hydrograph pulse and then began to decline during hydrograph recession. However, this decline was punctuated by a single sample with high concentration of all solutes. When the second event began, concentrations increased with discharge and declined after the hydrograph peak. An exception to this pattern was observed for DOC, where the first sample taken on the rising limb was highest of all observed samples (Figure 3-9d). End member pairs typically showed that OUT concentrations were greater than US, and that DS1 concentrations fell in between the two.

3.4.4 Isolating SCM effects

To further explore the influence of SCMs on stream concentrations, we compared water samples taken synchronously at the OUT and DS1 cross-sections across the entire sampling period. For UL1, the outlet could not be sampled directly, so samples taken from the SCM-mitigated US-R tributary were used as previously described in Section 3.1.2. Water sampled from OUT (UP1, SP1 and SL1) and US-R (UL1) is collectively referred to as the SCM sample. The average time difference between the paired samples was 15.2 min at UP1, 5.38 min at UL1, 9.25 min at SP1, and 18.6 min at SL1.

Generally, the results show that in-stream solute concentrations decreased downstream of the SCM confluence at the urban sites, but increased at the suburban sites. At both urban sites, mean NO_x-N concentrations were significantly lower in the SCM effluent compared to in-stream (Figure 3-10a). At the suburban sites, the mean NO_x-N concentrations in

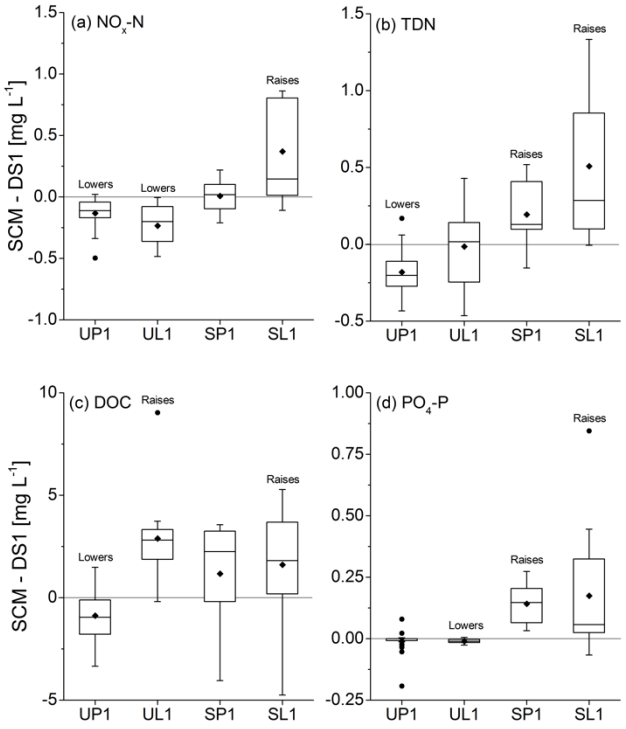

Figure 3-10: Boxplots showing the difference of concentrations of NO_x-N (a), TDN (b), DOC (c), and PO_4-P (d) for all paired samples of SCM water and stream at DS1. Observed differences greater than 0 indicate that SCMs raised solute concentrations in the stream downstream of the confluence, while those below 0 indicate that SCMs lowered solute concentrations in the stream downstream of the confluence. Because the outlet of the monitored SCM at UL1 could not be sampled directly, the paired samples are between the mitigated US-R tributary and the mixture of the mitigated and unmitigated tributaries at DS1. If the mean of the differences were significantly greater than zero (paired t-test, $p<0.05$), they are marked with "raises" to show that SCMs increased concentrations relative to the stream concentrations, while if they were significantly less than zero they are marked with "lowers". Number of paired samples at each site varied with each solute, but was from 24-33 at UP1, 12-16 at UL1, 8-9 at SP1 and 11-17 at SL1.

SCM water were not different than in-stream at SP1, but were significantly higher at SL1. Average TDN concentrations in SCM water were significantly lower than in-stream at UP1, not different at UL1 and higher than in-stream at the suburban sites (Figure 3-10b). Differences in DOC concentrations corresponded to SCM type with higher concentrations in SCM water at the wetland sites (UL1 and SL1), but no difference at SP1 and reduced concentrations at UP1 (Figure 3-10c). We observed greater PO_4-P

concentrations in SCM water compared to DS1 at all suburban sites and either lower (UL1) or similar (UP1) concentrations in the urban sites (Figure 3-10d).

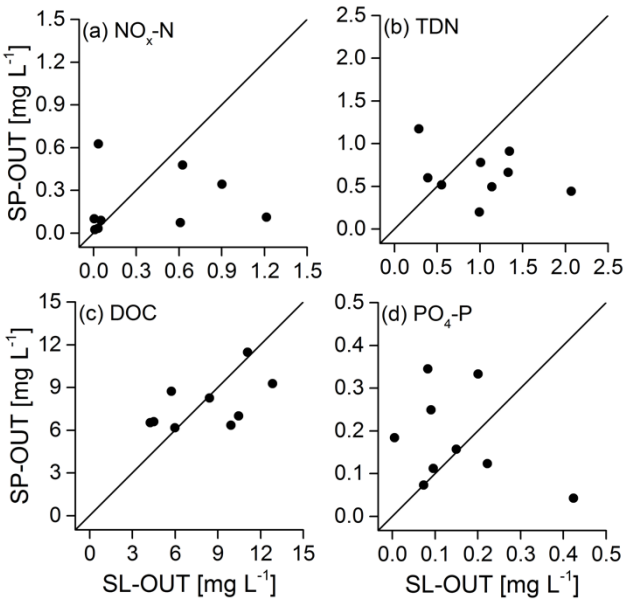

Figure 3-11: Temporally paired samples taken at SP-OUT vs. SL-OUT for NO_X-N (a), TDN (b), DOC (c), and PO_4-P (d). Because the land use draining into both the wet pond SCM (SP-OUT) and wetland SCM (SL-OUT) is similar and the samples were taken at the same time, variation away from the one-to-one line can be attributed to SCM type

To assess the effects of SCM type, we performed a paired t-test on synchronous samples taken at SL-OUT and SP-OUT. Only the suburban outlet pair was used for this analysis because directly sampling the outlet water at UL1 was not possible due to the submerged outlet structure. The average absolute value of time between paired samples taken at SL-OUT and SP-OUT was 43.7 minutes. Because of high variability among the sample pairs, no significant difference between SP-OUT and SL-OUT emerged for any of the solutes. However, patterns of the ratios reveal interesting trends (Figure 3-11). A majority of the data points for TDN fall below the one-to-one line, indicating that this wetland SCMs may produce higher N concentrations, all else being equal. Conversely, most PO_4-P pairs

plot on the SP-OUT side of the one-to-one line, and the DOC pairs cluster tightly around the one-to-one line.

3.5 Discussion

3.5.1 Times of elevated nutrient and carbon export

We found that at the four sites monitored in this study, storm events were important times of nutrient export. Average concentrations in the months of October 2011 and February 2012 were higher during storms that baseflow, and the total mass exported during storms during the intensively sampled month of October 2011 was higher than during baseflow at all sites for all solutes (Figure 3-2). Even in February 2012, which was the 8th driest February on the 72 yr record, stormflow contributed 20-70% of total solute mass exported across all sites and solutes (Figure 3-2). This finding is consistent with results from Baltimore, MD where a majority of the N (NO_x-N and total N) was exported during large flow events (Shields et al. 2008).

Concentration patterns during individual events also underscore the importance of storms as times of increased nutrient export. Concentrations of all solutes peaked at or near the time of peak discharge, and declined during hydrograph recession (Figures 3-6 though 3-9). Our observations of in-stream solute enrichment during storm events agrees with the concentration pattern of an urban watershed in Oregon observed by Poor and McDonnell (2007), who attribute this pattern to solutes accumulating on urban surfaces between storm events and subsequent flushing when it rains. Our results showed that the timing of peak N species concentrations corresponded with peak discharge, which indicates that N

sources are transport limited, and may be derived from the impervious surfaces that contribute during peak discharge. When hydrologic events occurred in rapid succession, concentrations were lower during the second hydrograph pulse. This behavior is possibly due to an exhaustion of the nutrient source from the impervious surfaces, without adequate time to re-accumulate (Figure 3-7). Similarly, Divers et al. (2014) used an isotopic N partition in urban Pittsburgh, PA to show that a greater portion of NO_x in the stream came from atmospheric deposition onto impervious surfaces during storms than during baseflow although the net effect of sewage inputs caused higher concentration during baseflow. These observed patterns contradicted other studies of urban streams. Hook and Yeakley (2005) showed that TDN concentrations in an urban watershed in Oregon were lower during storms than during baseflow because nitrogen enters the stream from either deep groundwater or riparian sources which contribute a larger portion of water during dry periods.

A notable exception to the accumulation and flushing pattern in our study was observed in the PO_4-P chemographs. Although concentrations were low and frequently below detection, PO_4-P concentrations tended to peak after the time of peak discharge. This delay of PO_4-P could be due to the fact that it is derived primarily from slower flow paths. For example, if the PO_4-P comes from soil stores or fertilizer applied to pervious areas, it would likely arrive in the stream later than PO_4-P deposited onto the hydrologically closer impervious surfaces. Despite this time lag, the pattern still showed a rise in concentrations associated with a rise in discharge. This pattern has been observed in

other studies in suburban areas. For example, Hathaway et al. (2012) also found earlier flushing of dissolved N species compared to PO_4-P in Raleigh, NC.

By design, SCMs affect watershed hydrology most dramatically during or shortly after peak flow during storm events (Jefferson et al. 2015; Roesner et al. 2001). As such, their ability to reduce solute loading and thereby improve nutrient water quality depends on whether or not solutes are exported by pathways engaged during storm events. We observed that storms were important times for export of reactive solutes, which demonstrates that SCMs are hydrologically connected when nutrient concentrations are highest.

In addition to storms acting as times of elevated solute export, seasonality also appeared to play an important role in the timing of solute export. For example, distinct differences in average concentrations of DOC and PO_4-P were observed between the months of October and February. For each site, February DOC concentrations were much greater than during October, both during storm and baseflow periods. These seasonal differences in concentrations led to greater DOC export during the month of February compared to October at all sites, despite storm volumes being less or approximately equal (e.g., October volume was 3% greater than during February at SL1, but DOC export was 33% lower). We hypothesize that the differences are due to the leaching of organic matter from fallen leaves. Leaf fall in the area typically occurs in late October or early November, and the leaves do not reemerge until well after February. Other studies have shown that leaf litter decay leads to increased stream DOC concentrations after season

leaf fall, and this period of leaf decomposition can last into February in North Carolina (Gulis and Suberkropp 2003; Meyer et al. 1998).

The average storm concentrations during the month of October for PO_4-P were higher than storm concentrations in February at each site. These seasonal differences were most dramatic at the two suburban sites, and we attribute this difference to seasonal variations in fertilizer application. Surveys of fertilizer application in both Baltimore, MD and Cary, NC indicate that fertilizer is not applied in the winter, but is applied on or more times between spring and fall (Law et al. 2004; Osmond and Platt 2000). Additionally, empirical studies show that PO_4-P applied to turfgrass leaches rapidly, so it is unlikely that any fall applications contributed during the month of February (Easton et al. 2007; Easton and Martin 2004). In our study watersheds, it likely that lawn fertilizer application continued through the summer until leaf off, elevating PO_4-P concentrations in October. Once application stopped in winter, concentrations decreased.

3.5.2 Land use controls solute sources and how SCMs affect stream concentrations

The distribution and density of land use categories throughout the watersheds were important controls on both the sources and processing of nutrients and carbon. We found that EMC and C_{MAX} of NO_x-N and TDN were significantly higher at the wetland watersheds (UL1 and SL1) than the wet pond watersheds (UP1 and SP1). Several paired samples of SCM outflow at the suburban sites had higher TDN concentrations at the wetland site (SL-OUT) than the wet pond site (SP-OUT), but the difference was not statistically significant. Wetlands typically have more oxic conditions than wet ponds,

which could lead to higher rates of nitrification and lower rates of denitrification, resulting in greater NO_x-N export (Devito et al. 2000; Hefting et al. 2003). However, the in-stream monitoring locations in this study were not solely influenced by a single SCM, but rather all sites were mitigated by two or more SCMs and most included both types of SCMs, which suggests that the SCM classification may not be the primary cause for our observed differences between the site pairs.

SCM type covaried with vegetation coverage: wet pond sites were more vegetated (73% at UP1 and 83% at SP1) compared to the wetland watersheds (57% at UL1 and 64% at SL1), and the difference in N species concentrations may be related to vegetation cover rather than SCM type. Figure 3-4 provides support for an inference that vegetated areas may control water N processing. The plots of NO_x-N vs. TDN at two high N sites (UL1 and SL1) do not separate by season, but the low N sites (UP1 and UL1) do show a seasonal difference. This seasonal difference at the more vegetated sites could be related to varying biological activity during these two times of the year. Bell et al. (In review) showed the importance of urban tree coverage on the annual water balance for 16 watersheds in Charlotte, NC (including the four studied here), which highlights the potential for urban forests to affect runoff volumes and potentially access nutrient rich water in surface and shallow subsurface flowpaths. Indeed, many studies in forested watersheds have shown high N retention (Henderson et al. 1978; Likens 2013; Swank and Vose 1997), which can be tied to biological processes such as N uptake and incorporation of organic matter into soil (Aber et al. 1991). In a comparative study of forested and suburban watersheds, Groffman et al. (2004) observed that a larger portion

of N was retained in a forested watershed (95%) compared to a nearby suburban one (75%) that received similar amounts of atmospheric N deposition. Therefore, we hypothesize that land use factors, particularly nutrient cycling by vegetation, may be a more important control than biogeochemical processes within the SCMs themselves leading to higher nitrogen concentrations.

As with N, land use controlled the concentration of PO_4-P during storm events. The mean values of EMC and C_{MAX} were higher at the suburban sites compare to the urban, where concentrations were often below detection. We attribute this to fertilizer application in the newly-developed residential areas of the suburban watersheds, as increased fertilizer application has been firmly linked to higher P concentrations (La Valle 1975). When comparing our two development categories, it is important to first highlight that increased fertilizer application in urban North Carolina has been negatively correlated to development age and related to property value by a concave downward parabola (Law et al. 2004; Osmond and Platt 2000). Indeed, the two suburban watersheds were approximately 40-50 years newer than the urban, and the value of the residential properties for sale in the suburban watersheds were ~$100,000 higher than those for sale in the urban (Mecklenburg County Register of Deeds 2016). C_{MAX} at SL1 was significantly higher than SP1, which could be due to more fertilizer application per unit area in the SL1 with 100% suburban residential development compared to SP1 with only 9%. The export of PO_4-P during storm events, quantified by the b flushing coefficient, was significantly slower at SL1 compared to SP1, which we attribute to the distribution of residential areas clustered closer to the watershed outlet in SP1, compared

to more evenly distributed throughout SL1. Together, the observed PO_4-P trends indicate that both the extent and location of urban development can affect the magnitude and timing of export during storms.

3.5.3 SCMs change stream solute concentrations

SCMs are key contributors to changes in solute concentrations at the stream-SCM confluence, but the direction of change depends on the land use and level of SCM mitigation. At the two urban sites, the land use upstream of the stream-SCM confluence is very similar to that within the SCM's subwatershed. At these sites, we showed that outflow from SCMs had lower concentrations than in the stream itself, implying that SCMs decrease concentration. Specifically, the SCMs significantly decreased concentrations of NO_x-N, TDN, and DOC at UP1 and NO_x-N and PO_4-P at UL1. Results for these two sites indicate that SCMs decrease concentrations of nutrients and carbon, and have the potential to decrease total mass export by lowering concentrations and decreasing flow volumes. Because land use in the SCM watersheds is similar to that of the rest of the watershed (e.g., the UP-OUT drainage area and UP1 have similar land use and impervious cover, see Figure 3-1 and Table 3-1), we assert that solute loading and processing is similar, and therefore the SCMs directly impact and decrease in-stream concentrations. This is supported by other studies that have demonstrated the ability for a single SCM to reduce decrease concentrations from urban runoff (Collins et al. 2010; Geosyntec Consultants and Wright Water Engineers 2012; Hunt et al. 2008; Kearney et al. 2013; Koch et al. 2014; Mallin et al. 2002). At larger scale, when comparing two

residential neighborhoods, Dietz and Clausen (2008) found that including smaller, distributed SCMs decreased total N and total P export relative to a neighborhood without SCMs. However, they did not report if these reductions were due to the observed decreases in runoff volume, or if stream concentrations also decreased.

In contrast, at the two suburban sites, the SCMs were found to increase in-stream solute concentrations, but the effects of the SCMs are difficult to disentangle from the watershed-scale effects (e.g., land use, distribution of impervious surfaces). At SP1, the addition of area mitigated by SCMs corresponded to the addition of urban surfaces to a mostly forested watershed. Indeed, the impervious cover fraction for the SP-OUT watershed is more than twice that of the entire SP1 watershed (Table 3-1). Therefore, we are unable to empirically separate the effects of SCMs from the addition of urban land use. The net result, however, was significant increases in TDN and PO_4-P below the stream-SCM confluence. At SL1, the land use upstream of the stream-SCM confluence is similar to the land use in the SCM watershed (Table 3-1, Figure 3-1), but this upstream area was also fully mitigated by SCMs. In fact, the upstream urban surfaces were mitigated by two SCMs, one of which was a pond that had so much storage capacity, that it rarely contributed to storm flow. This implies that the upstream water during storms at this site was not urban surface runoff but rather it came from the same sources as during periods of baseflow. Therefore, at SL1 we also attribute the increase in concentration from SCM water due to the addition of urban surface runoff, in a way similar to SP1. Together, results from the suburban sites show that even if SCMs are able to lower

outflow concentrations relative to inflow, the addition of nutrients from urban surfaces can outweigh these benefits, and ultimately increase in-stream concentrations.

3.6 Conclusions

We analyzed nutrient (NO_x-N, TDN and PO_4-P) and carbon (DOC) concentrations from two urban and two suburban watersheds in Charlotte, NC to determine if SCMs were able to change the water quality in stream ecosystems downstream of the stream-SCM confluence. The ability of SCM's to change stream concentrations has implications for protecting local stream ecosystems and downstream lakes and estuaries by reducing total mass loading. We showed that storm events were key times of nutrient and carbon export, both because concentrations increased during storms and because a large fraction of water volume and nutrient mass was exported during storms. This has important implications for the effectiveness of the SCMs in these watersheds, as they contribute most significantly to runoff during and after times of elevated discharge (Jefferson et al. 2015). We also found that seasonality is an important control on concentrations of DOC PO_4 due to leaf fall and decay and fertilizer application, respectively.

We also found that SCMs change stream water quality throughout storms, although the direction of this transformation depended on the spatial distribution of developed surfaces and SCMs in the watershed. In the urban watersheds, SCMs reduced in-stream concentrations immediately downstream. In these watersheds, land use in the area drained by the SCMs was comparable to that throughout the remainder of the watershed. However, in the suburban watersheds, the land use drained by the SCM at the watershed

outlet had significantly more runoff-contributing urban area than the rest of the watershed, resulting in elevated concentrations downstream of the SCM confluence. As a result, even if individual SCMs decrease watershed-derived nutrients, SCM outflow can locally increase stream solute concentrations because their presence corresponds to the addition of urban surfaces with greater nutrient sources. Collectively, these results imply that retrofitting SCMs in urban watersheds will decrease concentrations of nutrients and carbon in the stream at the watershed outlet, but new urban development accompanied by SCMs may increase stream concentrations.

We observed differences in in-stream N concentrations based on SCM type, however these were confounded by land use. TDN and NO_x-N concentrations were lower at wet pond sites but these were also the watersheds with more forest cover. The type of SCM may influence N transformation rates within the SCM as wetland redox conditions could lead to elevated rates of nitrification and suppressed denitrification compare to wet ponds. Additionally, forested soils may stimulate soil respiration and biological N assimilation resulting in greater N retention in watersheds with greater forested areas. While selection of SCM type (e.g., wetland vs wet pond) and design of the system (e.g., residence time, volume retention) will likely influence nutrient cycling with the SCM, our results also suggest that preserving forested areas within the watershed may be an important strategy to reduce N concentrations in urban streams.

PO_4-P concentrations were higher in the suburban sites with newly-developed residential areas, which likely receive more P from fertilizer. Additionally, clustering urban surfaces

near the outlet caused faster export of PO_4-P relative to water, suggesting that the spatial distribution of fertilized areas affected the timing the PO_4-P export during storms. Source reduction through the use of P-free fertilizers in lawns may be an effective strategy for limiting PO_4-P export form these watersheds.

3.7 References

Aber JD, Melillo JM, Nadelhoffer KJ, Pastor J, Boone RD (1991) Factors Controlling Nitrogen Cycling and Nitrogen Saturation in Northern Temperate Forest Ecosystems. Ecol Appl 1:303-315 doi:10.2307/1941759

Aitkenhead-Peterson JA, Steele MK, Nahar N, Santhy K (2009) Dissolved organic carbon and nitrogen in urban and rural watersheds of south-central Texas: land use and land management influences. Biogeochemistry 96:119-129 doi:10.1007/s10533-009-9348-2

American Public Health Association (APHA), American Water Works Association (AWWA), Water Environment Federation (WEF) (2005) Standard Methods for the Examination of Water and Wastewater, 21st Edition.

Bedan ES, Clausen JC (2009) Stormwater Runoff Quality and Quantity From Traditional and Low Impact Development Watersheds1. J Am Water Resour As 45:998-1008 doi:10.1111/j.1752-1688.2009.00342.x

Bell CD, McMillan SK, Clinton SD, Jefferson AJ (In review) Hydrological Response to Stormwater Control Measures in Urban Watersheds. J Hydrol

Bernhardt ES, Band LE, Walsh CJ, Berke PE (2008) Understanding, managing, and minimizing urban impacts on surface water nitrogen loading. Ann NY Acad Sci 1134:61-96

Bertrand-Krajewski J-L, Chebbo G, Saget A (1998) Distribution of pollutant mass vs volume in stormwater discharges and the first flush phenomenon. Water Res 32:2341-2356 doi:http://dx.doi.org/10.1016/S0043-1354(97)00420-X

Boström B, Andersen J, Fleischer S, Jansson M (1988) Exchange of Phosphorus Across the Sediment-Water Interface. In: Persson G, Jansson M (eds) Phosphorus in Freshwater Ecosystems, vol 48. Developments in Hydrobiology. Springer Netherlands, pp 229-244. doi:10.1007/978-94-009-3109-1_14

Brauman KA, Daily GC, Duarte TKe, Mooney HA (2007) The nature and value of ecosystem services: an overview highlighting hydrologic services. Annu Rev Environ Resour 32:67-98

Charlotte-Mecklenburg Stormwater Services (CMSWS) (2013) Charlotte-Mecklenburg BMP Design Manual (Revised Edition).

Collins KA et al. (2010) Opportunities and challenges for managing nitrogen in urban stormwater: A review and synthesis. Ecol Eng 36:1507-1519 doi:http://dx.doi.org/10.1016/j.ecoleng.2010.03.015

Devito KJ, Fitzgerald D, Hill AR, Aravena R (2000) Nitrate Dynamics in Relation to Lithology and Hydrologic Flow Path in a River Riparian Zone. J Environ Qual 29 doi:10.2134/jeq2000.00472425002900040007x

Diehl TH (2008) A Modified Siphon Sampler for Shallow Water. US Geological Survey Scientific Investigations Report 2007-5282

Dietz ME, Clausen JC (2008) Stormwater runoff and export changes with development in a traditional and low impact subdivision. J Environ Manage 87:560-566 doi:http://dx.doi.org/10.1016/j.jenvman.2007.03.026

Divers MT, Elliott EM, Bain DJ (2014) Quantification of Nitrate Sources to an Urban Stream Using Dual Nitrate Isotopes. Env Sci Tech 48:10580-10587 doi:10.1021/es404880j

Duan S, Kaushal SS, Groffman PM, Band LE, Belt KT (2012) Phosphorus export across an urban to rural gradient in the Chesapeake Bay watershed. J Geophys Res-Biogeo 117:G01025 doi:10.1029/2011jg001782

Duncan JM, Groffman PM, Band LE (2013) Towards closing the watershed nitrogen budget: Spatial and temporal scaling of denitrification. J Geophys Res-Biogeo 118:1105-1119 doi:10.1002/jgrg.20090

Easton ZM, Gérard-Marchant P, Walter MT, Petrovic AM, Steenhuis TS (2007) Identifying dissolved phosphorus source areas and predicting transport from an urban watershed using distributed hydrologic modeling. Water Resour Res 43:n/a-n/a doi:10.1029/2006WR005697

Easton ZMP, Martin A (2004) Fertilizer source effect on ground and surface water quality in drainage from turfgrass. J Environ Qual 33:645

Gagrani V, Diemer JA, Karl JJ, Allan CJ (2014) Assessing the hydrologic and water quality benefits of a network of stormwater control measures in a SE U.S. Piedmont watershed. J Am Water Resour As 50:128-142 doi:10.1111/jawr.12121

Geosyntec Consultants I, Wright Water Engineers I (2012) International Stormwater Best Management Practices (BMP) Database Pollutant Category Summary Statistical Addendum: TSS, Bacteria, Nutrients, and Metals.

Groffman PM, Boulware NJ, Zipperer WC, Pouyat RV, Band LE, Colosimo MF (2002) Soil Nitrogen Cycle Processes in Urban Riparian Zones. Env Sci Tech 36:4547-4552 doi:10.1021/es020649z

Groffman PM, Law NL, Belt KT, Band LE, Fisher GT (2004) Nitrogen fluxes and retention in urban watershed ecosystems. Ecosystems 7:393-403

Gulis V, Suberkropp K (2003) Leaf litter decomposition and microbial activity in nutrient-enriched and unaltered reaches of a headwater stream. Freshwater Biol 48:123-134 doi:10.1046/j.1365-2427.2003.00985.x

Hale R, Turnbull L, Earl S, Childers D, Grimm N (2015) Stormwater Infrastructure Controls Runoff and Dissolved Material Export from Arid Urban Watersheds. Ecosystems 18:62-75 doi:10.1007/s10021-014-9812-2

Hathaway JM, Tucker RS, Spooner JM, Hunt WF (2012) A Traditional Analysis of the First Flush Effect for Nutrients in Stormwater Runoff from Two Small Urban Catchments. Water Air Soil Poll 223:5903-5915 doi:10.1007/s11270-012-1327-x

Hatt BE, Fletcher TD, Walsh CJ, Taylor SL (2004) The Influence of Urban Density and Drainage Infrastructure on the Concentrations and Loads of Pollutants in Small Streams. Environ Manage 34:112-124 doi:10.1007/s00267-004-0221-8

Hefting MM, Bobbink R, de Caluwe H (2003) Nitrous Oxide Emission and Denitrification in Chronically Nitrate-Loaded Riparian Buffer Zones. J Environ Qual 32 doi:10.2134/jeq2003.1194

Henderson GS, Swank WT, Waide JB, Grier CC (1978) Nutrient Budgets of Appalachian and Cascade Region Watersheds: A Comparison. Forest Sci 24:385-397

Hook A, Yeakley JA (2005) Stormflow Dynamics of Dissolved Organic Carbon and Total Dissolved Nitrogen in a Small Urban Watershed. Biogeochemistry 75:409-431 doi:10.1007/s10533-005-1860-4

Hunt WF, Smith J, Jadlocki S, Hathaway J, Eubanks P (2008) Pollutant Removal and Peak Flow Mitigation by a Bioretention Cell in Urban Charlotte, N.C. J Environ Eng-ASCE 134:403-408 doi:doi:10.1061/(ASCE)0733-9372(2008)134:5(403)

Jefferson AJ, Bell CD, Clinton SM, McMillan SK (2015) Application of isotope hydrograph separation to understand contributions of stormwater control measures to urban headwater streams. Hydrol Process 29:5290-5306 doi:10.1002/hyp.10680

Kearney MA, Zhu W, Graney J (2013) Inorganic nitrogen dynamics in an urban constructed wetland under base-flow and storm-flow conditions. Ecol Eng 60:183-191 doi:http://dx.doi.org/10.1016/j.ecoleng.2013.07.038

Koch BJ et al. (2015) Suburban watershed nitrogen retention: Estimating the effectiveness of stormwater management structures. Elementa-Sci Anthropoc 3:000063

Koch BJ, Febria CM, Gevrey M, Wainger LA, Palmer MA (2014) Nitrogen Removal by Stormwater Management Structures: A Data Synthesis. J Am Water Resour As 50:1594-1607 doi:10.1111/jawr.12223

La Valle PD (1975) Domestic sources of stream phosphates in urban streams. Water Res 9:913-915 doi:http://dx.doi.org/10.1016/0043-1354(75)90041-X

Law N, Band L, Grove M (2004) Nitrogen input from residential lawn care practices in suburban watersheds in Baltimore County, MD. J Environ Plann Man 47:737-755

Leopold LB (1968) Hydrology for urban land planning: A guidebook on the hydrologic effects of urban land use. USGS Circular 554

Lewis DB, Grimm NB (2007) Hierarchical regulation of nitrogen export from urban catchments: Interactions of storms and landscapes. Ecol Appl 17:2347-2364 doi:10.1890/06-0031.1

Likens GE (2013) Biogeochemistry of a forested ecosystem. 3 edn. Springer-Verlag, New York

Mallin MA, Ensign SH, Wheeler TL, Mayes DB (2002) Pollutant Removal Efficacy of Three Wet Detention Ponds. J Environ Qual 31:654-660 doi:10.2134/jeq2002.6540

Mecklenburg County Register of Deeds (2016) http://meckrod.manatron.com/. Accessed 12/2015

Mecklenburg County GIS (2013) 2012 Mecklenburg County Tree Canopy / Landcover. http://maps.co.mecklenburg.nc.us/openmapping/data.html. Accessed June 2015

Meyer LJ, Wallace BJ, Eggert LS (1998) Leaf Litter as a Source of Dissolved Organic Carbon in Streams. Ecosystems 1:240-249 doi:10.1007/s100219900019

O'Driscoll M, Clinton SM, Jefferson AJ, Manda A, McMillan SK (2010) Urbanization effects on watershed hydrology and in-stream processes in the Southern United States. Water 2:605-648

Osmond DL, Platt JL (2000) Characterization of suburban nitrogen fertilizer and water use on residential turf in Cary, North Carolina. HortTechnology 10:320-325

Passeport E et al. (2013) Ecological Engineering Practices for the Reduction of Excess Nitrogen in Human-Influenced Landscapes: A Guide for Watershed Managers. Environ Manage 51:392-413 doi:10.1007/s00267-012-9970-y

Paul MJ, Meyer JL (2001) Streams in the urban landscape. Ann Rev Ecol Syst:333-365

Perniel M, Ruan R, Martinez B (1998) Nutrient removal from a stormwater detention pond using duckweed. Appl Eng Agric 14:605-609

Petrone KC (2010) Catchment export of carbon, nitrogen, and phosphorus across an agro-urban land use gradient, Swan-Canning River system, southwestern Australia. J Geophys Res-Biogeo 115:n/a-n/a doi:10.1029/2009JG001051

Poor CJ, McDonnell JJ (2007) The effects of land use on stream nitrate dynamics. J Hydrol 332:54-68 doi:http://dx.doi.org/10.1016/j.jhydrol.2006.06.022

R Core Team (2013) R: A language and environment for statistical computing. R Foundation for Statistical Computing, Vienna, Austria

Roesner L, Bledsoe B, Brashear R (2001) Are best-management-practice criteria really environmentally friendly? Journal of Water Resources Planning and Management 127:150-154 doi:doi:10.1061/(ASCE)0733-9496(2001)127:3(150)

Selbig WR, Bannerman RT (2008) A Comparison of Runoff Quantity and Quality from Two Small Basins Undergoing Implementation of Conventional and Low-Impact-Development (LID) Strategies: Cross Plains, Wisconsin, Water Years 1999-2005.

Shields CA et al. (2008) Streamflow distribution of non-point source nitrogen export from urban-rural catchments in the Chesapeake Bay watershed. Water Resour Res 44:W09416

Sickman JO, Zanoli MJ, Mann HL (2007) Effects of Urbanization on Organic Carbon Loads in the Sacramento River, California. Water Resour Res 43:n/a-n/a doi:10.1029/2007WR005954

Smart MM, Jones JR, Sebaugh JL (1985) Stream-Watershed Relations in the Missouri Ozark Plateau Province1. J Environ Qual 14:77-82 doi:10.2134/jeq1985.00472425001400010015x

State Office of Nort Carolina - CRONOS (2013) http://www.nc-climate.ncsu.edu/cronos/. Accessed 4 April 2013

Swank WT, Vose JM (1997) Long-term nitrogen dynamics of Coweeta Forested Watersheds in the southeastern United States of America. Global Biogeochem Cy 11:657-671 doi:10.1029/97GB01752

Taylor GD, Fletcher TD, Wong THF, Breen PF, Duncan HP (2005) Nitrogen composition in urban runoff—implications for stormwater management. Water Res 39:1982-1989 doi:http://dx.doi.org/10.1016/j.watres.2005.03.022

Toet C, Hvitved-Jacobsen T, Yousef YA (1990) Pollutant Removal and Eutrophication in Urban Runoff Detention Ponds. Water Sci Technol 22:197-204

Vidon P, Hubbard LE, Soyeux E (2009) Seasonal solute dynamics across land uses during storms in glaciated landscape of the US Midwest. J Hydrol 376:34-47 doi:http://dx.doi.org/10.1016/j.jhydrol.2009.07.013

Walker WW (1985) Urban nonpoint source impacts on a surface water supply.

Walker WW (1987) Phosphorous removal by urban runoff detention basins. Lake Reserv Manage 3:314-326 doi:10.1080/07438148709354787

Walsh CJ, Fletcher TD, Ladson AR (2005) Stream restoration in urban catchments through redesigning stormwater systems: looking to the catchment to save the stream. J N Am Benthol Soc 24:690-705 doi:10.1899/04-020.1

Waschbusch R, Selbig W, Bannerman R (1994) Sources of phosphorus in stormwater and street dirt from two urban residential basins in Madison. Wisconsin 95:1999

Winter JG, Duthie HC (2000) Export coefficient modeling to asses phosphorus loading in an urban watershed. J Am Water Resour As 36:1053-1061 doi:10.1111/j.1752-1688.2000.tb05709.x

CHAPTER 4. A MODEL OF HYDROLOGY AND WATER QUALITY IN STORMWATER CONTROL MEASURES

4.1 Abstract

The impervious surfaces, efficient drainage networks, and increased loading of urban watersheds causes increased water runoff and nitrogen (N) export which lead to eutrophication in downstream river and estuary ecosystems. Stormwater control measures (SCMs), such as wet ponds, are a management strategy that can reduce runoff and N export by providing additional water storage and by creating an ecosystem that promotes N retention and removal. This work develops and explores a computer model that simulates hydrologic and water quality processes of SCMs. The SCM model is incorporated into RHESSys, a watershed hydro-ecological model, so it can be used to answer questions about the function of SCMs across scales from individual SCMs to whole watersheds. Data from a wet pond SCM in Charlotte, NC was used for model calibration and validation. The hydrologic component of the SCM model successfully simulated distributions of observed storm event outflow volumes and duration without any calibration. Through calibration, the model simulated distributions of observed outflow concentrations of both nitrate (NO_3) and ammonium (NH_4). A global sensitivity analysis highlighted the five water quality parameters that should be targeted during calibration when applying the model to other regions or during future empirical studies to

restrict model parameter uncertainty. Finally, the model simulated changes in inorganic N removal under varying hydrometeorological conditions, N loading, and SCM design scenarios. Simulations show that increasing air temperatures by 10°C can increase removal efficiency of NO_3 from 0.52 to 0.61and NH_4 from 0.56 to 0.66. Mass removal of NH_4 was insensitive to changes in inflow N concentrations, but removal of NO_3 decreased under higher N loading simulations. Finally, results showed that deeper SCMs have greater inorganic N removal efficiencies because they have more stored volume of relatively N-deplete water, and therefore a greater capacity to dilute relatively N-rich inflow. This emphasizes the importance of this design parameter, but also the importance of N-uptake between events which can lower SCM concentrations before storms, and thus intensify the dilution process.

4.2 Introduction

The urbanization of undeveloped watersheds causes increased rainfall runoff and mass export of nitrogen (N) (Leopold, 1968; Peierls et al., 1991; Howarth et al., 1996). Reductions in transpiration, groundwater recharge, and temporary storage from the replacement of vegetation with impervious surfaces are the causes of increased runoff volumes (Dunne and Leopold, 1978; Arnold and Gibbons, 1996; Bell et al., In review). N loading to urban watersheds is elevated from imported food, fertilizer, and heightened atmospheric deposition (Bernhardt et al., 2008). This additional N load is not efficiently retained or removed by the watershed's biological processes because residence times are reduced by storm drainage networks, notably storm pipes that route water and nutrients

from the upland impervious surfaces directly to the stream, bypassing the riparian zone (Groffman et al., 2002; Groffman et al., 2004; Taylor et al., 2005). Increased water runoff, increased N loading, and decreased N processing cause urban streams to have high N export and contribute to river and coastal eutrophication (Castro et al., 2003).

To reduce urban N export and thus protect downstream aquatic ecosystems, the United States federal government has established the National Pollutant Discharge Elimination System (NPDES) {, 40 CFR Part 122`, 2011 #13}. This program requires that state governments issue permits to municipalities before they are allowed to discharge stormwater runoff into any receiving stream. These NPDES permits usually stipulate targets for reductions in mass loading of a number of solutes, that often include N (Collins et al., 2010).

One way that municipalities can meet the water quality targets is to require that stormwater control measures (SCMs) be included on site at locations of new and re-development to mitigate any hydrologic impacts of the build out. SCMs are depressions in the urban landscape that receive and store rainwater runoff, which provides hydrologic benefits like reductions in runoff volume and peak discharge. Stored water that evaporates between rain events can lead to a reduction in nutrient loads to downstream aquatic ecosystems, as loads are often correlated to runoff volumes (Hale et al., 2015). In addition to reducing runoff volume, SCMs can reduce peak flow by retaining runoff, and slowly releasing it to the stream. This phenomenon, sometimes referred to as peak shaving (Roesner et al., 2001), is accomplished by promoting infiltration and by

restricting surface water outflow though a designed outlet structure. Outlet structures are vertical risers affixed with one or more openings that reduce the rate at which stored water leaves the SCM. The openings are typically orifices or weirs. The elevation and size of riser's openings depends on design goals stipulated by the local stormwater ordinance. Some SCM types, like wet ponds, permanently store surface water to create an aquatic ecosystem that is both functional and aesthetically pleasing. The depth of this permanent pool is based on the elevation of the lowest orifice on the outlet structure. Additionally wet ponds will have an emergency spillway that routes overflow out of the wet pond to the stream during extreme events.

Within SCMs, vegetation and dynamic redox states caused by hydrologic fluctuations create an ecosystem that is a potential hot spot for biogeochemical activity, which can transform or remove nutrients from the water column. Terrestrial vegetation, which populates the perimeter of wet ponds and the entire area of wetlands or bioretention cells, and algae within ponded water assimilate dissolved inorganic N species like ammonium (NH_4) and nitrate (NO_3) and incorporate the molecules into their cell structure. The plants and algae later release this N as organic N during senescence, often stimulated by changing seasons. Collectively, SCMs that facilitate the processes of assimilation and senescence convert inorganic N to organic N. Under aerobic conditions, microbial communities transform NH_4 to NO_3 (i.e., nitrification), which produces energy used by the microbes in ATP synthesis. While these transformation processes are important to nutrient cycling within the SCM, none of them truly remove N from the environment. Denitrification, the energy-yielding conversion of NO_3 to nitrous-oxide (N_2O) or nitrogen

(N_2) gases, is a microbial process that does remove N from the aquatic system. SCMs generally have high concentrations of NO_3, organic carbon (C), reducing conditions, and extended residence times. As such, they are ideal locations to promote removal via denitrification (Collins et al., 2010).

Removal and retention processes within SCMs enable them to reduce the mass of N that is exported relative to inflow (Mallin et al., 2002; Hunt et al., 2008; Collins et al., 2010; Kearney et al., 2013; Koch et al., 2014). The amount of reduction has been demonstrated to vary substantially, and the causes for this variation are attributed to differences in inflow concentrations, climate, land use, location, and SCM properties including size, age, and type (Barrett, 2005; Hunt et al., 2012; Geosynthetic Consultants and Wright Water Engineers, 2014; Koch et al., 2014). Despite this variability, most municipalities assume a single, static removal rate when planning for compliance to their NPDES permit.

Similarly, many of the watershed models currently used for simulation of urban hydrology and water quality do not adequately account for the variability of N removal and retention by SCMs. Many widely-used watershed models simulate hydrologic processes of SCMs and therefore address the advection component of nutrient loading, but do not include any water quality processes within the SCM (e.g., the Environmental Protection Agency's SWMM v. 5.1 and SUSTAIN, see Rossman (2015)). The watershed models that do account for changes in N concentrations, typically only use a first order rate reduction with some irreducible or background concentration (e.g., MUSIC model of Wong et al. (and LTHIA-LID of Ahiablame et al. (2012)). None of

these models account for the dynamic behavior of the SCM ecosystem, and the important controls of seasonality, SCM design, and system memory.

This work addresses these shortcomings by developing a process-based hydrologic and water quality model of a wet pond SCM. The SCM routines are added to a spatially distributed, processed-based hydro-ecological model called the Regional Hydro-Ecological Simulation System (RHESSys) (Tague and Band, 2004). Because RHESSys is spatially distributed, users are able to simulate different configurations of SCMs and urban areas across a landscape. Because the SCM routines are process-based, they are able to simulate changes in N removal efficiency under different environmental conditions and SCM designs. The applications of this novel modeling approach for SCMs are wide reaching as it can be a tool for optimizing design of individual SCMs as well as SCM implementation throughout a watershed to maximize hydrologic and water quality benefits in urban watersheds.

4.3 Methods

A simple realization of RHESSys was used to explore newly-developed model routines of hydrological and ecological processes within SCMs. A global sensitivity analysis was then performed to gain understanding of the system dynamics. The model was calibrated, validated, and parameter uncertainty and sensitivity were quantified. With the model parameter uncertainty constrained, inorganic N retention and removal was quantified within a single SCM under varied environmental forcing and SCM design scenarios.

4.3.1 Overview of the RHESSys model

RHESSys is a community-based research tool, and a number of recent modifications have been made to hydrologic and biogeochemical cycling modules since it was documented by Tague and Band (2004). An hourly timestep version of RHESSys (version 5.19, available online at: https://github.com/RHESSys/RHESSys) was expanded to include the SCM hydrologic and water quality routines. RHESSys is a spatially-explicit, process-based, hydro-ecological model that simulates water, carbon and nitrogen cycling with lateral and vertical redistribution. RHESSys distributes the watershed area into a series of patches, the spatial unit where mass balances of water, carbon and nitrogen are computed. Lateral redistribution of surface and subsurface water between neighboring patches depends on topographic and soil characteristics. All surface water that exceeds the soils storage capacity is routed to one or more downslope patches within one timestep, whereas only a portion of the patch's subsurface water store is routed to the downslope patches. An exponential transmissivity decay model determines the portion of subsurface flow. RHESSys also models vertical redistribution of water through the soil profile, which is discretized into a root zone layer, an unsaturated soil layer, a saturated soil layer, and a deep groundwater layer. Infiltration from the surface into the soil profile follows the Green-Ampt model (Green and Ampt, 1911), and infiltrated water moves vertically through the layers based on hydraulic conductivity and pressure gradient at the boundary of the saturated and unsaturated zones. Water can also move vertically from the root zone layer through vegetation back to the atmosphere via transpiration, simulated

using the Penman-Monteith model (Monteith, 1965). Evaporation from canopy and ground surface detention stores also follows the model of Penman (Monteith, 1965).

RHESSys simulates vegetation and soil carbon and nitrogen cycling similar to dynamic global vegetation models like CTEM, 3PG and Biome-BGC (Running and Hunt, 1993; Landsberg and Waring, 1997; Arora and Boer, 2003). The model includes vegetation litterfall, respiration, assimilation, and the allocation of biomass accumulation through photosynthesis into separate plant physiological components. The vegetation's canopy attenuates radiation following Beer's law. Incoming radiation, which is partitioned into diffuse and direct components, drives photosynthesis at variable rates based on sun exposure and other controls including moisture and nutrient availability. Soil and litter decomposition models are similar those used in Biome-BGC (Running and Hunt, 1993), and nitrification and denitrification follow Century N-GAS (Parton et al., 1996). Other authors have used RHESSys to answer to numerous questions about hydrologic and water quality across ecoregions, and have applied it successfully in urban areas (Tague and Pohl-Costello, 2008; Mittman et al., 2012; Shields and Tague, 2012; Shields and Tague, 2014).

4.3.2 SCM model development

The RHESSys SCM model has two novel components: a hydrologic routing component that simulates the rate of surface water outflow from an SCM patch to downslope patches, and a water quality routine that simulates C and N cycling associated with algae growth,

death, respiration, and settling within the SCM. Figure 4-1 shows these new state variables and fluxes within an SCM.

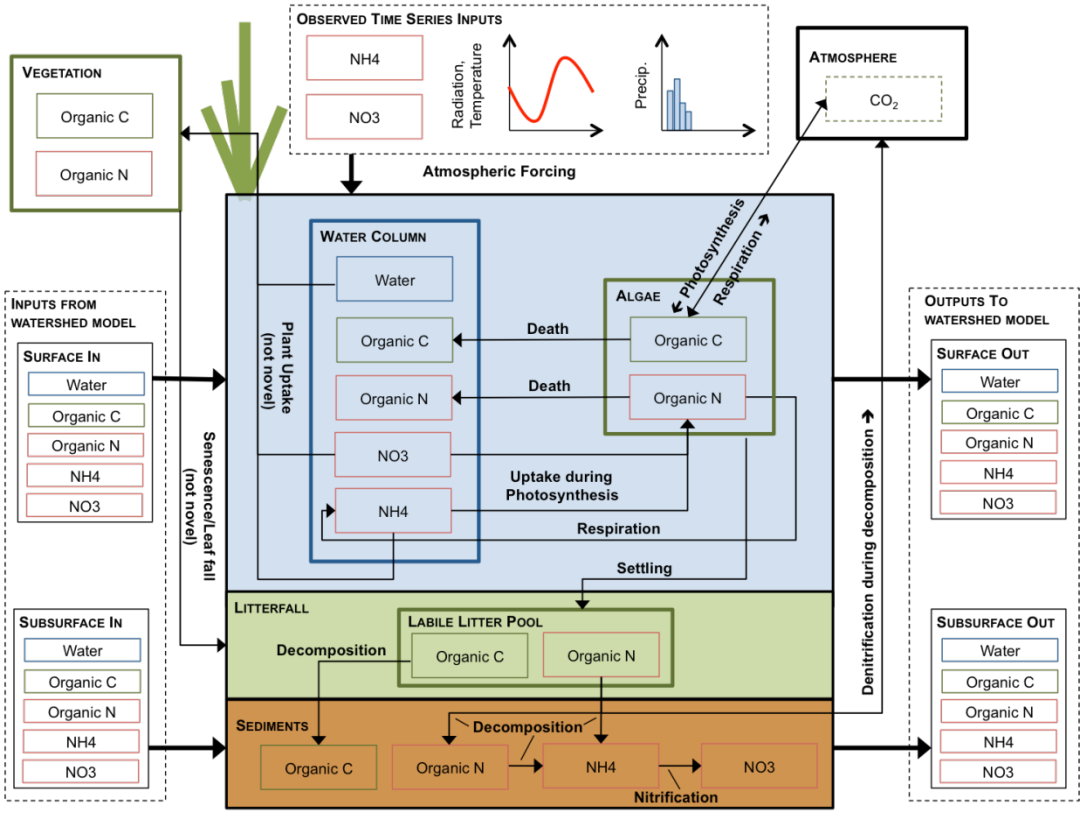

Figure 4-1: Diagram of state variables and fluxes within SCM model, as well as connection of the SCM model to the RHESSys watershed model.

4.3.2.1 Hydrologic routing model

For hydrologic routing, the model assumes the SCM to be rectangular frustum, the design of which is specified by parameters detailing surface area, length to width ratio, side slope, and outlet structure design. Equation 4.1 is used to represent the balance of water in the pond:

$$\frac{dV}{dt} = -E - Q_{out} + Q_{in} - I + PPT \qquad \text{(Eq. 4.1)}$$

where V is the pond volume [m], E = evaporation [m hr^{-1}], Q_{out} is the volume leaving pond [m hr^{-1}], Q_{in} is the volume entering pond [m hr^{-1}], I is infiltration to soil beneath the pond [m hr^{-1}], and PPT is incident precipitation [m hr^{-1}]. The RHESSys watershed model simulates Q_{in} using the surface routing processes described above, and simulates E based on estimates of radiation and windspeed at the SCM surface. PPT is net precipitation computed by subtracting any interception losses by canopy layers above the SCM from a time series input, using existing RHESSys routines that account for both storage and evaporation of intercepted water by canopies. Computation of Q_{out} is done using equations that model flow over the weirs and through the orifices of the outlet structure. These equations are dependent on pond depth, and subsequently on V (see Appendix A for more details). Therefore, the routine uses a finite-difference approximation, referred to as the Storage-Outflow method (see Wurbs and James (2002)), to solve the differential equation for Q_{out} and V. This solution is unstable at the hourly time step used by the hillslope routing routines, so the routine subdivides the hour into one-minute time steps, and assumes Qin, I, PPT and E are uniform over the hour.

4.3.2.2 Algae growth model

Algae growth is a critical component to C and N cycling within an SCM, particularly wet detention ponds that are continually inundated with water. The new SCM routine simulates the processes of algal growth, respiration, settling, and death. For algae, represented by mass of cholorphyll-a (chl-a), the mass balance follows that of the well-tested stream water quality model QUAL2K (Pelletier and Chapra, 2003), adapted

slightly for application to SCMs. The SCM is modeled as a continuous stirred-tank reactor. Equation 4.2 describes the mass balance:

$$\frac{da}{dt} = k_g' a - k_r' a - k_d' a - \frac{Q_{out}}{V} a + \frac{Q_{in}}{V} a_{in} - \frac{v_{s,a}}{H} * a \qquad \text{(Eq. 4.2)}$$

where a is the mass of chl-a in the SCM [kg chl-a m^{-1}], k_g' is the effective first order growth rate [d^{-1}], k_r' is the effective first order respiration rate [d^{-1}], k_d' is the effective first order death rate [d^{-1}], a_{in} is the mass of chl-a entering the SCM [kg chl-a m^{-1}], v_s is the settling velocity of algae [m d^{-1}], and H is the average pond depth [m]. Because algal growth, death, and respiration are all dependent on SCM water temperature, the routine includes a simple empirical model of water temperature as a function of air temperature developed by Stefan and Preud'homme (1993) (Appendix B).

A full description of the algae growth model, including the temperature, nutrient and light controls, is found in Appendix C. Generally, the effective algal growth rate is quantified by a base growth rate parameter (k_g) that is augmented by temperature and inhibited by availability of light and nutrients (N and phosphorous (P)). The RHESSys watershed model contains a radiation attenuation regime which estimates the radiation at the pond surface. This incident radiation is also attenuated through ponded water at a rate that increases with higher concentrations of chl-a. NH_4, is a more reduced form of inorganic N, so algae preferentially assimilate it over NO_3 based on a parameter and the relative abundance of both species (see Appendix D for more details) (Dortch, 1990). The routine models death and respiration as a parameterized first order loss base rate (k_d and k_r respectively) that increases with water temperature. Algae death releases N to the

water column as dissolved organic nitrogen (DON), whereas respiration releases N to the water column as NH_4. Death also returns algal carbon (C) to the water column as dissolved organic carbon (DOC), and respiration releases C to the atmosphere as carbon dioxide. Algae can enter the SCM with water from an upstream SCM, and exit with water outflow. The SCM model also simulates advection of DOC, DON and inorganic N with water from the watershed model (Appendix D). Finally, algae settles to a labile litter pool with relatively low C to N ratios, where it is decomposed and nitrified or denitrified, depending on the simulated chemical and physical conditions. Algal litter decomposition routines follow the existing leaf litter decomposition routines in RHESSys, modeled after BIOME-BGC (Running and Hunt, 1993).

4.3.3 Calibration and validation dataset

A wet pond SCM located in Charlotte, NC (35°15'37.2" N, 80°47'29.9" W) was used to calibrate and validate the SCM model routines. Charlotte-Mecklenburg Stormwater Services (CMSWS) monitored hydrology and water quality at a wet pond SCM, called the North Tryon Wet Pond (NTWP), from April 2008 – May 2011 as part of its Pilot Stormwater Control Management Program (CMSWS, 2016). NTWP is a 0.7 acre SCM serving 12.5 acres of urban residential development, which retains a permanent pool depth of 1.52 m (5.0 ft) above the deepest part of the pond. The sampling protocol, described by CMSWS (2015), included monitoring flow and water quality for storm events flowing into and out of the SCM. Data obtained from the county during the monitoring period described total inflow and outflow volume for 23 discrete events, as

well as inflow and outflow duration for 22 events. Additionally, the data documents the event mean concentrations (EMC) of NO_3 and NH_4 for 25 events entering and 29 events leaving the SCM, which was used for analysis of the water quality model. The discrepancy in the number of inflow and outflow samples is due to some events being sampled successfully at the inlet but not the outlet, or vice versa. Similarly, more data describing event water quality than hydrology was used because duration was not reported for all the hydrologic events sampled. This data limitation is addressed using a stochastic analysis approach, discussed later.

A simple four patch representation of NTWP and its watershed was used to perform all simulations in RHESSys. The four (4) patches were the (1) NTWP watershed, (2) NTWP itself, (3) a single downstream terrestrial patch, and (4) a single stream patch. These patches were hydrologically connected in series in the order listed. For this paper, the processes of the contributing watershed were not simulated in order to focus on the processes in the SCM only. This allowed for examination of the parameter sensitivity of the new SCM model routines only. To test the SCM component of the model, time series of precipitation and atmospheric deposition of NO_3 and NH_4 (described in detail below) were used to simulate inflow into the SCM from the NTWP watershed. Volumes assumed an effective contributing area of 7.9 ha, which is 63% of the actual watershed area, based on relationships between observed rainfall and inflow.

Because hydrologic and water quality data from SCM monitoring programs are typically recorded as discrete events, a time series of inflow and outflow was not available.

Therefore, a stochastic approach was used to generate a synthetic time series of water, NO_3, and NH_4 inflow to force the SCM model. This was done by first selecting the best-fitting of five candidate probability density functions (PDF) through observations of inflow volume, inflow event duration, and EMC of both NO_3 and NH_4 made at NTWP. The goodness-of-fit of the five candidate PDFs was quantified by the Akakie Information Criteria (AIC) and the Kolmogorov-Smirnov statistic (D). The candidate distributions were the normal, log-normal, gamma, Weibull, and exponential. The "fitdistplus" package in the R programming language and software environment was used to fit PDFs and quantify goodness-of-fit (Delignette-Muller and Dutang, 2014; R Core Team, 2014). Because many of the NH_4 values observed were below detection, a left-truncated distribution (truncated at 0.0 mg-N L^{-1}) was fit through the observations using the "EnvStats" R package (Millard, 2013). PDFs were also fit through observations of the interarrival times for rain events with a cumulative rainfall $\geq$ 2.54 mm, using a minimum antecedent dry period of 6 hr, as suggested by Hydroscience Inc. (1979) and Driscoll et al. (1989). Interarrival time of these rain events was assumed to correspond to that of SCM inflow events. The rainfall data was taken from a United States Geological Survey gage ~1 km away at Hidden Valley Elementary School (Site no: 351604080470845, data downloaded from: http://nc.water.usgs.gov/char/rainfall.html). Table 4-1 describes the selected PDFs, the PDF's parameters, and goodness-of-fit quantified by Kolmogorov-Smirnov statistic (D). Only D, which quantifies the maximum difference in probability between two empirical cumulative distribution functions (CDFs), is reported in Table 4-1 because AIC only has value when compared relative to other model permutations.

Table 4-1: Description of best-fit PDFs of the variables used to generate stochastic inflow time series. In this table, the abbreviation "sd" stands for standard deviation.

Variable	Distribution	Distribution Parameters	Kolmogorov-Smirnov statistic (D)
Volume	Lognormal	mean = 1.78, sd =0.135	0.091
Duration	Gamma	shape = 2.15, rate = 0.00298	0.12
Interarrival Time	Exponential	rate = 0.00783	0.077
EMC of NO_3	Gamma	shape = 2.52, rate = 10.1	0.082
EMC of NH_4	Truncated Lognormal	mean = -2.13, sd =0.620	0.13*

* D value reported is the largest distance between empirical and fitted PDF to the right of the truncation only

The continuous PDFs of inflow volume, duration, interarrival period, and EMC were randomly sampled 131 times to generate characteristics of 131 discrete storm events. These synthetic events were then merged in time, resulting in an inflow water and N time series that spanned a period of 2 years from 10/01/2011 to 10/01/2013 (i.e., 2012 and 2013 water years). Inflow volume was distributed over the duration of the event using a triangular distribution, which peaked in the middle of the event (i.e., an isosceles triangle). Inflow mass of organic N for each time step during an event was determined by dividing the inflow volume at that time step by the randomly generated EMC. In addition to this stochastic inflow data, observed times series of maximum and minimum daily temperature from the National Oceanic and Atmospheric Administration's meteorological station at Charlotte-Douglas Airport (KCLT) for the same time period were used to force the model.

4.3.4 Calibration, validation and sensitivity analysis

The 2012 water year was used as a spin up period for water, algae, and N state variables, and the analyses described below were performed on the 2013 water year only.

4.3.4.1 Hydrologic validation

The geometry and design of the wet pond and outlet structure at NTWP are documented in two reports (McKim & Creed, 2006; CMSWS, 2015). Because the design parameters controlling hydrologiv bevaior were known (Table 4-2), they were not calibrated. The parameters were validated by comparing simulated vs. observed CDFs of outflow volume and duration from discrete events only. A discrete event was defined as the period of time between the start of inflow into the SCM until the resulting outflow concluded; a

Table 4-2: NTWP design parameters used for water volume validation, as well as water quality calibration, validation, and sensitivity analysis. Also shown is the range of outlet structure parameters varied to quantify how the permanent pool design height affects inorganic N removal.

SCM Parameter Name	Value	Permanent pool design scenario range	Unit	Reference
Maximum SCM Height	4.57	3.35-5.79 by 0.305	m	CMSWS (2015)
Length:Width Ratio	1.5	--	$m\ m^{-1}$	CMSWS (2015)
Side Slope (H:V)	2	--	$m\ m^{-1}$	CMSWS (2015)
Infiltration Rate	0.006096	--	$m\ d^{-1}$	CMSWS (2013)
Riser Length	0.365	--	m	McKim and Creed (2009)
Riser Weir Coefficient	3.33	--		Wurbs and James (2002)
Riser Orifice Coefficient	0.6	--		Wurbs and James (2002)
Riser Height	3.05	1.83-4.27 by 0.305	m	McKim and Creed (2009)
Number of Orifices	1	--		McKim and Creed (2009)
Orifice Diameter	0.144	--	m	McKim and Creed (2009)
Orifice Coefficient	0.6	--		Wurbs and James (2002)
Orifice Height	1.52	0.305-2.74 by 0.305	m	McKim and Creed (2009)

definition guided by the sampling protocol (CMSWS, 2015). If inflow from an event occurred prior to the cessation of the previous event, both events were excluded from analysis. Twenty discrete events were identified over the 2013 water year.

4.3.4.2 Water quality model parameter uncertainty, sensitivity, and calibration

A Monte Carlo approach was used to perform a global sensitivity analysis of state variables to water quality parameters (following the procedure outlined by Marino et al. (2008)), and to quantify parameter uncertainty (following the Generalized Likelihood Uncertainty Estimation (GLUE) procedure of Beven and Binley (1992)). The twelve water quality parameters are grouped into three groups of four: first order rate parameters, growth-limiting nutrient parameters, and physical parameters (Table 4-3). A Latin hypercube sampling (LHS) technique was used to generate 10,000 parameters sets for Monte Carlo simulation (McKay et al., 1979). The "spartan" package in R was used to perform the LHS (Alden et al., 2015). The parameters were assumed to follow a uniform distribution across the ranges listed in Table 4-3. These ranges were taken from peer-reviewed literature, referenced also in Table 4-3.

The relationship between the concentrations of two water quality state variables (NO_3, NH_4) and the water quality parameters was assumed to be non-linear and monotonic. Therefore, partial rank correlation coefficient (PRCC) was used to measure model sensitivity. The PRCC quantifies the strength of linear correlation between the rank of a given state variable and the rank of each parameter from the 10,000 simulations. The PRCC between the two water quality state variables and each of the twelve parameters

was computed at the beginning of each day during the simulations. This sensitivity analysis was performed through time to explore how the strength of the relationship between SCM concentrations and these parameters changed with season and times of different water and nutrient loading.

Table 4-3: Description of water quality parameters and ranges used for Monte Carlo sensitivity analysis, uncertainty estimation, and calibration

Group	Symbol	Description	Unit	Low	High	Reference
Rate	k_g	Base growth rate of chl-A in algae	d^{-1}	1.5	10	Cho and Ha (2010)
Rate	k_d	Base death rate of chl-A in algae	d^{-1}	0	1	Cho and Ha (2010)
Rate	k_r	Base respiration rate of chl-A in algae	d^{-1}	0	1	Cho and Ha (2010)
Rate	v_s	Settling rate of algae as chl-A	m d^{-1}	0	5	Cho and Ha (2010)
Nutrient	k_{sn}	Half saturation concentration of nitrogen	mg-N L^{-3}	0.005	0.02	Chapra (1997)
Nutrient	k_{sp}	Half saturation concentration of Phosphorous	mg-P L^{-1}	0.001	0.005	Chapra (1997)
Nutrient	P	Phosphorous concentration in the SCM	mg-P L^{-1}	0.01	0.1	Unpublished observation
Nutrient	k_{pn}	Constant of preferential NH_4 uptake, over NO_3	mg-NH_4 L^{-1}	0.01	0.1	Tetra Tech, Inc. (2009)
Physical	θ_g	Constant for k_g dependency on temperature	--	1.053	1.08	Chapra (1997)
Physical	θ_d	Constant for k_d dependency on temperature	--	1.072	1.088	Chapra (1997)
Physical	θ_r	Constant for k_r dependency on temperature	--	1.072	1.088	Chapra (1997)
Physical	I_s	Optimum radiation level for algae growth	kJ $m^{-2}d^{-1}$	9414	11506	Chapra (1997)

The GLUE procedure was used to calibrate water quality parameters and to assess their uncertainty. This method acknowledges potential equifinality in the parameter sets, and therefore results in a range of acceptable parameter sets rather than one optimum set. First, an initial, prior likelihood distribution was assigned to all 10,000 parameter sets.

The prior distributions of each parameter were assumed to be uniform, with bounds set by literature and physical constraints. Simulations were run using all 10,000 parameter sets. Next, a threshold of acceptable model performance was determined, and the parameters sets that did not meet this threshold were discarded. The Kolmogorov-Smirnov D test statistics between CDFs of observed and simulated outflow EMCs were used to determine acceptability. All parameter sets that produced a Kolmogorov-Smirnov D < 0.2 for both NO_3 and NH_4 were deemed acceptable. Only the CDFs of EMCs above the detection limit, 0.05 mg-N L^{-1} for NO_3 and 0.1 mg-N L^{-1} for NH_4, were compared with the D statistic. With acceptable parameter sets identified, a likelihood measure for each parameter set was computed. These measures were then rescaled to create likelihood weights with a cumulative sum equal to 1. The likelihood measure used was the sum of Kolmogorov-Smirnov D for both NO_3 and NH_4 (D_{sum}), and the likelihood weight was computed as in Equation 4.3:

$$W_i = \frac{\frac{\max(D_{sum}) - D_{sum,i}}{\max(D_{sum}) - \min(D_{sum})}}{\sum_i \frac{\max(D_{sum}) - D_{sum,i}}{\max(D_{sum}) - \min(D_{sum})}} \quad \text{(Eq. 4.3)}$$

where W is the likelihood weight, $max(D_{sum})$ and $min(D_{sum})$ are the maximum and minimum D_{sum} of all acceptable parameter sets, respectively, and i represents each acceptable parameter set. This function gives parameter sets with a lower D_{sum} greater weight. The distributions of simulated outflow EMC of both NO_3 and NH_4 from the prior parameter distribution were compared to the same distribution from the posterior to gain insight to the parameter uncertainty.

4.3.4.3 Model sensitivity to environmental inputs

A final sensitivity analysis was performed to determine how the model responded to changes in air temperature, inflow volume, and inflow NO_3 and NH_4. This analysis identified environmental controls on the model and addressed the limitations of synthetically generated inflow based on relatively few observed measurements from the SCM. First, a reference time series of each model input was established. The reference temperature scenario was the actual daily temperatures of the 2012 and 2013 water years. The 2013 water year demonstrated typical air temperatures, as the average annual air temperature was in the 40^{th} percentile of the of the water years 1949-2013 on record at KCLT. The reference inflow volume scenario was the synthetically generated time series for the NTWP SCM as described above. The reference scenario used for inflow N concentrations was the synthetically generated inflow time series used during calibration, multiplied by a factor of three. The distributions of the 3x augmented concentrations corresponded with the 25^{th}, 50^{th} and 75^{th} percentiles of NO_3 inflow concentrations into retention ponds reported in the International Stormwater BMP Database (Geosynthetic Consultants and Wright Water Engineers, 2014).

To consider SCM behavior outside of the reference scenario, either air temperature, inflow volume, or inflow NH_4 and NO_3 concentrations were systematically perturbed, while the other inputs were left at reference scenario values. Temperature was varied from -5°C to +5°C, by increments of 1°C. Karl et al. (2009) has summarized climate change projections, and projected an maximum likely increase of annual average

temperature of 5°C above the 1961-1979 average by the year 2099 for Charlotte, NC. Because monitored inflow volumes were used instead of precipitation to calibrate and validate the model, climate change projections were not used to simulate possible environmental variability. Rather, the reference scenario inflow volumes were increased and decreased by 2%, 5%, 10%, and 20%. For these volume perturbations, N mass inflow was simultaneously altered to keep inflow EMCs constant. Finally, the reference concentrations of both NO_3 and NH_4 were varied by factors of 1/6, 1/2, 1/3 (equal to our observed concentrations), 2, 3 and 6. All 11 temperature, 7 inflow volume, and 7 inflow nitrogen scenarios were run across the all of the acceptable parameter sets.

4.3.5 SCM design scenario testing

Because the design of an SCM will likely affect processing of N and C, the depth of the permanent pool was varied to determine how this design parameter affected N retention and removal. NTWP has a permanent pool depth of ~1.52 m (5.0 ft). The depth of the permanent pool was varied from the actual depth, across a range of 0.30 m to 2.74 m by increments of 0.30 m (1.0 ft to 9.0 ft by 1.0 ft). The SCM design parameter ranges that reflect these permanent pool designs are shown in Table 4-2. As with the environmental input sensitivity analysis, these scenarios were run across the entire range of acceptable parameter sets from the GLUE analysis.

4.4 Results

4.4.1 Hydrologic Validation

SCM design parameters were taken directly from monitoring data at NTWP, and therefore were not calibrated (Table 4-2). Figure 4-2a shows the CDFs of modeled and observed event outflow volume using those parameters. The Kolmogorov-Smirnov D between observed and modeled volume was 0.197. Thirty-one percent of the observed inflow events did not produce any outflow, while 23% of the modeled events had no outflow. The CDFs of outflow volumes aligned best in the middle quartiles. In the upper quartile, observed outflow volumes were generally larger than those modeled, excluding the largest modeled outflow event which was 2.4 times greater than the largest observed outflow volume. The Kolmogorov-Smirnov D between modeled and observed CDFs of outflow duration was 0.274 (Figure 4-2b). The model underestimated the duration of

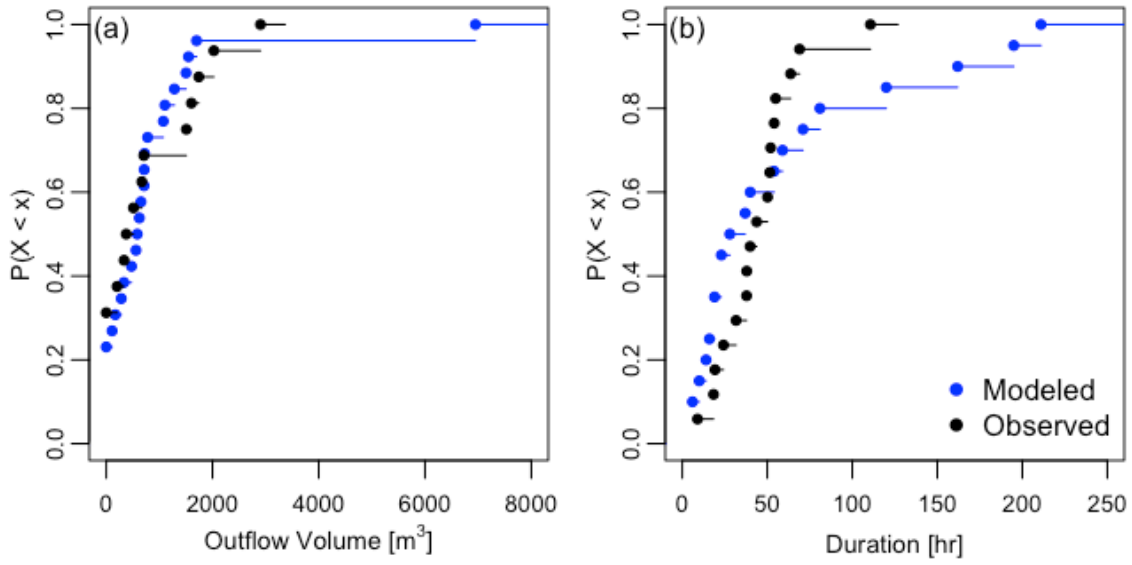

Figure 4-2: Validation of hydrologic model by comparing modeled and observed CDFs of outflow volume (a) and event duration (b).

events through the lower three quartiles, above which the model tended to over predict event duration.

4.4.2 Water quality parameter global sensitivity analysis

To explore global sensitivity of the model to water quality parameters, daily time series of the PRCC values between both SCM NO_3 and NH_4 concentration and the 12 selected parameters were computed (Table 4-3). Figures 4-3 and 4-4 show the strength of the correlation between the 12 selected parameter sets and NO_3 and NH_4, respectively, through the year and relative to different inflow conditions (panel a). Higher positive PRCC values indicate a stronger positive correlation between the state variable and the parameter, whereas lower negative values indicate a stronger negative trend. Values around zero mean less correlation, and therefore less sensitivity. Figure 4-3b shows the PRCC values for the first order parameters. The PRCC was consistently below -0.5 for k_g, but was predominately above 0.5 for k_d. The parameter k_d did not show a seasonal pattern, whereas k_g showed a stronger negative correlation in the colder months (Nov.-Mar.). The PRCC for k_r and v_s also showed a seasonal pattern: they were more positive in the colder months (Nov.-Mar.) and were either negative (k_r) or near zero (v_s) in the warmer growing months (May-Oct.). The sub-seasonal patterns were inverted, v_s was more positively sensitive (peaks) on days when k_r was less positively sensitive (troughs). The sensitivity of SCM NO_3 to the nutrient (Figure 4-3c) and physical (Figure 4-3d) parameters was not as strong as the first order algae parameters, as the PRCC values for all parameters but one were between -0.13 and +0.25. The parameter, k_{sn}, was

consistently positively correlated to NO_3, and the strength of this correlation, which peaked at 0.5, increased continually between inflow events.

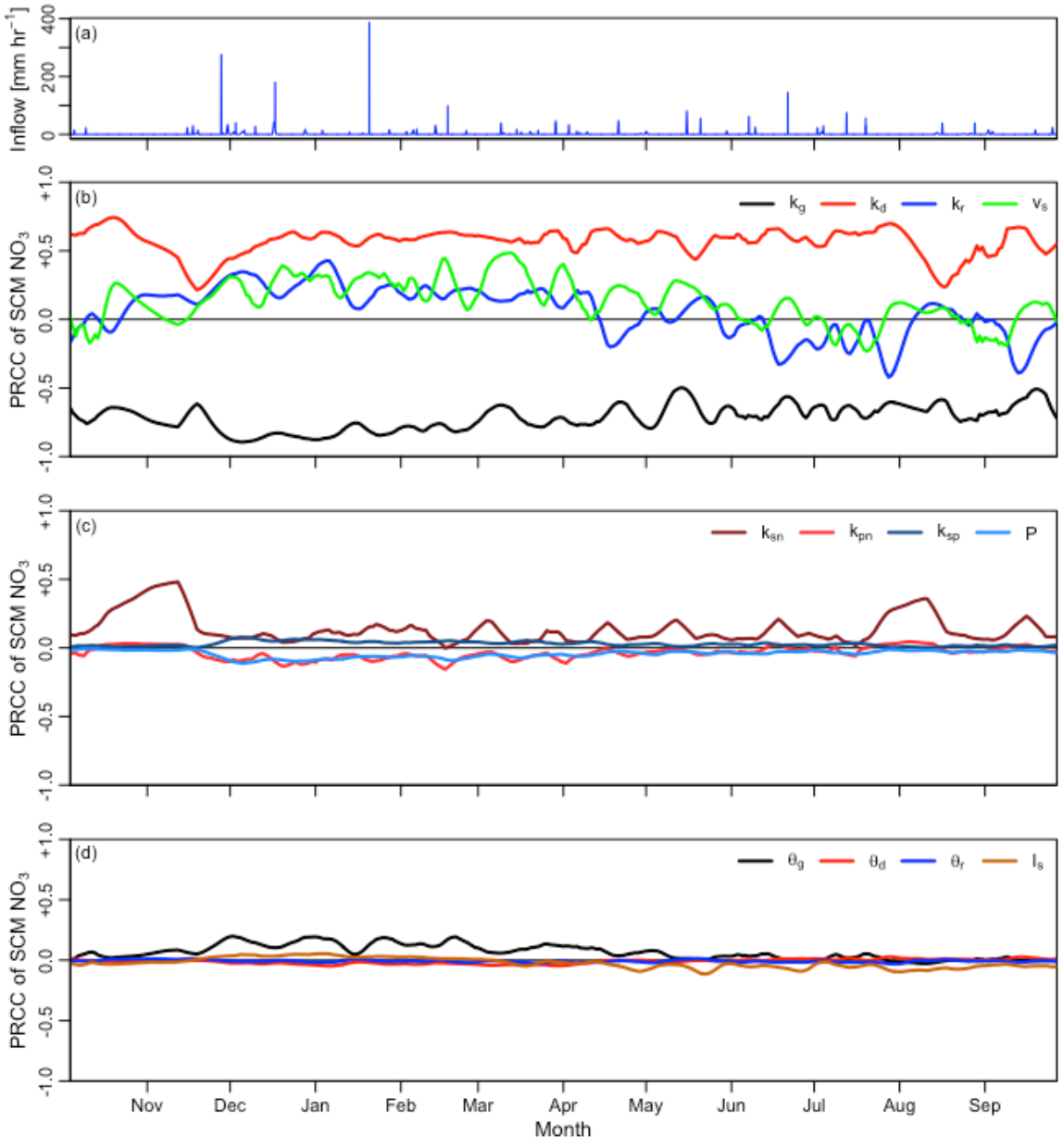

Figure 4-3: Global sensitivity, quantified by a PRCC, of SCM NO3 concentrations to model parameters. Subplot (a) shows the inflow time series, and a 7-day moving average of parameter sensitivity grouped into the remaining subplots by first order rates (b), nutrient limitation parameters (c), and physical parameters (d).

The sensitivity of NH_4 concentrations to the 12 water quality parameters followed similar patterns as for NO_3 (Figure 4-4). The first order algae parameters showed much stronger control than the physical and nutrient parameters (Figure 4-4b). As with NO_3, the

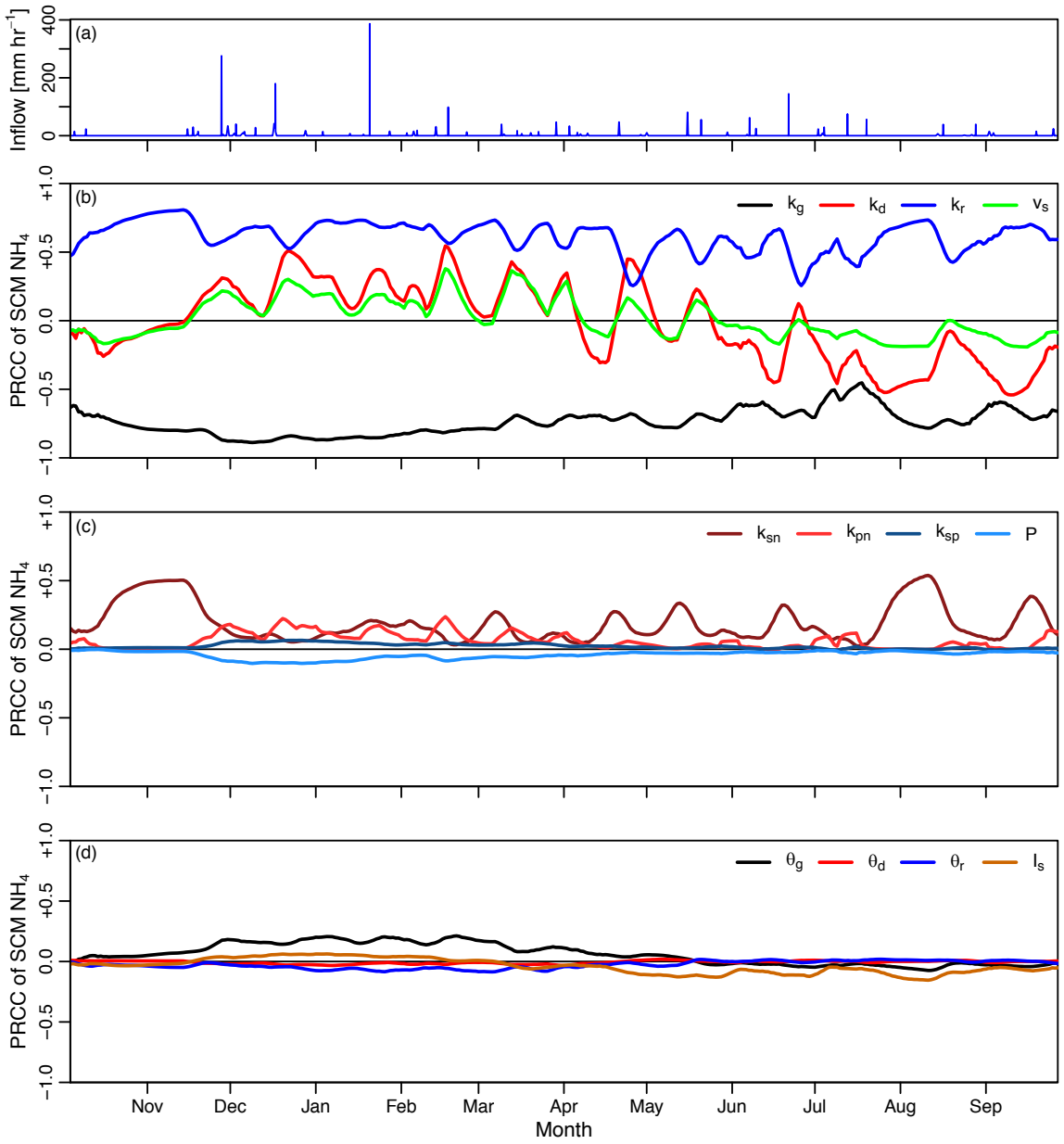

Figure 4-4: Global sensitivity, quantified by a PRCC, of SCM NH_4 concentrations to model parameters. Subplot (a) shows the inflow time series, and a 7-day moving average of parameter sensitivity grouped into the remaining subplots by first order rates (b), nutrient limitation parameters (c), and physical parameters (d).

strongest negative correlation was between NH_4 and k_g. For both NO_3 and NH_4, k_g showed a seasonal pattern as colder months had a greater negative PRCC than the warmer months. However, the strongest positive correlation was between NH_4 and k_r. The other two parameters, k_d and v_s, tracked each other both seasonally (positive during the colder months of Nov. – Apr., and negative during warmer months of May – Nov.) and sub-seasonally. The sub-seasonal peaks in PRCC of these two parameters occurred at the same time as the troughs in PRCC of the respiration parameter, and these variations correspond with inflow events. As with NO_3, the nutrient (Figure 4-4c) and physical (Figure 4-4d) parameters showed weak (-0.16 to +0.25) PRCC values through time, apart from k_{sn}, which was elevated during the dry period to a peak PRCC of 0.50.

To further explore the effect of both season and hydrologic conditions on these PRCC values, a simple correlation analysis between the daily time series of PRCC for the five most sensitive model parameters and the average daily air temperature and depth of water in the SCM was performed (Table 4-4). The correlations between the parameters and air temperature agreed with the qualitative observations of the time series described above. NO_3 and NH_4 were more sensitive to k_g during the warmer months. NO_3 concentrations were also slightly more sensitive to k_g values when depth of water was low. The sensitivity of both inorganic N parameters to k_{sn} was not correlated with temperature. When analyzing the effects of hydrologic conditions on the NO_3 concentration sensitivity, sensitivity was more negatively correlated to k_{sn} during wetter periods. The remaining parameters all showed weaker (< 0.3) correlations. The same phenomena were true for

NH_4, as model sensitivity to k_{sn} decreased during wetter periods. NH_4 concentrations also showed increased sensitivity to v_s and k_s to increased SCM water depth

Table 4-4: Correlation coefficients between PRCC values of NO_3 and NH_4 and the average daily SCM water depth and daily air temperature for the 5 most sensitive water quality parameters. Correlations greater than 0.5 are highlighted with bold text.

Parameter	Temperature		Depth	
	NO_3	NH_4	NO_3	NH_4
k_g	**0.50**	**0.67**	-0.24	-0.06
k_d	0.00	**-0.70**	-0.04	0.47
k_r	**-0.65**	-0.36	0.19	-0.27
v_s	**-0.51**	**-0.62**	0.27	**0.53**
k_{sn}	0.00	0.07	**-0.72**	**-0.67**

4.4.3 Water quality parameter uncertainty and calibration

Of the 10,000 initial water quality parameter sets, only 246 met the acceptability criteria that the Kolmogorov-Smirnov D statistic between modeled and observed CDFs of both NO_3 and NH_4 must be less than 0.2. Figure 4-5 shows the envelopes of the 1-99th percentiles of simulated outflow EMC of both inorganic N species before (dark grey) and after (light grey) applying this acceptability filter. Constraining the parameters reduced the uncertainty of EMC, which is reflected in the horizontal width of the grey envelopes in Figure 4-5. The average horizontal distance of contraction of the simulated CDF envelopes was 0.145 mg L^{-1} for NO_3 and 0.099 mg L^{-1} for NH_4.

Additionally, Figure 4-5 shows the weighted ensemble mean of all the acceptable parameter sets which aggregates the 246 simulations based on performance. Acceptable parameter set weights ranged from 0 to 0.0086, which was 2.1 times the average (or

uniform) weight. The absence of observed NO_3 and NH_4 values below the 45th and 85th percentiles, respectively, was due to an abundance of samples below analytical detection making it difficult to determine the goodness-of-fit of the parameters below these percentiles. However, all observations above these percentiles, save the highest observed NH_4, fell within the posterior envelope. Observed values of NO_3 outflow deviated from the ensemble mean at higher percentiles, as the model over predicted EMCs above 0.1 mg-N L^{-1}.

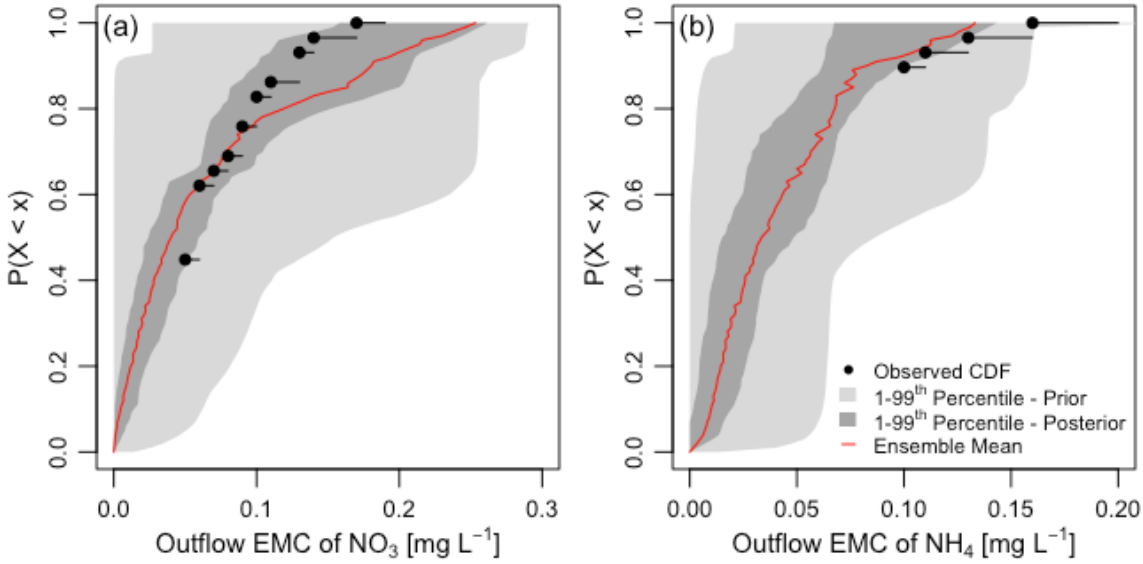

Figure 4-5: Evaluation of uncertainty from model parameters by comparing the range of simulated CDFs of NO_3 (a) and NH_4 (b). All 10,000 parameter sets are reflected in the prior distribution (light gray), whereas only the 246 acceptable parameter sets are shown in the posterior distribution (dark gray). The red line represents the aggregated ensemble mean of all 246 acceptable parameter sets, weighted by performance.

4.4.4 Model sensitivity to environmental inputs

To quantify how N removal efficiency varied with environmental input, either air temperature, inflow volume, or inflow N concentrations was systematically altered, while the other two inputs were kept constant. N removal fraction was calculated as the

difference between mass inflow and mass outflow, divided by the mass inflow. Figure 4-6 shows how the mass removal fraction of inorganic N changes with temperature. Results showed that as temperature increased, so did the mass removal fraction. Figure 4-6 also shows that at higher temperatures, the width of the parameter uncertainty envelope widens. The removal of NH_4 was greater than removal of NO_3 for all simulated temperature regimes. Figure 4-7 shows how changing inflow water volumes, but keeping concentrations constant, influenced mass removal fraction. As with temperature, NH_4 removal was greater than NO_3 removal across all simulated inflow volumes. As inflow volume increased, mass removal fraction decreased. Additionally, the parameter uncertainty envelope did not change significantly with volume. Finally, the effect that changing N inflow concentrations had on removal fraction was tested. Figure 4-8 shows that, for NO_3, increased concentrations result in decreased removal efficiencies. For NH_4,

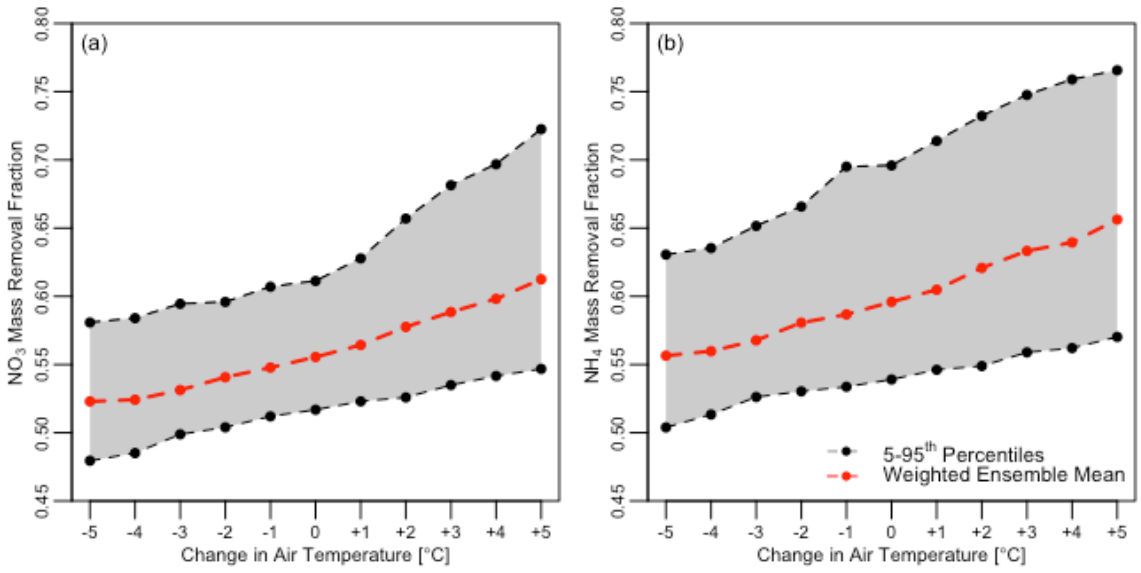

Figure 4-6: Changes in mass removal of NO_3 (a) and NH_4 (b) with changes in air temperature, relative to a reference scenario, the 2013 water year.

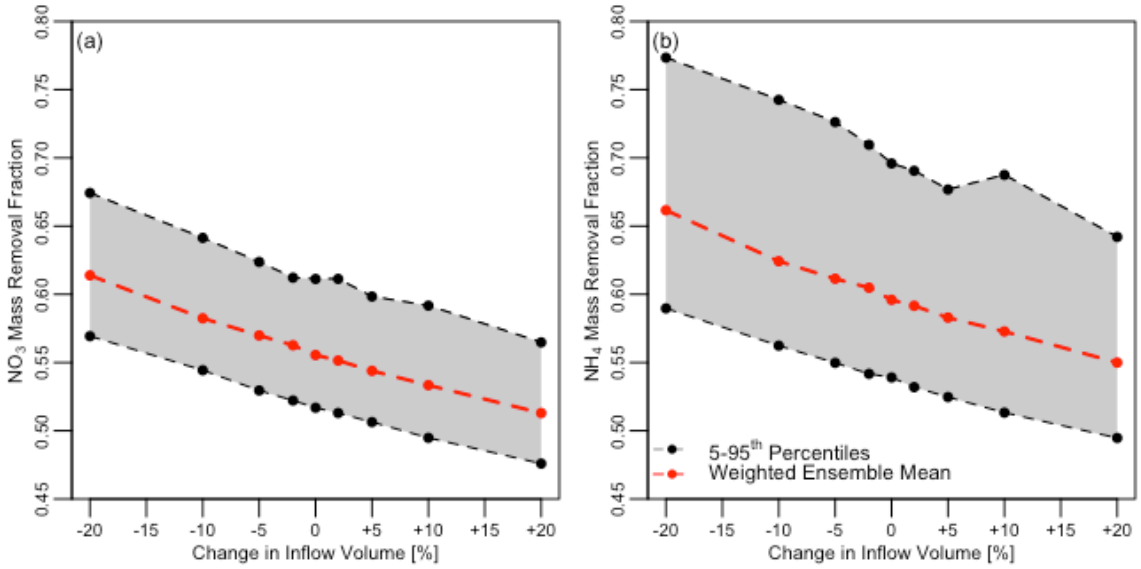

Figure 4-7: Changes in mass removal of NO_3 (a) and NH_4 (b) with changes in inflow volume, relative to a reference scenario. Inflow nitrogen mass changes with water volume in order to keep concentrations constant.

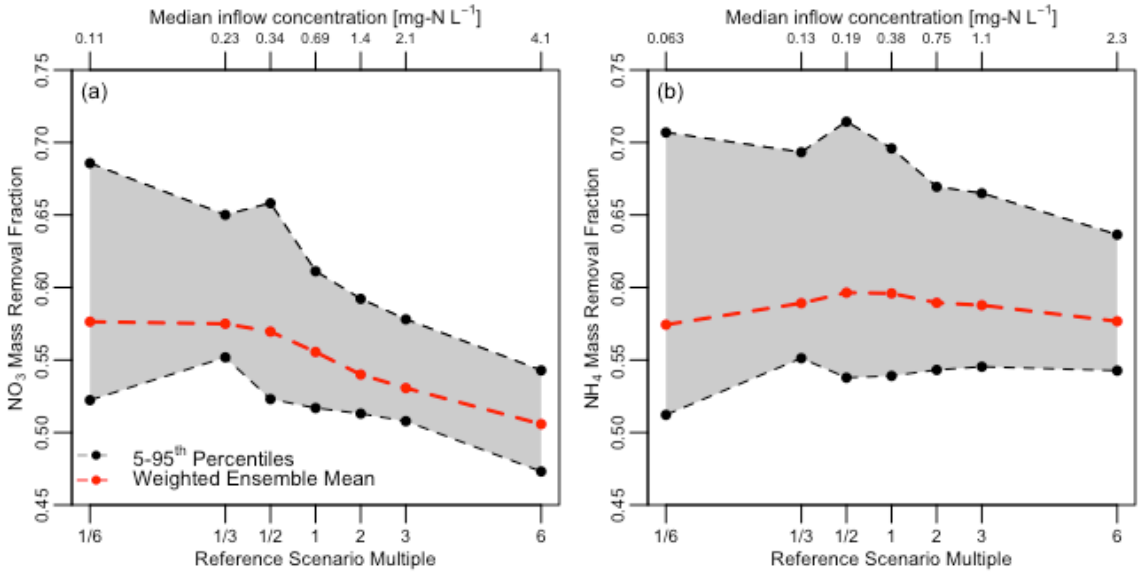

Figure 4-8: Changes in mass removal of NO_3 (a) and NH_4 (b) with changes in inflow concentrations of both N species. The bottom x-axis shows the multiple of inflow concentration relative to the reference scenario, while the top x-axis shows the median concentration of each scenario. The x-axis is scaled so that the multiples on either side of 1 are plotted linearly, rather than the concentration. For example, this scaling causes the multiples 1/3 and 3 to be an equal distance from one.

removal efficiencies remained between 0.58 and 0.60 across all inflow scenarios. For both NO_3 and NH_4, the parameter uncertainty envelope shrunk with increased inflow concentrations, although the effect was more exaggerated for NO_3. For the lowest N concentration simulation, removal of NO_3 was greater than NH_4, the only time this relative difference was observed in all environmental input simulations.

4.4.5 SCM design scenario testing

To quantify how different SCM designs change N removal, the depth of the permanent pool in NTWP was varied. Figure 4-9 shows how mass removal fraction of both NO_3 and NH_4 changes with the depth of the permanent pool. In both cases, increased pool depth caused increased removal. Removal increased approximately linearly until the observed depth of 1.524 m, after which the slope began to decline but still remained

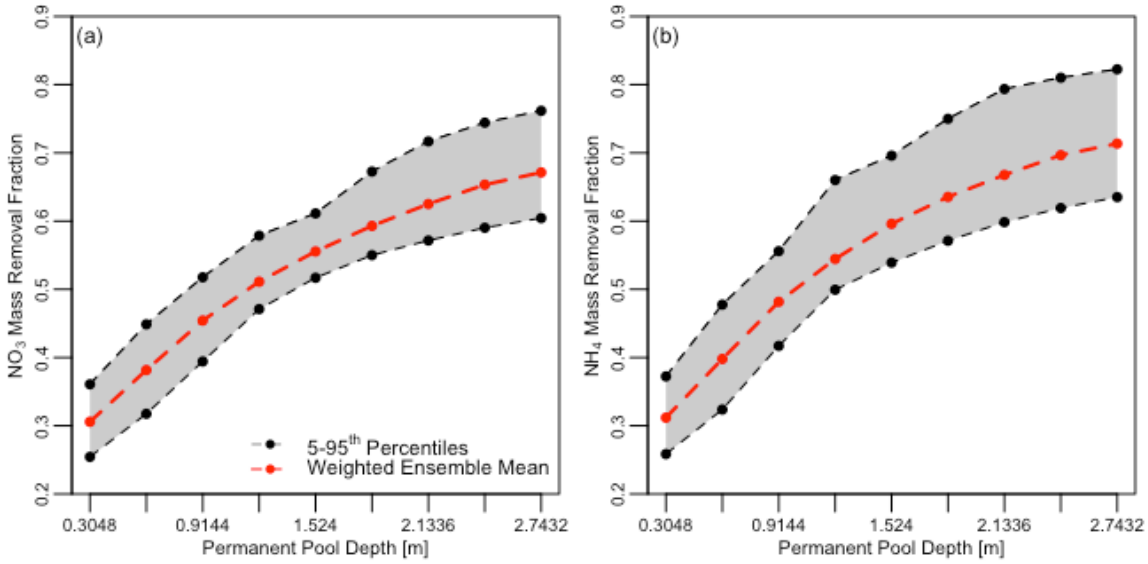

Figure 4-9: Changes in mass removal of NO3 (a) and NH4 (b) with change in depth of the SCM permanent pool

positive. The ensemble means of removal fraction varied dramatically across the range of simulate depths, ranging from 0.31 to 0.67 for NO_3 and 0.31 to 0.71 NH_4.

4.5 Discussion

4.5.1 Model evaluation

Validation of the SCM hydrologic model is critically important for urban water quality modeling, because mass export of solutes from urban watersheds is directly tied to runoff volume and density of SCMs within the basin (Hale et al., 2015). An important first step is accurate simulation of water retention and routing. This work presents a new model that successfully replicates the distribution of observed outflow volumes through the lower three quartiles without any calibration (Figure 4-2a). This result underscores the model's ability to capture the effects that SCMs have on the water balance in urban areas, which is one of the benefits that SCMs provide. Although the model generally under predicted observed outflow volumes in the upper quartile, issues with both observation and simulated values during larger events exist. First, uncertainty in the rating curves at both inlets and the outlet at higher stages, a problem that has been explored for gauging river discharge (e.g., Clarke (1999)). Additionally, because the inflow record was generated stochastically, event volume, duration, and antecedent dry period were grouped randomly. It is possible that the durations and dry periods paired with the large volume events introduced uncertainty to the model.

The model was also able to reasonably reproduce the distribution of event outflow duration without calibration. Simulating event outflow duration is important for

capturing the effects that SCMs have on timing of stream discharge. Despite the success, the routine under predicted the duration of outflow during storm events through the first three quartiles and over predicted the duration in the upper quartile (Figure 4-2b). Again, this could be due to both to limitations in the observation procedure and the stochastic modeling framework. If sampling was stopped prior to complete cessation of the hydrograph due to logistical reasons, it could lead to this discrepancy. As with the large volume events, the random paring of inflow volume and antecedent dry periods to the generated inflow durations could introduce variation in the simulation results. Still, 70% of the modeled outflow events had ceased within 60.5 hours of initiation, which corresponds to the designed drain down time of 48 hr (McKim & Creed, 2006) plus 12.5 hr, the median observed duration of inflow (data not shown).

The GLUE framework was used to both quantify parameter uncertainty, and to constrain plausible parameter sets to a reasonable range. The ensemble mean, which reflects a performance-weighted average of all acceptable parameter sets, predicted NO_3 EMC well up through the third quartile, but over-predicted NO_3, in the upper quartile. NH_4 EMC estimates closely matched observed EMCs. As with the modeled outflow volumes, the stochastic pairing of inflow N concentrations with inflow volume, duration, and interarrival times could be the source of some of the variability at these higher percentiles.

Additionally, a global sensitivity analysis was performed to determine the correlation between simulated SCM NO_3 and NH_4 concentrations and twelve water quality model parameter values. This analysis provided insight into the behavior of the model, but also

identified the parameters that should be constrained either through empirical observation or through calibration to limit model uncertainty. Of the 12 parameters, the base growth rate, k_g, demonstrated the strongest control on both state variables over the course of the simulation. This result is expected as algae growth relates directly to inorganic N uptake, and therefore faster growth rates will be negatively correlated to both NO_3 and NH_4 concentrations. Other parameters that showed strong, positive correlations to NO_3 and NH_4 were k_d (base death rate) and k_r (base respiration rate) respectively. The reason for the correlation to NH_4 is clear, as the model routines cause algal respiration to release NH_4 directly to the water column. However, the correlation between NO_3 and k_d is not as direct, as algae death does not release NO_3. The cause for the correlation could be realted to a secondary control. Algae death removes the stock of chl-a without adding inorganic N, therefore limiting growth by reducing the stock chl-a, resulting in less NO_3 uptake. The final first order rate parameter, v_s, also demonstrated strong control on both NO_3 and NH_4, although the direction on the correlation changed seasonally. As with k_d, v_s does not directly affect the mass balance of inorganic N, but it removes algal chl-a stocks which limits growth and subsequent N uptake.

Collectively, the four first order rate parameters of the algae submodel exerted far stronger control on inorganic N concentrations than the 4 nutrient limitation parameters and 4 physical parameters. The only parameter of the remain 8 nutrient limitation and physical parameters with an absolute value of PRCC greater than 0.2 was k_{sn}: the half saturation constant of Michaelis-Menten uptake of inorganic N during chl-a growth (Figures 3b and 4b). We attribute the strong sensitivity of the SCM model behavior to

this parameter to the fact that available N frequently limits algal growth. This could be due, in part, to inflow concentrations at NTWP being relatively low compared to other similar systems. The distribution of inflow NO_3 concentrations at NTWP were approximately 1/3 lower than those reported in the International Stormwater BMP Database (Geosynthetic Consultants and Wright Water Engineers, 2014).

In addition to informing model behavior, the global sensitivity analysis also highlights the parameters that contributed the most to model uncertainty. This uncertainty could be constrained either through calibration, application of literature-based parameters that govern algal community dynamics in other systems, or additional monitoring and experimentation. Future application of the SCM model in other regions should minimize parameter uncertainty by calibrating the four first order growth parameters (k_g, k_r, k_d, and v_s), as well as k_{sn}.

4.5.2 Environmental controls on water quality model sensitivity

Analyzing how sensitivity to model parameters changes through time illuminates the change of system dynamics with season, under different hydrologic conditions, and N availability. Model sensitivity of both inorganic N species changed with air temperature and therefore season. The time of year strongly controlled sensitivity of modeled NO_3 to k_g, k_r and v_s and also sensitivity of modeled NH_4 to k_g, k_d and v_s. The strength of correlation for the two loss parameters (k_r and v_s for NO_3 and k_d and v_s for NH_4) is opposite to the growth term, k_g. In the colder months, when k_g exerted a weaker effect on the inorganic N concentrations, greater loss parameter values lead to lower algae stocks.

Lower stocks of algae lead to less gross uptake, and therefore greater N concentrations. This explains the positive correlation between inorganic N concentrations and the loss parameters. However, during the warm months, the correlation with the loss parameters approached zero or even goes negative. This may be because N uptake during growth quickly assimilates any release of inorganic N. Understanding the environmental controls on model sensitivity adds to fundamental knowledge of the system dynamics and provides useful information for future users looking to parameterize the model under different environmental conditions.

Additionally, results showed that increasing temperatures exaggerated the effects of parameter uncertainty. Figure 4-6 shows that as input temperature increased, the envelope of the 5-95th percentile of simulated inorganic N removal fraction widened. Three of the first order rate parameters (k_g, k_r and k_r), the group identified as demonstrating the most control on SCM inorganic N concentrations, were all influenced positively by temperature. Therefore, warmer temperatures caused increased rates of chl-a cycling, likely causing the divergence of simulated N concentrations relative to the mean. The implications of this are that parameter values must be carefully constrained if simulations are done in places with warmer climates or during years of higher temperatures. Changing sensitivity of simulated water quality variables to ecological model parameters with season was also shown by Yi et al. (2016) using a more complex, but similar model of algae growth in a lake ecosystem.

SCM water depth, a proxy for recent hydrologic and N input, also influenced model parameter sensitivity. The PRCC of both NO_3 and NH_4 showed stronger positive correlation to k_{sn} when SCM depth was lowered, indicating that this parameter exerts greater control during dry periods (Table 4-4). Because k_{sn} controls the degree to which N concentrations limit growth, the parameter increased in importance between inflow events as the stocks of inorganic N gradually depleted through algae N assimilation. Therefore, higher values of k_{sn} lead to less N uptake between events and greater inorganic N concentrations. This remaining N rich water could be flushed out of the system during subsequent rain events, ultimately decreasing the ability of the SCM to remove inorganic N. This highlights that N availability constrained algae N uptake between storm events when concentrations declined, more than it did during events when N is high. PRCC sensitivity values of NH_4 to k_d and v_s increased when SCM pond depth increased. This could be because these two chl-a loss fluxes are of greater importance when N concentrations are high, immediately after inflow events.

Unlike temperature, increased event inflow volume did not influence parameter uncertainty. Increased N concentrations, however, led to a reduction in parameter uncertainty. The cause for this could be that, as constraints on growth from N limitation are removed, model simulations become more homogeneous. Application of the SCM model at low-N sites where N limitation dominates must account for the potential for parameter uncertainty to influence simulation results.

4.5.3 Environmental and design control on N removal by SCMs

Reduction of mass export of nutrients, including NO_3 and NH_4, is often a stated goal of stormwater management plans (e.g., City of Charlotte (2015)). These plans often stipulate that SCMs are a strategy to reduce export, and post-construction compliance permits are issued on the assumption that SCMs of a given type (e.g., wet pond, wetland) remove a constant fraction of inflow mass on average. This removal fraction is based on a broad dataset of multiple studies (e.g., International Stormwater Database) or limited, local empirical studies. These assumptions ignore watershed condition, nutrient loading to the SCM, performance deterioration/enhancement through time and other hydrometeorological forcing (Koch et al., 2014). The model developed here uses a calibrated SCM model to test how mass removal of NO_3 and NH_4 changes with air temperature, inflow volume, and inflow N concentrations. Estimated mass removal efficiencies for both N species across all scenarios tested fell between 0.30-0.65, in line with those reported in the International Stormwater BMP Database (Geosynthetic Consultants and Wright Water Engineers, 2014). For all scenarios tested, the ensemble mean of mass removal fraction of NH_4 was greater than that for NO_3. The cause for this is likely due to the simulated algal community preferentially assimilating and removing NH_4 from the water column over NO_3 when both are in abundance. This phenomenon, which has been explored in detail by Dortch (1990), is due to the structure of the two inorganic N ions that allows NH_4 to be more readily utilized by algae.

Varying average annual air temperature from 10.7°C to 20.7°C increased the ensemble mean of the mass removal fraction of NO_3 from 0.52 to 0.61, and the mass removal fraction of NH_4 from 0.56 to 0.66 (Figure 4-6). The cause for this moderate increase in removal was increased rates of algal biomass turnover, which caused more net inorganic N uptake. This N was then converted to organic forms, which were settled and or advected from the system. The control of temperature and seasonality on the ability of these SCMs to remove N is supported by a field study by Roseen et al. (2009), who showed that removal efficiencies of inorganic N in stormwater wet ponds were lower in winter months compared to summer.

While the relationship between the efficiency of inorganic N removal and air temperature was monotonic for both species, the effect of changing nitrogen concentrations was not as clear. For NH_4, mass removal efficiency was relatively unchanged across all the simulated inflow (Figure 4-8b). Because algae preferentially assimilated NH_4 over NO_3, any additional inflow or release of NH_4 during respiration is quickly assimilated. NO_3, however, showed moderately decreased uptake when the median inflow concentrations increased above ~0.2 mg-N L-1 (Figure 4-8a). Thus, there is a threshold concentration at which algae can no longer effectively utilize additional NO_3. This result indicates that wet pond SCMs promoting algae growth have better potential to remove NH_4 at high concentrations compared to NO_3. There may also exist a threshold concentration of NH_4 where algae growth becomes saturated. This saturation has been observed in batch studies of algae treating wastewater with NH_4 at a concentrations as high as 129 mg L^{-1} (Aslan and Kapdan, 2006). However, even the scenario with the highest distribution

inflow concentrations explored here (which ranged from 0.37 - 7.0 mg-N L^{-1}), a substantial fraction (> 50%) of NH_4 was removed.

The influence of inflow volume on inorganic N mass removal was also tested. Results showed that increased inflow volume caused inorganic N removal by the SCM to decrease (Figure 4-7). This highlights that, even if N inflow concentrations remain static, N removal efficiency in wetter years is likely to decrease. Additionally, if impervious surfaces (and the increased N loading associated with them) are added to in the SCM's watershed, increases in runoff for a given rain event will also lead to a decreases in SCM N removal. Finally, the controls of permanent pool depth of the SCM on inorganic N removal were tested. Results showed that increasing the permanent pool from 0.30 m to 2.74 m increased the ensemble mean of NO_3 removal from 0.31 to 0.67 and NH_4 from 0.31 to 0.71. These changes are substantially greater than changes associated with temperature and input concentration scenarios, highlighting the importance of pond depth as a design parameter. While each additional 0.30 m of permanent pool depth led to increased N removal, the change in removal began to flatten above 1.52 m. These results are contrary to those observed by Koch et al. (2014), who found that the removal efficiency of NH_4 from individual inflow events increased in BMPs with shallower depths and lower volumes. This discrepancy could be because the Koch et al. (2014) study included both wetland and wet pond style SCMs, or because they were only able to analyze removal from individual events, rather than over a complete annual cycle.

The cause for increased inorganic N mass removal efficiency with both decreased inflow volume and deeper pool depth is likely due to the same phenomenon: the dilution of relatively N-replete inflow water by relatively N-deplete SCM water. Figure 4-10 shows that for all permanent pool depth simulations, concentrations in the pond are lower than the inflow. The same was true for the inflow volume scenarios (data not shown). For both sets of model permutations, as the ratio of SCM pool volume to inflow volume increased, so did mass removal of inorganic N. Therefore, deeper permanent pools, or similarly lower inflow volumes, allow for more dilution of the inflow volume. One reason SCMs may have lower concentrations than inflow water may be due to the prevalence of N-limited algae growth between events, a phenomena highlighted in the previous discussion of the k_{sn} parameter. Additionally, shallower permanent pools, with their decreased volume, cause the same mass of algae to exist at higher concentrations.

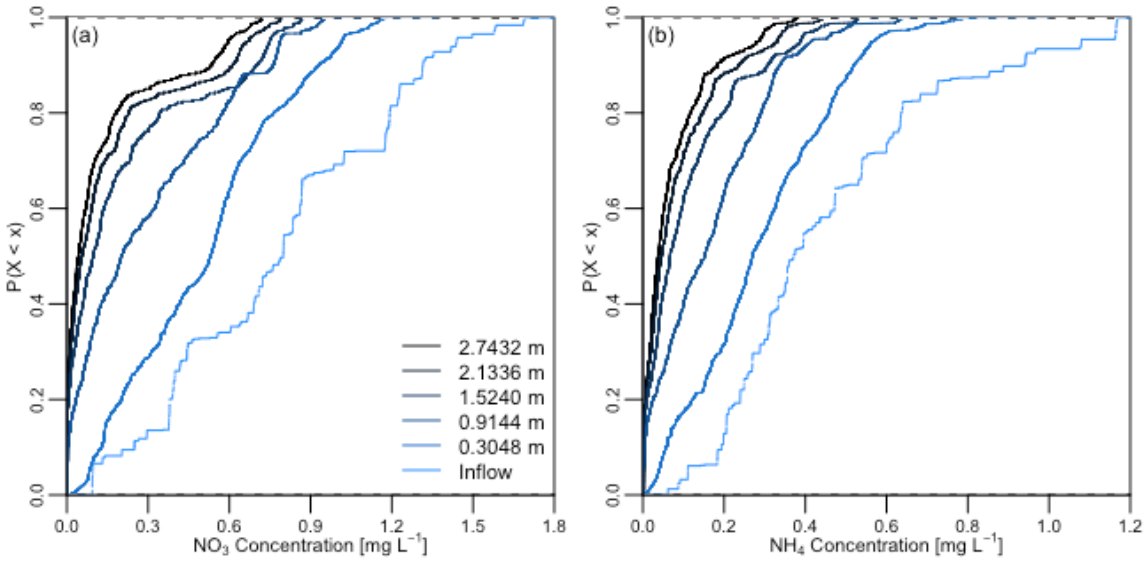

Figure 4-10: CDFs of pond concentrations of NO3 (a) and NH4 (b) at different permanent pool depths, compared to inflow concentrations.

These higher chl-a concentrations increase the effect of self-shading, which reduces light availability and limits N uptake through growth. This could lead to greater inorganic N concentrations in shallower ponds. Because most outflow occurs 1-5 days after inflow (Figure 4-2b), which are times of ample N for algae growth, biological activity over the course of the storm event is not as important for N removal as the mixing process that dilutes inflow with inter-event SCM water, which has low inorganic N concentrations.

4.6 Conclusions

The hydrologic and water quality model of a wet pond SCM described in this paper is novel because it uses eco-hydrological process, rather than a simple first order removal efficiency, to simulate retention and removal of inorganic N from urban runoff. It improves on existing watershed models of SCMs because it can account for changes in N retention due to controls hydrometeorological forcing, nutrient loading, and SCM geometric design. Because the model is installed in RHESSys, a spatially distributed watershed model, it can be used to test stormwater management scenarios at larger spatial scales. This work limited the modeling environment to just a single SCM with one upstream and two downstream patches, in order to focus on internal SCM process by controlling inputs to the SCM, rather than introducing additional variability associated with running the watershed model at the full scale. Future work will use a full RHESSys-SCM watershed model to investigate the effectiveness of multiple and spatially distributed SCMs within a watershed.

The model reproduced observed hydrology without calibration, and it simulated the distribution of outflow NO_3 and NH_4 concentrations after calibration of water quality parameters. Using a global sensitivity analysis of water quality parameters, results showed that 5 parameters dominated NO_3 and NH_4 concentrations in the SCM. These 5 parameters should be the target of empirical studies or calibration during future model applications. Additionally, results showed that model sensitivity to and uncertainty from these parameters changed with season and hydrologic condition. Notably, higher temperatures and lower inorganic N inputs increased model uncertainty to these parameters. Therefore, careful calibration is required if the model is applied in watersheds with warmer climates or low N concentrations in runoff.

Because the model is process based, it was able to simulate how changes in air temperature, inflow N concentrations, inflow water volume, and SCM design influenced the ability of the SCM to retain and remove inorganic N. Increasing air temperature caused increase removal of both NO_3 and NH_4, which has implications for the success of SCMs in different regions and under climate. However, changes in N removal efficiency, were relatively moderate over a fairly substantial (10 °C) temperature range and suggest that other factors, such as pond depth are likely to play a more substantial role in explaining variation in SCM performance within a given region and over time. Similarly, changes in inflow concentration did not affect NH_4 removal efficiency, but greater concentrations caused removal of NO_3 to slight decrease. The difference is likely due to algae preferentially assimilating NH_4 over NO_3. This implies that removal efficiency of NO_3 by SCMs in high N watersheds may decrease.

Finally, decreased inflow volumes and increased SCM permanent pool depths led to relatively large increases in inorganic N removal. Because SCM concentrations were always lower than inflow concentrations, we attribute this to increased dilution of inflow water. Additionally, model sensitivity to N uptake parameters increased during dry periods, when algae growth was N limited. Together, these results show that N removal is dependent on both the physical process of mixing of inflow and SCM water during storm events, and biological processes that reduce SCM inorganic N concentrations between events. This finding has direct implications for design of SCMs, that more water storage will result in greater inorganic N removal efficiency.

4.7 References

Ahiablame, L.M., Engel, B.A., Chaubey, I., 2012. Representation and evaluation of low impact development practices with L-THIA-LID: An example for site planning. Environment and Pollution, 1(2): 1.

Alden, K. et al., 2015. spartan: Simulation Parameter Analysis R Toolkit ApplicatioN: Spartan.

Arnold, C.L., Gibbons, C.J., 1996. Impervious surface coverage: the emergence of a key environmental indicator. Journal of the American Planning Association, 62(2): 243-258.

Arora, V.K., Boer, G.J., 2003. A Representation of Variable Root Distribution in Dynamic Vegetation Models. Earth Interactions, 7(6): 1-19.

Aslan, S., Kapdan, I.K., 2006. Batch kinetics of nitrogen and phosphorus removal from synthetic wastewater by algae. Ecol Eng, 28(1): 64-70.

Barrett, M.E., 2005. Performance Comparison of Structural Stormwater Best Management Practices. Water Environment Research, 77(1): 78-86.

Bell, C.D., McMillan, S.K., Clinton, S.D., Jefferson, A.J., In review. Hydrological Response to Stormwater Control Measures in Urban Watersheds. J Hydrol.

Bernhardt, E.S., Band, L.E., Walsh, C.J., Berke, P.E., 2008. Understanding, managing, and minimizing urban impacts on surface water nitrogen loading. Ann NY Acad Sci, 1134(1): 61-96.

Beven, K., Binley, A., 1992. The future of distributed models: model calibration and uncertainty prediction. Hydrol Process, 6(3): 279-298.

Castro, M.S., Driscoll, C.T., Jordan, T.E., Reay, W.G., Boynton, W.R., 2003. Sources of nitrogen to estuaries in the United States. Estuaries, 26(3): 803-814.

Chapra, S.C., 2008. Surface water-quality modeling. Waveland Press, Inc., Long Grove, IL.

City of Charlotte, 2015. City of Charlotte NPDES MS4 Permit Program Stormwater Management Program Plan.

Clarke, R.T., 1999. Uncertainty in the estimation of mean annual flood due to rating-curve indefinition. J Hydrol, 222(1–4): 185-190.

CMSWS, 2015. LSC Hidden Valley North Tryon Wet Pond Project - Final Monitoring Report, Charlotte-Mecklenburg Stormwater Services, Charlotte, NC.

CMSWS, 2016. City of Charlotte - Pilot Stormwater Control Measure (SCM) Program.

Collins, K.A. et al., 2010. Opportunities and challenges for managing nitrogen in urban stormwater: A review and synthesis. Ecol Eng, 36(11): 1507-1519.

Delignette-Muller, M.L., Dutang, C., 2014. fitdistrplus: An R Package for Fitting Distributions. J. Stat. Softw, 64(4): 1-34.

Dortch, Q., 1990. The interaction between ammonium and nitrate uptake in phytoplankton. Marine ecology progress series. Oldendorf, 61(1): 183-201.

Driscoll, E.D., Palhegyi, G.E., Strecker, E.W., Shelley, P.E., 1989. Analysis of storm event characterisitcs for selected rainfall gages throughout the United States. In: EPA (Ed.), Oakland, CA.

Dunne, T., Leopold, L.B., 1978. Water in environmental planning. New York, 818p.

Geosynthetic Consultants, I., Wright Water Engineers, I., 2014. International Stormwater Best Management Practices (BMP) Database Pollutant Category Summary Statistical Addendum: Solids, Bacteria, Nutrients, and Metals, http://www.bmpdatabase.org/.

Green, W.H., Ampt, G., 1911. Studies on Soil Phyics. The Journal of Agricultural Science, 4(01): 1-24.

Groffman, P.M. et al., 2002. Soil Nitrogen Cycle Processes in Urban Riparian Zones. Env Sci Tech, 36(21): 4547-4552.

Groffman, P.M., Law, N.L., Belt, K.T., Band, L.E., Fisher, G.T., 2004. Nitrogen fluxes and retention in urban watershed ecosystems. Ecosystems, 7(4): 393-403.

Hale, R., Turnbull, L., Earl, S., Childers, D., Grimm, N., 2015. Stormwater Infrastructure Controls Runoff and Dissolved Material Export from Arid Urban Watersheds. Ecosystems, 18(1): 62-75.

Howarth, R.W. et al., 1996. Regional nitrogen budgets and riverine N & P fluxes for the drainages to the North Atlantic Ocean: Natural and human influences. In: Howarth, R. (Ed.), Nitrogen Cycling in the North Atlantic Ocean and its Watersheds. Springer Netherlands, pp. 75-139.

Hunt, W., Smith, J., Jadlocki, S., Hathaway, J., Eubanks, P., 2008. Pollutant Removal and Peak Flow Mitigation by a Bioretention Cell in Urban Charlotte, N.C. J Environ Eng-ASCE, 134(5): 403-408.

Hunt, W.F., Davis, A.P., Traver, R.G., 2012. Meeting Hydrologic and Water Quality Goals through Targeted Bioretention Design. J Environ Eng-ASCE, 138(6): 698-707.

Hydroscience Inc., 1979. A statistical method for assesment of urban stormwater loads - impacts - controls. In: EPA (Ed.), Washington, D.C.

Karl, T.R., Melillo, J.M., Peterson, T.C. (Eds.), 2009. Global climate change impacts in the United States. Cambridge University Press.

Kearney, M.A., Zhu, W., Graney, J., 2013. Inorganic nitrogen dynamics in an urban constructed wetland under base-flow and storm-flow conditions. Ecol Eng, 60: 183-191.

Koch, B.J., Febria, C.M., Gevrey, M., Wainger, L.A., Palmer, M.A., 2014. Nitrogen Removal by Stormwater Management Structures: A Data Synthesis. J Am Water Resour As, 50(6): 1594-1607.

Landsberg, J.J., Waring, R.H., 1997. A generalised model of forest productivity using simplified concepts of radiation-use efficiency, carbon balance and partitioning. Forest Ecology and Management, 95(3): 209-228.

Leopold, L.B., 1968. Hydrology for urban land planning: A guidebook on the hydrologic effects of urban land use. USGS Circular 554.

Malcom, H.R., 1989. Elements of urban stormwater design. North Carolina State University, Raleigh, NC, USA.

Mallin, M.A., Ensign, S.H., Wheeler, T.L., Mayes, D.B., 2002. Pollutant Removal Efficacy of Three Wet Detention Ponds. J. Environ. Qual., 31(2): 654-660.

Marino, S., Hogue, I.B., Ray, C.J., Kirschner, D.E., 2008. A methodology for performing global uncertainty and sensitivity analysis in systems biology. Journal of Theoretical Biology, 254(1): 178-196.

McKay, M.D., Beckman, R.J., Conover, W.J., 1979. Comparison of Three Methods for Selecting Values of Input Variables in the Analysis of Output from a Computer Code. Technometrics, 21(2): 239-245.

McKim & Creed, I., 2006. Hidden Valley Pond Discharge Orifice.

Millard, S.P., 2013. EnvStats, an R Package for Environmental Statistics. Wiley Online Library.

Mittman, T., Band, L.E., Hwang, T., Smith, M.L., 2012. Distributed Hydrologic Modeling in the Suburban Landscape: Assessing Parameter Transferability from Gauged Reference Catchments1. J Am Water Resour As, 48(3): 546-557.

Monteith, J., 1965. Evaporation and environment, Symposium Society Experimental Biology on The State and Movement of Water in Living Organisms, pp. 205-234.

Parton, W. et al., 1996. Generalized model for N2 and N2O production from nitrification and denitrification. Global Biogeochem Cy, 10(3): 401-412.

Peierls, B.L., Caraco, N.F., Pace, M.L., Cole, J.J., 1991. Human influence on river nitrogen. Nature, 350(6317): 386-387.

Pelletier, G., Chapra, S., 2003. QUAL2K: a modeling framework for simulating river and stream water quality: documentation and users manual. Civil and Environmental Engineering Dept., Tufts University, Medford, MA.

R Core Team, 2014. R: A language and environment for statistical computing. R Foundation for Statistical Computing, Vienna, Austria.

Riley, G.A., 1956. Oceanography of Long Island Sound, 1952-54, 15. Bingham Oceanographic Laboratory.

Roesner, L., Bledsoe, B., Brashear, R., 2001. Are best-management-practice criteria really environmentally friendly? Journal of Water Resources Planning and Management, 127(3): 150-154.

Roseen, R.M. et al., 2009. Seasonal Performance Variations for Storm-Water Management Systems in Cold Climate Conditions. J Environ Eng-ASCE, 135(3): 128-137.

Rossman, L.A., 2015. Storm water management model user's manual, version 5.1. National Risk Management Research Laboratory, Office of Research and Development, US Environmental Protection Agency Cincinnati.

Running, S.W., Hunt, E.R., 1993. Generalization of a forest ecosystem process model for other biomes, BIOME-BGC, and an application for global-scale models. Scaling physiological processes: Leaf to globe: 141-158.

Shields, C., Tague, C., 2014. Ecohydrology in semiarid urban ecosystems: Modeling the relationship between connected impervious area and ecosystem productivity. Water Resour Res: n/a-n/a.

Shields, C.A., Tague, C.L., 2012. Assessing the Role of Parameter and Input Uncertainty in Ecohydrologic Modeling: Implications for a Semi-arid and Urbanizing Coastal California Catchment. Ecosystems: 1-17.

Steele, J.H., 1962. Environmental control of photosynthesis in the sea. Limonology and Oceanography, 7(2): 137-150.

Stefan, H.G., Preud'homme, E.B., 1993. Stream temperature estimatino from air temperature. J Am Water Resour As, 29(1): 27-45.

Tague, C., Pohl-Costello, M., 2008. The Potential Utility of Physically Based Hydrologic Modeling in Ungauged Urban Streams. Annals of the Association of American Geographers, 98(4): 818-833.

Tague, C.L., Band, L.E., 2004. RHESSys: regional hydro-ecologic simulation system-an object-oriented approach to spatially distributed modeling of carbon, water, and nutrient cycling. Earth Interactions, 8(19): 1-42.

Taylor, G.D., Fletcher, T.D., Wong, T.H.F., Breen, P.F., Duncan, H.P., 2005. Nitrogen composition in urban runoff—implications for stormwater management. Water Res, 39(10): 1982-1989.

Wong, T.H.F., Fletcher, T.D., Duncan, H.P., Coleman, J.R., Jenkins, G.A., 2002. A Model for Urban Stormwater Improvement Conceptualisation, Global Solutions for Urban Drainage, Portland, Oregon, pp. 1-14.

Wurbs, R.A., James, W.P., 2002. Water resources engineering. Prentice Hall Upper Saddle River, NJ.

Yi, X., Zou, R., Guo, H., 2016. Global sensitivity analysis of a three-dimensional nutrients-algae dynamic model for a large shallow lake. Ecological Modelling, 327: 74-84.

CHAPTER 5. MODELING CHANGES IN HYDROLOGY AND NITROGEN EXPORT BY CONNECTING URBAN IMPERVIOUS SURFACES TO STORMWATER CONTROL MEASURES

5.1 Abstract

The addition of impervious surfaces during urban development increases runoff and nutrient loads. The problems of impervious surfaces are exaggerated by storm pipe networks that directly connect them to streams, because pipe networks bypass many of the urban ecological zones where important hydrologic and biogeochemical process occur. Stormwater control measures (SCMs) are a management strategy that disrupts the connectivity between urban impervious surfaces and stream networks, and aims to restore the beneficial processes that are lost during urbanization. This work uses a RHESSys model of a watershed in Charlotte, NC to simulate runoff under different scenarios of urban surface connectivity to SCMs to develop a simple predictive relationship between watershed condition and N loads. The metric unmitigated imperviousness (UI), which is the percent of the watershed area covered by an impervious surface that is unmitigated by SCMs, quantified watershed condition. Result showed that as SCM mitigation decreased, or as UI increased from 3% to 15%, runoff ratios and nitrite+nitrate (NO_x) and total dissolved nitrogen (TN) loads increased by 26% (21-32%), 14% (3-26%) and 13% (2-25%), respectively. The shape of the relationship between these variables and UI was linear, which indicates that mitigation of any impervious surfaces will result in

proportional reductions at the range of UI in this study. Loads of ammonium (NH_4), however, decreased linearly with increases in UI, demonstrating that increased SCM mitigation increased stream NH_4 concentrations drastically enough to overcome reductions in water runoff volumes. The simulated change in NH_4 loads between the most and least mitigation scenarios was -37% (-73% to +37%). These results have implications for watershed managers seeking to reduce impacts to stream and lake ecosystems from impervious surface runoff by mitigating them with SCMs

5.2 Introduction

During the process of urbanization, the land surface is covered with roads, parking lots and buildings necessary to support the urban economy. These impervious surfaces limit the infiltration of rainfall and cause increased runoff volumes during more frequent and intense flood events, which negatively impact stream ecosystems (Leopold, 1968; Arnold and Gibbons, 1996; Paul and Meyer, 2001; O'Driscoll et al., 2010). While the extent of urban impervious surfaces is an important control on watershed scale hydrology, the hydrologic connectivity of these surfaces to stream networks through constructed drainage channels and storm sewers is also very important (Alley and Veenhuis, 1983; Shuster et al., 2005; Walsh et al., 2005; Walsh and Kunapo, 2009; Dewals et al., 2012; Shields and Tague, 2014; Bell et al., In review-a). These drainage networks cause runoff, rich in nutrients like nitrogen (N), to bypass biologically active zones in both the terrestrial and riparian environments, which limits the ability of urban ecosystems to remove or retain the excess nutrients imported as food and fertilizer (Groffman et al.,

2004; Hatt et al., 2004; Bernhardt et al., 2008; Kaushal and Belt, 2012; Duncan et al., 2013).

Stormwater control measures (SCMs) are a management strategy aimed at interrupting the connectivity of urban impervious surfaces and the stream network. Some examples of SCMs are detention ponds, constructed wetlands, or smaller bioretention basins that collect and store stormwater runoff in a surface depression. This stored runoff is temporarily retained until it leaves the SCM as surface outflow through a designed outlet structure, infiltration or evaporation. Retention of water in SCMS decreases the connectivity between urban surfaces and the streams, and has the potential to reduce peak discharges and discharge response times (Horner et al., 2001; Villarreal et al., 2004; Hood et al., 2007; Jarden et al., 2015). Water stored in SCMs may also evaporate. The presence of SCMs has been shown to reduce total runoff volumes in urban watersheds (Gagrani et al., 2014; Hale et al., 2015).

Additionally, SCMs may increase water and nutrient residence times, promoting biological activity, and ultimately reducing nutrient export by urban streams. SCMs are typically vegetated, and this vegetation has the potential to uptake dissolved N from the retained stormwater. Some SCMs retain a permanent pool of water, which allows aquatic algae communities to also assimilate N, removing it from the water column. Because SCMs receive runoff during storm events, they have very dynamic hydrologic conditions. This, in turn, creates rapidly changing redox conditions in pond sediments that can promote the microbial processes of nitrification and denitrification that can also lead to

removal of N. Together, these processes within SCMs may reduce concentrations of N in outflow compared to inflow, although the amount of reduction is highly variable (Mallin et al., 2002; Barrett, 2005; Hunt et al., 2008; Collins et al., 2010; Kearney et al., 2013; Geosynthetic Consultants and Wright Water Engineers, 2014; Koch et al., 2014).

There is a large body of research that documents the relationship between the percentage of watershed area covered by impervious surfaces, typically referred to as total imperviousness (TI), and changes to hydrologic and water quality regimes (see reviews by Arnold and Gibbons (1996); Brabec (2009)). A smaller number of studies have examined the role of connectivity of these surfaces by relating stream hydrology and water quality to a watershed's effective imperviousness (EI). EI is the fraction of watershed area that is covered by an impervious surface that is directly connected to the stream network through artificial drainage. Modeling studies have shown that EI is an important factor for predicting hydrologic behavior, but less is know about the controls on water quality (Lee and Heaney, 2003; Guo, 2008; Dewals et al., 2012; Shields and Tague, 2014). SCMs are designed to restore hydrographs to mimic the hydrographs prior to development (Roesner et al., 2001). Therefore, the mitigation of impervious areas with SCMs could be a way to effectively disconnect impervious areas from the stream, and therefore reduce EI (Walsh et al., 2005). However, the effect of disconnecting impervious surfaces through the use of SCMs is less well documented.

This work uses RHESSys, a fully distributed, process-based watershed model, to develop an empirical relationship between a metric that describes both urban impervious surface

connectivity and mitigation to watershed response, quantified by water runoff and nitrogen export. The watershed metric unmitigated imperviousness (UI), a is the fraction of the watershed populated by impervious surfaces that are connected directly to the stream by storm pipes. This excludes impervious surfaces that are mitigated by SCMs or that are undrained by storm infrastructure. This metric is analogous to EI and it quantifies the interaction of impervious surfaces and their connection to either SCMs or the stream directly. Bell et al. (In review-a) found UI to be the best of a suite of urban impervious surface connectivity metrics at predicting hydrologic record flashiness. Since UI is inherently bounded by the watershed's TI, the ratio of the two (UI/TI) is another metric that characterizes the fraction of TI that is directly connected to the stream. This is analogous to directly connected impervious area (DC, DCI, or DCIA) used in other studies analyzing the effects of EI on hydrology and stream ecosystem health (Lee and Heaney, 2003; Walsh et al., 2005; Walsh and Kunapo, 2009; Shields and Tague, 2014).

Because RHESSys is spatially explicit, it can systematically change connectivity of urban surfaces between SCMs or the stream network directly at a very high spatial resolution. This allows for rigorous testing different connectivity scenarios. Additionally, because RHESSys is process based, it can simulate the dynamic effects that SCMs have on water quantity and quality across seasons, storm event sizes, and antecedent conditions. Therefore the goal of the study is to use RHESSys to characterize the relationship between connectivity of impervious surfaces (expressed though UI) and hydrologic and water quality regimes by systematically varying connectivity of a residential watershed in Charlotte, NC. Identifying this relationship will provide managers with insights on what

levels of SCM implementation that can be targeted to effectively disconnect urban impervious surfaces and to protect stream ecosystems.

5.3 Methods

5.3.1 Site Description

The Beaverdam Creek (BD) watershed is an actively urbanizing watershed in Charlotte, North Carolina that has been the subject of a 10-year stormwater monitoring effort by Charlotte-Mecklenburg Stormwater Services (CMSWS) and documented by Allan et al. (2013). BD consists of 5 subwatersheds, of which the subwatershed named "BD4" is the

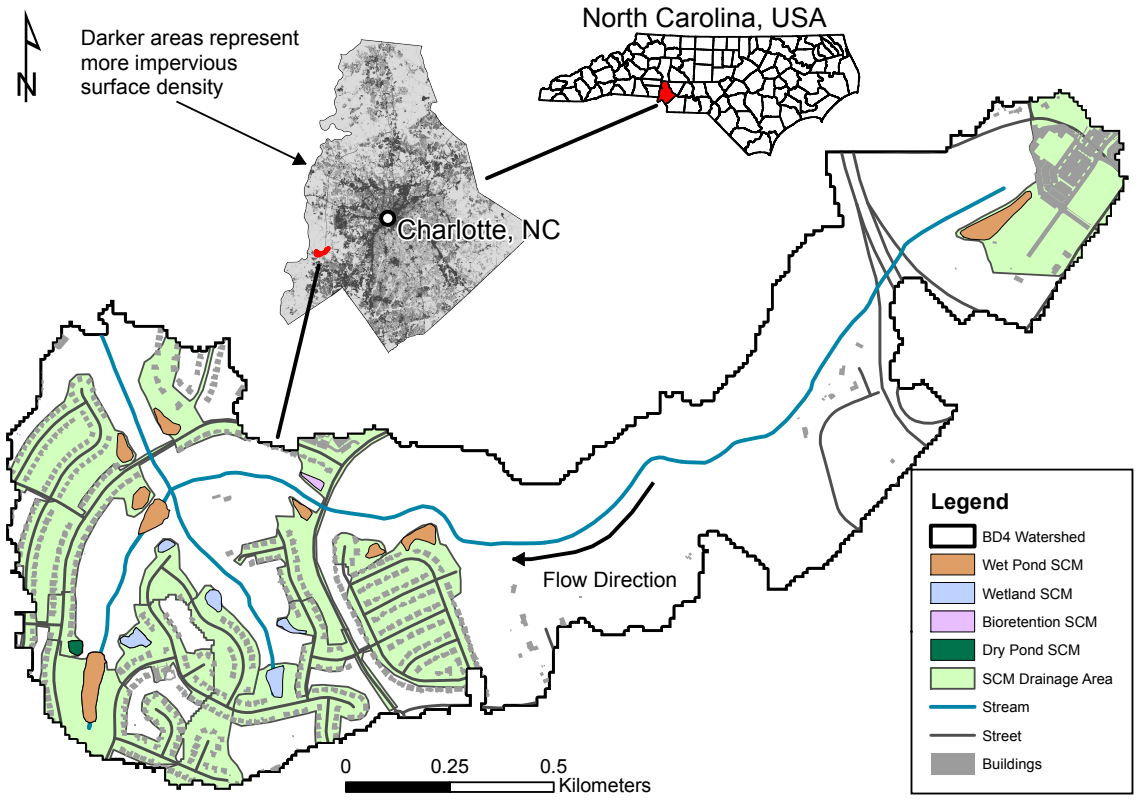

Figure 5-1: Map of BD4, showing location of SCMs and the urban surfaces that they mitigate

most developed. BD4 is the subject of this study, and has also been studied in the past by Gagrani et al. (2014). BD4 is a 1.7 km^2 in area and is built out with a medium-density residential neighborhood in the lower watershed, and an interstate exchange and commercial shopping center in the upper watershed (Figure 5-1). These impervious surfaces, which cover 15% of the watershed, are treated by a total of 16 SCMs: 1 dry pond, 1 bioretention basin, 5 wetlands, and 9 wet ponds. Soils in the BD4 watershed are generally sandy clay and sandy loams, with a dominant "B" hydrologic soils group classification (USDA-NRCS, 2010). The middle of the watershed was largely undeveloped at the time of the study, although has since been developed. A 70-100 m forested buffer populates the riparian areas along the BD4 channel

5.3.2 Model Description

A Regional Hydro-Ecological Simulation System (RHESSys) watershed model was used to simulate hydrological and ecological process in the BD4 watershed. RHESSys is an open-source computer model documented by Tague and Band (2004), but has been expanded significantly since then. This study used a version of RHESSys that includes routines that simulate the hydrologic and ecological processes within SCMs in addition to terrestrial processes (available at: https://github.com/RHESSys/RHESSys/tree/scm) (Bell et al. In review-b)

RHESSys is fully distributed in space, and simulates processes that affect cycling and advection of water, C and N. The "patch" is the fundamental spatial unit used by RHESSys to simulate these processes. Each patch is populated by consistent soil,

vegetation, and topographic properties. Subsurface water is routed between adjacent patches based on topographic and soil characteristics. The amount of subsurface water routed to downslope patches is computed using an exponential transmissivity decay model. This subsurface water can migrate to one or more downstream patches. Surface water that exceeds infiltration potential and a parameterized detention storage depth is immediately routed to downstream patches. SCM patches retain ponded surface water for longer periods of time, at a depth parameterized by the design of the SCM outlet structure. Outflow from the SCM through the outlet structure is modeled based on a series of weir and orifice equations (Bell et al., In review-b). At this time, RHESSys does not explicitly simulate discharge in storm pipes. However, it does have the ability to route surface flow between any two (or more), non-adjacent patches which approximates the connectivity of storm pipes.

RHESSys also simulates vertical redistribution of water within patches. This includes evaporation from surface detention stores (for example, from SCMs) and soil and transpiration by vegetation. Both evaporation and transpiration are modeled using that of Penman-Monteith (Monteith, 1965). Infiltration into the soil profile is model by the Green-Ampt equation (Green and Ampt, 1911). Infiltrated water moves vertically through subsequent soil layers including a root zone layer, saturated and unsaturated soil layers, and a deep groundwater reservoir.

RHESSys also models vegetation processes including C and N uptake during photosynthesis, and subsequent release during litterfall and respiration in each patch.

RHESSys allocates assimilated C and N to different physiological stores, based on parameters described by White et al. (2000). These vegetative processes are analogous to those modeled by dynamic global vegetation models including CTEM, 3PG and Biome-BGC (Running and Hunt, 1993; Landsberg and Waring, 1997; Arora and Boer, 2003). RHESSys simulates diffuse and direct radiation attenuation through the vegetation canopy using Beer's law. Litter decomposition and soil respiration follow the routines of Biome-BGC (Running and Hunt, 1993), and microbial N cycling follows that of Century N-GAS (Parton et al., 1996). In addition to terrestrial vegetation, this version of RHESSys also simulates the carbon and nitrogen cycling of algae in the aquatic ecosystem within the SCMs (Bell et al., In review-b). Algae uptake inorganic forms of N from the water column during photosynthesis, release ammonium (NH_4) during respiration, and release dissolved organic forms of C and N during death.

5.3.3 Data

To construct the distributed model of the BD4 watershed, spatial data describing the soils, vegetation coverage, location of impervious surfaces, location of SCMs, and pipe network connectivity was obtained. Soil data was taken from the NRCS's Web Soil Survey (Soil Survey Staff, 2013), and vegetation data from North Carolina University's Gap Analysis Program database (http://www.basic.ncsu.edu/ncgap/). There were five major classes of vegetation in the watershed: coniferous forest, deciduous forest, riparian forest, lawns, and non-vegetated areas. The allometry and phenology of these five vegetation classes were parameterized from the RHESSys vegetation default file database.

A digital elevation model, an impervious surface coverage map, and pipe network data were downloaded from the Mecklenburg County Open Mapping GIS database (http://maps.co.mecklenburg.nc.us/openmapping/). Because the landscape within BD4 is actively changing, spatial data that best described the watershed during 2009 water year was used in all cases. Spatial data that did not match BD4 during this time period was manually altered using high-resolution aerial photography from 2009, also downloaded from Mecklenburg county database. The aerial photography was also used to identify the locations of the 16 SCMs. Field surveys were used to characterize the geometry of these SCMs, specifically the design of outlet structure. Bell et al. (In review-b) contains a list of geometric parameters required to describe an SCM.

From these spatial datasets, a map of patches with consistent soil, land cover, and topography was constructed. The BD4 watershed was discretized into 10 x 10 m square patches. This allowed for explicit routing between urban surfaces at a relatively high spatial resolution. An exception to this patch size was the SCM patches, for which the patch area was equal to the footprint of the existing SCM. RHESSys uses files called "flowtables" to specify the subsurface and surface routing between patches based on topographic position. However, stormwater infrastructure in urban environments often routes water across the boundaries of these topographical subwatersheds. Therefore, the surface flowtables were altered to reflect the routing between urban impervious surfaces and the SCM subwatersheds in the existing watershed. To do this, the subwatersheds of each SCM were manually delineated using the digital elevation model, storm network pipe data, site design plans, and field visits (Figure 5-1). Additionally, the flowtable

Table 5-1: List of time series data sources used to force and calibrate the BD4 model. When necessary, we aggregate data from multiple sites to form a single composite record. The composition method is also listed.

Parameter(s)	Source	Site ID(s) Used	Composition Method	Reference/Repository
Hourly rainfall, daily rain duration	USGS Charlotte-Mecklenburg Rainfall Record	350623080583801 35084208057280	Theissen Polygon	http://nc.water.usgs.gov/char/rainfall.html
Daily wet NO_3 and NH_4 deposition	National Atmospheric Deposition Program: NTN	BA41 NC25 NC36 NC45 SC06	Inverse-Distance Weighted Average, only applied on days with rainfall at BD4	http://nadp.isws.illinois.edu/data/ntn/
Daily dry NO_3 and NH_4 deposition	EPA Clean Air Status and Trends Network (CASTNET)	ESP127 GAS153 COW137 PNF126 CND125	Inverse-Distance Weighted Average	http://java.epa.gov/castnet/clearsession.do
Daily maximum and minimum air temperature	NOAA National Climatic Data Center	KCLT	--	http://www.ncdc.noaa.gov/
Daily discharge	Beaverdam Creek Watershed Monitoring Report	BD4	--	Allan et. al (2013)
Monthly NO_3, NH_4, and TN export	Beaverdam Creek Watershed Monitoring Report	BD4	--	Allan et. al (2013)

was edited to reflect impervious surfaces connected to the stream directly, i.e. not to mitigated by an SCM.

Table 5-1 lists the time series data from 2009 and data sources used to drive and calibrate the model. Hourly rainfall, daily wet and dry N deposition, and daily air temperature forced the model. The model was calibrated using observed daily discharge and monthly nitrogen export data. In some cases, time series from observed data at multiple collection sites were aggregated into one record to account for large distances between sampling points and the watershed (e.g., N deposition data) or spatial heterogeneity within the watershed (e.g., rainfall).

5.3.4 Hydrologic calibration and parameter uncertainty estimation

Prior to calibration, soil stores of C and N were spun up by simulating the model for a period of 600 years until soil state variable varied by < 5% over a 10 year period. Additionally, vegetation nitrogen and carbon stores were spun up for a period of 20 years, as this correlates to the age of the riparian forest. Repeated input data from the 2000-2010 water years forced the model during spin up. Then, a Monte Carlo calibration approach, along with a Generalized Likelihood Uncertainty Estimation (GLUE) was used to assess uncertainty of the calibrate parameters (Beven and Binley, 1992). For the Monte Carlo simulations, 10,000 sets of seven groundwater parameters were generated using a Latin Hypercube Sampling (LHS) (McKay et al., 1979) technique in “spartan” package in R (Alden et al., 2015). Table 5-2 contains a description of the calibrated groundwater parameters.

Table 5-2: Description and range of groundwater parameters varied during hydrologic calibration

Parameter	Description	Unit	Parameter Value Range*	Scalar Low	Scalar High
k	Saturated hydraulic conductivity at the ground surface	m d^{-1}	0.731-1.55	0.1	2000
svalt1	Pore size index (PSI)	unitless	0.088-0.204	0.5	2
svalt2	PSI air entry pressure	m	0.218-0.630	0.5	2
Parameter	Description	Unit		Parameter Low	Parameter High
gw1	Fraction of rainwater bypassing rootzone to deeper reservoir	unitless		0	0.05
gw2	Drainage coefficient from deeper reservoir	d^{-1}		0	0.1
m	Decay of saturated hydraulic conductivity with depth	m^{-1}		0.1	1.2
depth	Depth of soil profile	m		1	10

***** These parameters are dependent on soil type, which varied spatially. We report the range of parameter values across soil types, and the scalar applied to each of these spatially distributed values.

The GLUE framework was used to quantify uncertainty in LHS-generated hydrologic parameter sets. This framework is quasi-Bayesian, and acknowledges that multiple parameters sets could reasonably predict streamflow. Therefore, rather than producing one optimum parameter set, GLUE produces a range of parameters, which are subsequently used during simulation experiments. To perform the GLUE procedure, an initial, or "prior", distribution of likelihood must be assigned to all parameter sets. The likelihood of all parameters was assumed to follow uniform distributions, and the ranges of the 7 distributions are shown in Table 5-2. Next, calibration simulations that spanned the 2008 and 2009 water years were run using all 10,000 parameters sets. The 2008 water year was used as a spin up period only, and the 2009 water year was used to compare simulated and observed daily discharge. Next, goodness-of-fit statistics were computed between simulated and observed watershed discharge at a daily timestep for all

10,000 simulations. Two goodness-of-fit statistics were computed: the Nash-Sutcliffe Efficiency of daily discharge (NSE) (Nash and Sutcliffe, 1970) and the percent bias of annual stream discharge (PBIAS). Next, a standard of performance that produced acceptable model results was determined. The performance standard was that the NSE must be at least 0.3 and PBIAS must be between -15% and +15%. Any parameter sets that did not meet this two-part standard were discarded from further analysis. Only 10 of the 10,000 parameter sets met these performance criteria. The 10 parameter sets retained populated the "posterior" distribution.

The next step of the GLUE methodology is to determine a likelihood measure of all the acceptable parameter sets. The likelihood measure combined the two goodness-of-fit statistics (NSE and PBIAS) combined, as shown in Equation 5.1:

$$L_i = \frac{NSE_i - \min(NSE)}{\max(NSE) - \min(NSE)} * \frac{\max(|PBIAS|) - |PBIAS_i|}{\max(|PBIAS|) - \min(|PBIAS|)} \qquad \text{(Eq. 5.1)}$$

where L is the likelihood measure of each posterior parameter set i, and *max()* and *min()* represent the maximum and minimum of the specified goodness-of-fit statistics. Next, a likelihood weight was determined by rescaling all the posterior L values so that their sum was equal to 1. Finally, these weights were used to perform a weighted average across all of the model output variable. This weighted average is called the ensemble mean.

The GLUE methodology can also be used to assess model sensitivity to parameters. Following the Hornberger-Spear-Young method (Hornberger and Spear, 1981; Young, 1983), comparing cumulative density functions (CDF) of the prior and posterior

parameter likelihood distributions informs model sensitivity to these parameters: the greater the differences in CDFs indicates greater sensitivity.

5.3.5 Water quality validation

Once hydrologic calibration had been completed, the model predictions were compared to observed monthly export and average concentrations of three N parameters: nitrate+nitrite (NO_x), ammonium (NH_4), and total dissolved nitrogen (TN). TN was assumed to be equal to the sum of NO_x, NH_4 and dissolved organic nitrogen. Allan et al. (2013) was the source of observed N export data. To express uncertainty in the validation simulations, all 10 acceptable groundwater parameters were paired with 25 water quality parameter sets that control algae C and N cycling within the SCMs. These 25 SCM water quality parameters were randomly selected from the 246 parameter sets deemed acceptable by a previous GLUE analysis that used the SCM routines in RHESSys to simulate inorganic N processing in a single SCM in Charlotte, NC (Bell et al., In review-b). Only 25 of the 246 acceptable parameter sets, or approximately 10%, were taken from the Bell et al. (In review-b) study to limit model run time. This produced a total of 250 simulations for validation: 10 groundwater parameters sets each paired to one of the 25 water quality parameter sets. The validation simulations also spanned the 2008 and 2009 water years, and output from the second year of simulation was compared to observations. Modeled seasonal patterns were evaluated by computing the Pearson's correlation coefficient (r) between observed and simulated monthly export and

concentration. The PBIAS mass export over the 2009 water year is reported to quantify the accuracy of modeled annual export.

5.3.6 Watershed connectivity scenario testing

To test how connectivity of impervious surfaces changed hydrologic and water quality regimes, the surface flowtable used in calibration was systematically altered to reflect different levels of UI/TI, and subsequently UI. Twenty-one different flow tables reflected BD4 realizations that span a range of UI/TI from 0.21-1.0 (Table 5-3). All 21

Table 5-3: Summary of the watershed impervious surface connectivity scenarios

Simulation	TI [%]	Interstate Impervious Surfaces [%]	Fraction of other* impervious surfaces connected to stream (x) [%]	Fraction of other impervious surfaces connected to SCM (1-x) [%]	UI [%]	UI/TI [%]
Existing	15	3.2	0	69†	12	75
1	15	3.2	0	100	15	100
2	15	3.2	5.0	95	15	96
3	15	3.2	10	90	14	92
4	15	3.2	15	85	14	88
5	15	3.2	20	80	13	84
6	15	3.2	25	75	12	80
7	15	3.2	30	70	12	76
8	15	3.2	35	65	11	72
9	15	3.2	40	60	11	68
10	15	3.2	45	55	10	65
11	15	3.2	50	50	9.3	61
12	15	3.2	55	45	8.7	57
13	15	3.2	60	40	8.1	53
14	15	3.2	65	35	7.5	49
15	15	3.2	70	30	6.9	45
16	15	3.2	75	25	6.3	41
17	15	3.2	80	20	5.7	37
18	15	3.2	85	15	5.1	33
19	15	3.2	90	10	4.5	29
20	15	3.2	95	5.0	3.9	25
21	15	3.2	100	0	3.2	21

* Other refers to impervious surfaces not associated with the interstate. This includes the residential and commercial areas treated by SCMs in the existing watershed (Figure 5-1)

† This value is not 100% because we assumed 50% of the rooftops were connected directly to the SCM via downspouts, and the other 50% drained to adjacent pervious surfaces.

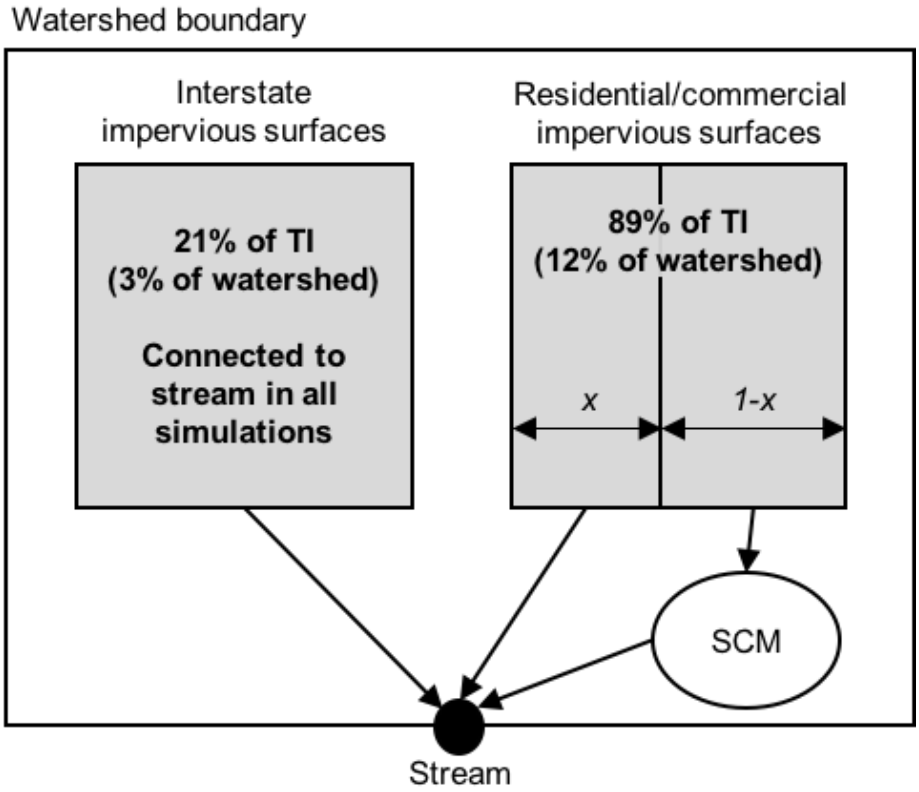

Figure 5-2: Graphical description of impervious surfaces (grey) connectivity scenarios. In all case, impervious surfaces associated with the interstate exchange were connected directly to the stream. We varied the parameter "x", which is the fraction of impervious surfaces mitigated by SCMs in the actual watershed, from 0 to 100%. The relative area of the boxes are not to scale

simulations used a TI of 15%. In all cases, the impervious surfaces associated with the interstate exchange in the middle part of BD4 were left disconnected to SCMs (Figure 5-1). This area accounts for the lowest UI/TI of all simulations being equal to 21%. These surfaces were never mitigated in the model because there is no SCM in the existing watershed. The 21 flowtables were manipulated so that impervious surfaces mitigated by SCMs in the actual watershed were routed either to an SCM or the stream directly. Figure 5-2 contains a graphical description of how connectivity varied across these 21

scenarios. The ratio of impervious surfaces that were connected to the stream (x) vs. SCM (1-x) were consistent between the sub watersheds of al 16 SCMs. For example, for simulation 2 (Table 5-3), 5% of the impervious surfaces in each of the 16 SCM subwatersheds was routed to the stream, whereas the remaining 95% was routed to the SCM. Impervious surface patches routed to the stream or to SCM were selected randomly. The result of these routing scenarios were 21 realizations of the BD4 watershed with UI values ranging from 0.3 to 0.15 (Table 5-3).

RHESSys then simulated water and N export for these 21 watershed connectivity scenarios for the 2008-2009 water years. To account for uncertainty in calibrated parameters, each of the 21 scenarios was parameterized with the 250 hydrologic and water quality parameter sets used in model validation. From these 250 simulations, hydrologic changes were determined by annual rainfall-runoff ratios, annual surface evaporation, and monthly surface evaporation for the 2009 water year. The mean value and one standard deviation from across the 250 simulations per each connectivity scenario is reported here. Flow duration curves were plotted to qualitatively characterize the hydrologic regimes. For clarity, only the mean of the 250 simulations from three UI scenarios is reported: scenarios 1, 11 and 21 (Table 5-3). Annual loads of NO_x, NH_4 and TN were also computed for each of the connectivity scenarios. As with the hydrologic variables, the mean and standard deviation of the 250 simulations for each connectivity scenario are reported.

5.4 Results

5.4.1 Hydrologic calibration, sensitivity analysis, and uncertainty estimation

During hydrologic calibration, only 10 of the 10,000 groundwater parameter sets met the performance criteria. The NSE and PBIAS of the 10 accepted parameters ranged from 0.301-0.338 and 8.7-14.9%, respectively. All acceptable parameter sets were greater than zero, which indicates the model consistently overestimates discharge. Figure 5-3 summarizes the simulated daily discharge for all 10,000 simulations, and compares them to observed. Comparing the posterior ensemble mean (red line) to observed discharges (black line) shows that that model tends to under predict high flows. Specifically, the model under predicted the peak of all 9 of the highest discharge events. Additionally, the model tends to extend recession of hydrograph over a period much longer than observed. These elevated hydrograph tails are the source for the overestimated total discharge volume.

Figure 5-3 also shows the range between the 5-95th percentiles of simulated discharge of the prior 10,000 simulations and only the posterior 10 simulations. The width of these 5-95th ensembles is substantially reduced for the posterior simulation compared to the prior. On average, the posterior ensemble is 0.807 mm narrower than the prior, with a maximum contraction of 11.3 mm on 6/4/2009. Figure 5-4 shows the differences in cumulative distribution functions (CDF) of all 7 hydrologic parameters between the prior and posterior distributions. A greater change in the CDFs indicates that the model is

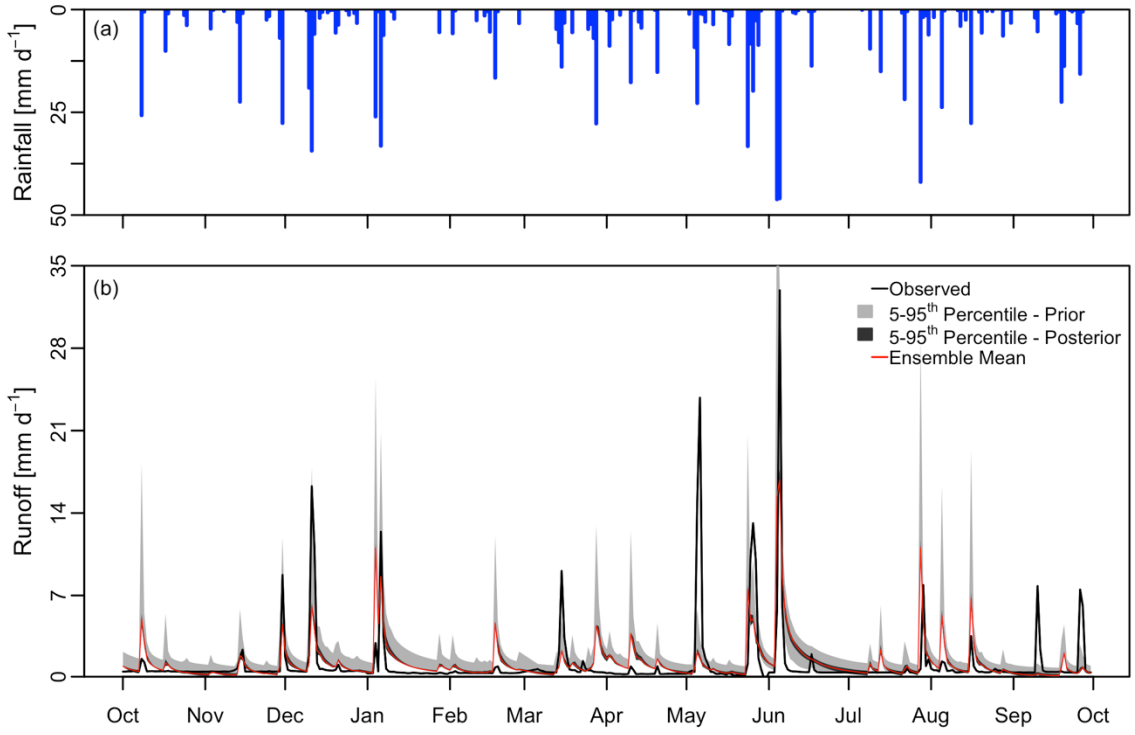

Figure 5-3: Results from hydrologic calibration and GLUE uncertainty estimation for the 2009 water year. Panel (a) shows the rainfall time series that forced the model, and panel (b) shows the observed hydrograph, and the 5-95th percentiles of the GLUE prior and posterior parameter envelopes, and a performance-weighted ensemble mean of the posterior parameter sets.

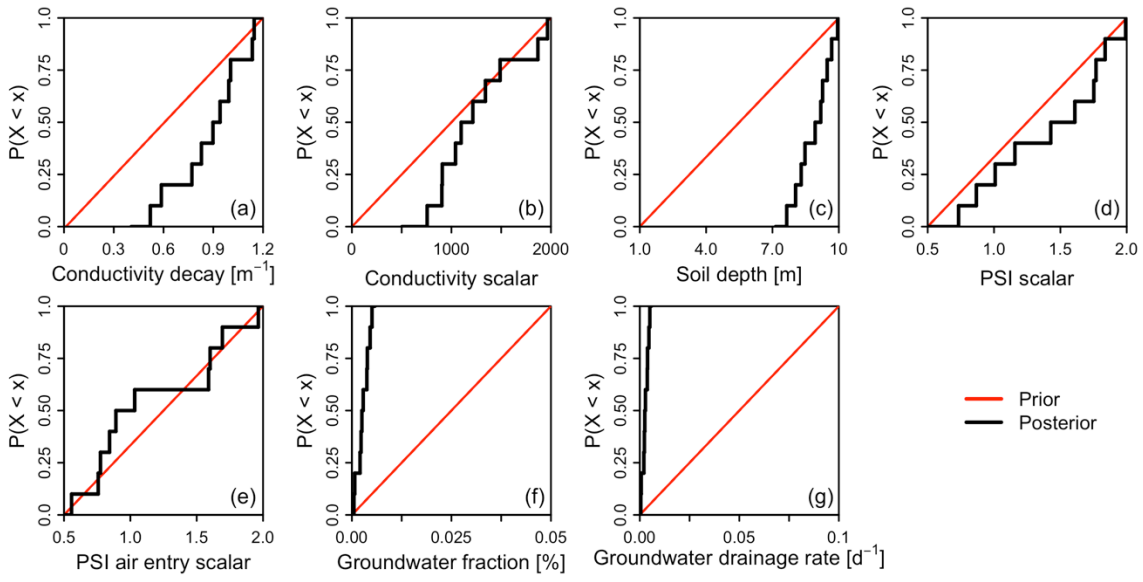

Figure 5-4: Comparison of prior and posterior CDFs of the 7 hydrologic parameters.

more sensitive to that parameter. The model appears to be least sensitive to the pore size index (PSI) and the PSI entry air pressure parameters. The model appears to be most sensitive to the deep groundwater entry fraction (gw1) and the deep groundwater drainage rate (gw2). Only the gw1 and gw2 values in the lowest 10^{th} percentile of the prior distribution made it through to the posterior. The model also shows sensitivity to hydrologically active soil depth, as only depths greater than 7.0 m were retained from the initial range of 1-10 m.

5.4.2 Water quality validation

Generally, the simulated monthly NO_x loads are reasonably well correlated to those observed ($r = 0.47$), although the model over predicts total export by 22% (Figure 5-5b). There is a distinct seasonal pattern of model performance, as the model tends to over predict NO_x loads during the time period spanning form October 2008 to February 2009, but under predict between May and September of 2009. For 9 of the 12 observed monthly NH_4 loads, the observed average concentrations were below the detection limit (0.01 mg-N L^{-1}), which means monthly load was estimated at 0 g m^{-2}. This makes comparing simulated and observed loads difficult. However, simulated flow-weighted mean monthly NH_4 concentrations were also consistently below that detection limit, spanning a range of 0.001-0.005 mg-N L^{-1}. The simulated loads that reflect these concentrations are shown in Figure 5-5c. Over the simulation period, the model underestimated total mass export of TN by 7% (Figure 5-5d). While the net N retention behavior was well modeled, monthly correlations of both TN load were negative (r=-

0.02), which indicates seasonal dynamics were not well captured. Overall, the simulated N loads were within reason, given that the estimates were generated without calibration.

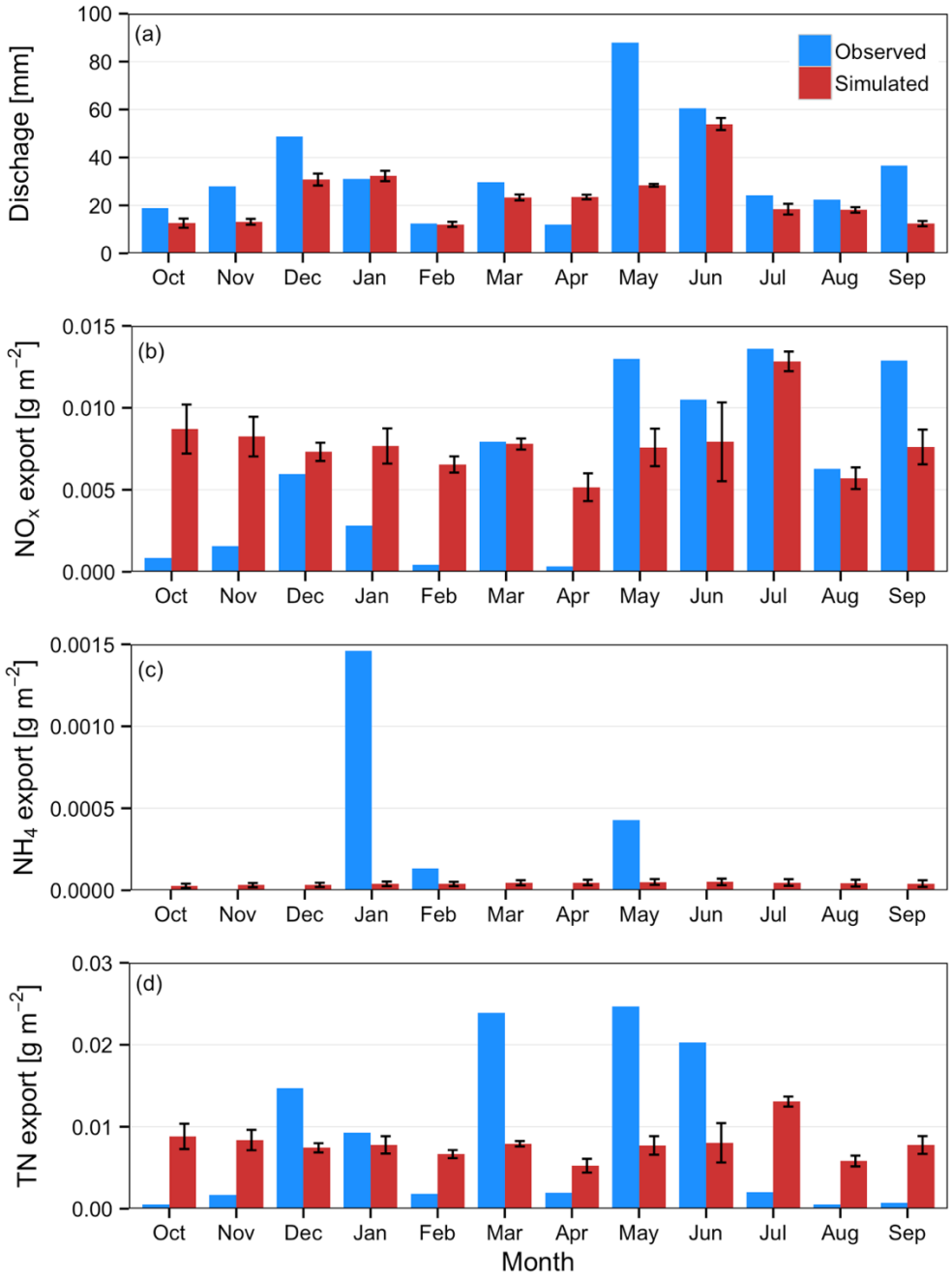

Figure 5-5: Observed vs. simulated monthly water and nitrogen mass export for the 2009 water year. Error bars on the simulations bar indicate one standard deviation from the mean of simulations using the 250 combinations of water quality and hydrologic parameters. Bars missing from the NH_4 plot in panel (c) indicate that observed concentrations were below detection.

5.4.3 Watershed connectivity scenario testing

For each of the connectivity scenarios, hydrologic behavior was quantified by annual runoff ratios, annual surface evaporation, and monthly surface evaporation. As the UI of the watershed increased, so, too did the runoff ratio (Figure 5-6). The scenario with the least connectivity to SCMs had 26% (21-32% within one standard deviation) more runoff volume than compared to the most connected scenario. The shape of the relationship between runoff ratios and UI is positive and linear, which indicates that each additional impervious surface that is connected to the SCM will result in a proportional reduction in runoff volume.

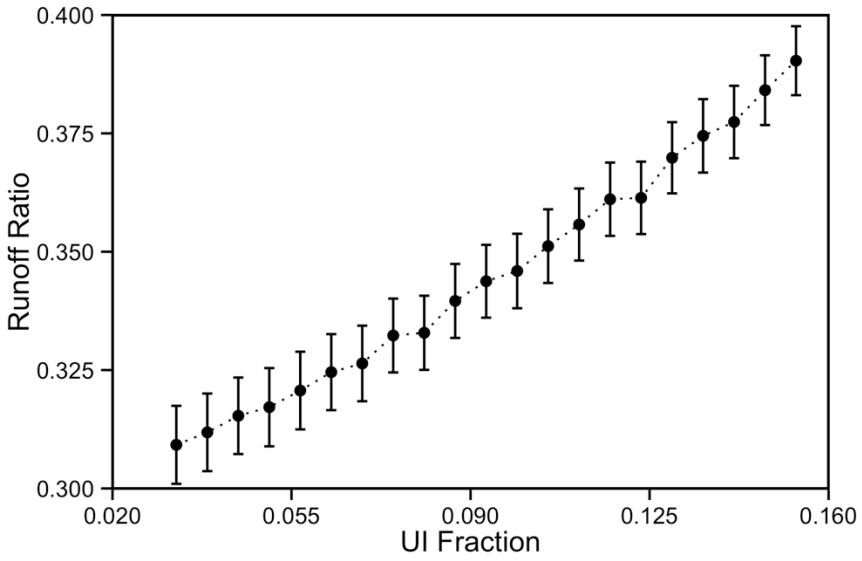

Figure 5-6: Changes to runoff ratios under the 21 impervious surface connectivity scenarios (quantified by UI). Filled circles represent the mean of the 250 parameter sets tested for each level of UI, and the error bars represent one standard deviation.

Figure 5-7 shows that as UI increases, annual surface evaporation decreased. While the two are intertwined, the shape of the relationship between evaporation and UI is markedly different than runoff ratio and UI. Instead of the simple, linear response, the

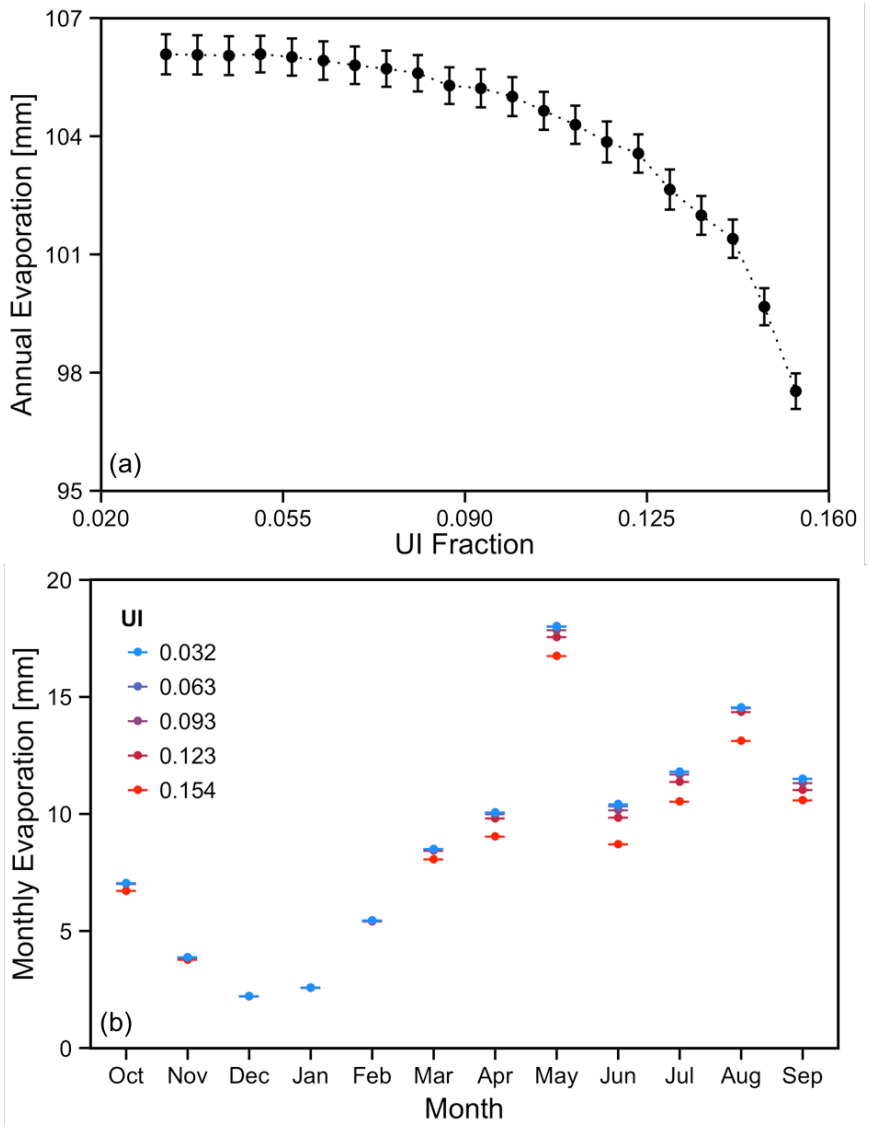

Figure 5-7: Panel (a) shows changes surface evaporation under the 21 impervious surface connectivity scenarios (quantified by UI). Filled circles represent the mean of the 250 parameter sets tested for each level of UI, and the error bars represent one standard deviation. Panel (b) shows only the mean estimated monthly evaporation for five select UI scenarios,

rate of change of evaporation with respect to UI increases at high levels of UI. Figure 5-7b shows monthly evaporation totals for five select connectivity scenarios (scenarios 1, 6, 11, 16, and 21). Between the months of November and February, evaporation totals across all levels of UI are relatively consistent. However, in the warmer months, it becomes clear that connectivity exerts a control on total evaporation, as there is more disparity in evaporation estimates between the connectivity scenarios. Figure 5-7b also shows that the low UI scenarios (e.g. scenarios 1, 6, and 11 with a UI of 0.032, 0.063 and 0.093, respectively) behave more similarly than the high UI scenarios. This reflects the shape of the evaporation vs. UI curve.

While simple metrics such as runoff ratios are useful indicators of hydrologic behavior, it is important to analyze the entire flow regime when evaluating how SCM implementation may effect stream ecosystems. To do this, we analyzed flow duration curve for three select connectivity scenarios (Figure 5-8). For clarity, the entire flow duration curves are separated into four separate panels, each representing a quartile of exceedance probability, and each with its own vertical scale (Figure 5-8). The flow duration curves show that greater levels of UI consistently result in higher discharge values. However, the flow duration curves converge at higher exceedance probabilities. The flow duration curves of the 0.093 and 0.153 UI scenarios cross 12 times in highest quartile of exceedance probability (Figure 5-8d), while they only cross 3 times throughout the rest of the range (Figure 5-8a-c).

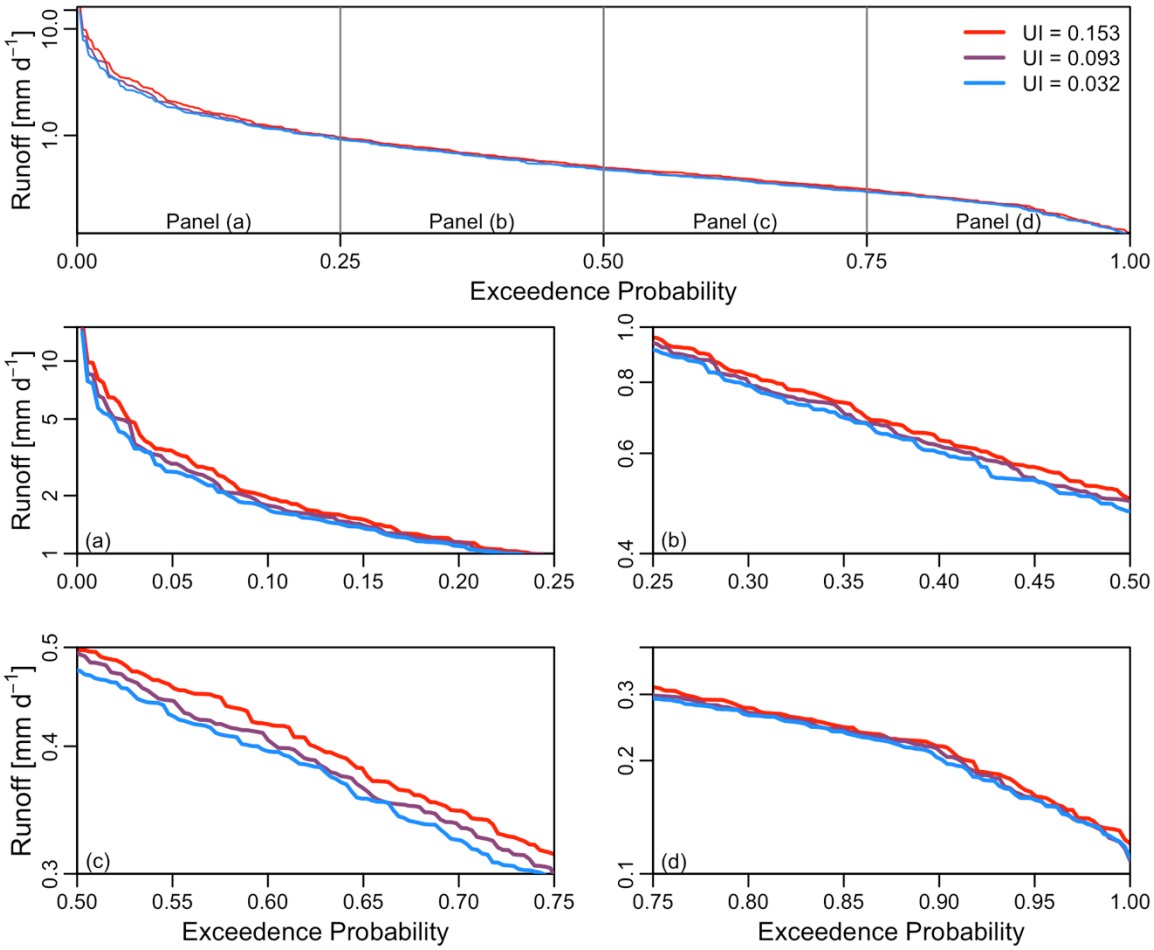

Figure 5-8: Flow duration curves between three select connectivity scenarios. For clarity, the curves are broken up into four sub-panels, each spanning a single quartile of exceedance probability, and each plotted on its own y-axis. Note the y-axis in all panels are on a logarithmic scale.

As impervious surfaces were more connected to SCMs, watershed export of NO_x and TN decreased (Figure 5-9a and 5-9b). The average change in total load between the least mitigated scenario relative to the most mitigated was 14% (3 to 26%) and 13% (2 to 25%) for NO_x and TN, respectively. The relationship between the load and UI was generally positive and linear. However, NH_4 loads show an opposite trend. As UI increased, average loads decreased. The percentage change between the least and most mitigated scenarios, relative to the most, for annual loads was -37% (-73% to +37%). Error bars,

indicating one standard deviation from the mean, for NH_4 were wide relative to changes in the mean across simulations, indicating that simulated NH_4 is sensitive to model parameters (Figure 5-9b). Because NH_4 loads were linearly related to UI in a direction opposite of runoff, increased loads were due to increased concentrations.

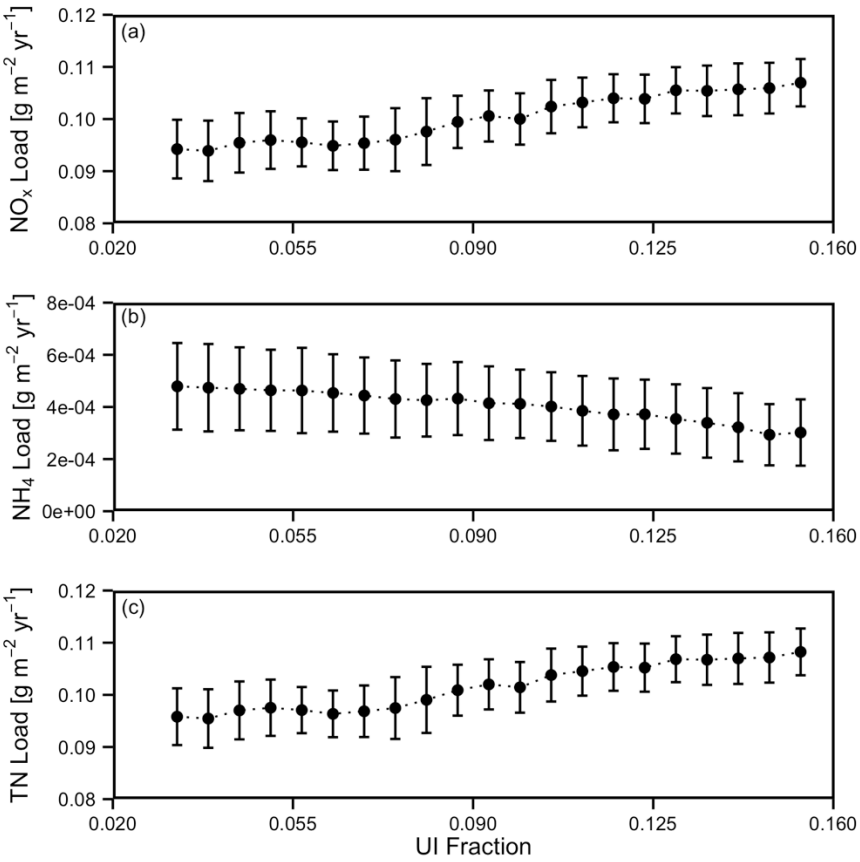

Figure 5-9: Changes in annual load of (a) NO_x, (b) NH_4 and (c) TN species across ranges of UI. Filled circles represent the mean of the 250 parameter sets tested for each level of UI, and the error bars represent one standard deviation.

5.5 Discussion

5.5.1 Model evaluation

Calibration of hydrologic parameters produced acceptable model performance at predicting daily streamflow. Typically, NSE values > 0.7 are deemed to demonstrate good performance, although this number can vary with sample size and outliers (McCuen et al., 2006). Here, only 10 of the 10,000 parameter sets used produced NSE values > 0.3. Application of the GLUE acceptability filter reduced model uncertainty by an average of 0.807 mm, which accounted for approximately 30% of total rainfall over the 2009 water year. The model did not successfully reproduce the flashiness of the urban system, as peak flows were under predicted and recession periods were extended. Additionally, the model showed sensitivity to both groundwater and soil depth parameters (Figure 5-4). These two results together indicate that the model may be simulating a greater fraction of subsurface flow than actually occurs, although there is no way to quantify this without experimental analysis of runoff sources. The model may also underrepresent the effects that urban development has on compaction of pervious surfaces, and how these areas can limit infiltration and become contributing source areas that contribute to runoff during rain events (Pitt et al., 2008; Miles and Band, 2015).

The model reasonable predicted seasonal dynamics of NO_x, as monthly loads were well correlated. However, seasonal dynamics of TN showed low correlation. Reproducing N export dynamics is challenging for a number of reasons. Correctly parameterizing the magnitude and timing of N loading is difficult, as there are many varying sources

including atmospheric deposition, and applied fertilizer (Bernhardt et al., 2008). Here, N deposition data was taken from the closest sites with available data, but these locations were at least 100 km away. This distance could cause issues for the model, as N deposition was the only external N source simulated. Additionally, there are clear limitations of the observed data. For four of the twelve months, the reported observed TN loading was less than reported NO_x. Still, the overall loads of the N species were only off by 7-22%, and therefore model performance was deemed sufficient.

5.5.2 Watershed connectivity

SCMs are designed to interrupt the connectivity between urban impervious surfaces and stream networks, and to promote hydrologic and biogeochemical processes that protect stream ecosystems. This work sought to explore how hydrologic and biogeochemical regimes of urban streams change as impervious surfaces are connected to SCMs. Results show that as more impervious surfaces are mitigated by SCMs, corresponding to a decrease in the watershed metric UI, annual runoff ratios decrease (Figure 5-7). The decrease in reduction is linearly proportional to decrease in UI across the range explored here (3-15%). Other studies have demonstrated the role that increased mitigation urban areas by SCMs has on reducing runoff volumes (Gagrani et al., 2014; Hale et al., 2015; Liu et al., 2015).

Using a simple water balance, runoff is equal to precipitation minus the sum of evaporation, transpiration, and storage. SCMs pond water, exposing it to sun and wind, and promoting evaporation. As shown in Figure 5-8, basin-wide surface evaporation

decreased as UI increased, particularly during summer months, when evaporation potential is high. The relationship between UI and surface evaporation is non-linear, which is different from the relationship between UI and runoff ratio. This implies that evaporation plays a less significant role in decreasing runoff ratios as UI decreases. Therefore, the processes of storage and transpiration must increase relative to evaporation to produce linear change in runoff ratios. The SCMs modeled here are not vegetated, so transpiration does not occur within an SCM patch. Therefore, it is likely increased infiltration and subsequent storage in soil or transpiration by plants that accounts for the decreased runoff ratios at low levels of UI. This is supported by monitoring results from Endreny and Collins (2009) who demonstrated the potential for groundwater mounding around SCMs from infiltration.

In addition to the overall water balance, the extent to which mitigation would change the distribution of discharge was analyzed. Figure 5-10 shows that increased UI leads to increased discharge across the entire flow regime. However, at lower exceedance probabilities, the flow duration curves for the three select connectivity scenarios began to merge, as the flow duration curves intersected more frequently. This suggests that the SCMs have a lesser effect on hydrology during dry periods compared to wet periods. This aligns with the design objective of many SCMs which are targeted at reducing peak discharges during large rain events, rather than fully restoring natural hydrologic regimes (Burns et al., 2012).

The effect that connecting urban impervious surfaces to SCMs on mass loads of NO_X, NH_4 and TN was also analyzed. NO_x and TN loads increased linearly with UI, indicating that increased mitigation results in proportional load reductions. The reduction in annual load is inextricably tied to the reduction in runoff volumes, so part of the reductions could be simply due to the hydrologic benefits of SCMs. These flow-driven load reductions have been observed in other studies (Gagrani et al., 2014; Hale et al., 2015).

However, NH_4 loads decreased with UI, despite these volume reductions. That implies that connecting impervious surfaces to SCMs causes concentrations to increase enough to cause greater N loads even when there is less water runoff. One possible explanation for this behavior is that algae growth and respiration is more active in watersheds with greater SCM connectivity because the SCMs receive more water and N from the landscape. The algae growth model in RHESSys is designed so that algae uptake N in both inorganic forms of NO_x and NH_4. Algae release a fraction of this assimilated N back to the water column as NH_4 during respiration (Bell et al., In review-b). Therefore, greater connectivity could stimulate this process, and lead to greater NH_4 export. Despite the increased load of NH4, the cumulative load of all N species is reduced as UI decreases.

While most of the relationships observed in this study were all linear, it is like that the nature of the relationship may change at different levels of TI, and subsequently UI. Increased abundance of impervious surfaces may demonstrate a saturation relationship in

runoff and load reductions, as was observed for annual evaporation. Future work should address how these relationships change at different levels of TI and subsequent mitigation.

5.6 Conclusions

This study used a spatially-distributed, process-based watershed model to simulate runoff and nitrogen loads under different scenarios of urban surface connectivity in a residential watershed in Charlotte, NC. Model simulations were used to systematically vary the fraction of impervious surfaces within the watershed that were connected either to the stream directly or first to an SCM. The purpose was to develop simple relationship between hydrologic and water quality variables relative to the watershed metric UI, which quantifies the extent of unmitigated impervious surfaces.

Results showed that linear decreases in UI of the range observed here (i.e., increased mitigation by SCMs) caused linear decreases in runoff ratios as well as NO_x and TN loads. Increased surface evaporation from SCMs accounted for part of the load reductions, particularly at higher levels of UI. However, at low levels of UI, soil storage and transpiration may be more important. No matter the processes, the linear shape of the relationship at this UI range implies that at the level of development considered in this study, any additional mitigation of impervious surfaces by SCMs will result in additional benefits to hydrology and N load. However, results showed that NH_4 load decreased with increases in UI. Therefore, additional mitigation of urban impervious surfaces by SCMs will produce increased NH_4 export. This increase can be attributed to algae communities within the SCMs converting NO_x to NH_4. However, loads of NH_4 are so low relative to

NO_x, that despite slight increases in NH_4 with more SCM mitigation, TN loads are still reduced.

5.7 References

Alden, K. et al., 2015. spartan: Simulation Parameter Analysis R Toolkit ApplicatioN: Spartan.

Allan, C.J., Diemer, J.A., Gagrani, V., 2013. Beaverdam Creek Watershed Monitoring Report 2005-2012, Charlotte, NC.

Alley, W., Veenhuis, J., 1983. Effective Impervious Area in Urban Runoff Modeling. Journal of Hydraulic Engineering, 109(2): 313-319.

Arnold, C.L., Gibbons, C.J., 1996. Impervious surface coverage: the emergence of a key environmental indicator. Journal of the American Planning Association, 62(2): 243-258.

Arora, V.K., Boer, G.J., 2003. A Representation of Variable Root Distribution in Dynamic Vegetation Models. Earth Interactions, 7(6): 1-19.

Barrett, M.E., 2005. Performance Comparison of Structural Stormwater Best Management Practices. Water Environment Research, 77(1): 78-86.

Bell, C.D., McMillan, S.K., Clinton, S.D., Jefferson, A.J., In review-a. Hydrological Response to Stormwater Control Measures in Urban Watersheds. J Hydrol.

Bell, C.D., Tague, C.L., McMillan, S.K., In review-b. A model of hydrology and water quality in stormwater control measures. Environmental Modeling and Software.

Bernhardt, E.S., Band, L.E., Walsh, C.J., Berke, P.E., 2008. Understanding, managing, and minimizing urban impacts on surface water nitrogen loading. Ann NY Acad Sci, 1134(1): 61-96.

Beven, K., Binley, A., 1992. The future of distributed models: model calibration and uncertainty prediction. Hydrol Process, 6(3): 279-298.

Brabec, E., 2009. Imperviousness and Land-Use Policy: Toward an Effective Approach to Watershed Planning. Journal of Hydrologic Engineering, 14(4): 425-433.

Burns, M.J., Fletcher, T.D., Walsh, C.J., Ladson, A.R., Hatt, B.E., 2012. Hydrologic shortcomings of conventional urban stormwater management and opportunities for reform. Landscape and Urban Planning, 105(3): 230-240.

Collins, K.A. et al., 2010. Opportunities and challenges for managing nitrogen in urban stormwater: A review and synthesis. Ecol Eng, 36(11): 1507-1519.

Dewals, B.J., Archambeau, P., Khuat Duy, B., Erpicum, S., Pirotton, M., 2012. Semi-Explicit Modelling of Watersheds with Urban Drainage Systems. Engineering Applications of Computational Fluid Mechanics, 6(1): 46-57.

Duncan, J.M., Groffman, P.M., Band, L.E., 2013. Towards closing the watershed nitrogen budget: Spatial and temporal scaling of denitrification. J Geophys Res-Biogeo, 118(3): 1105-1119.

Endreny, T., Collins, V., 2009. Implications of bioretention basin spatial arrangements on stormwater recharge and groundwater mounding. Ecol Eng, 35(5): 670-677.

Gagrani, V., Diemer, J.A., Karl, J.J., Allan, C.J., 2014. Assessing the hydrologic and water quality benefits of a network of stormwater control measures in a SE U.S. Piedmont watershed. J Am Water Resour As, 50(1): 128-142.

Geosynthetic Consultants, I., Wright Water Engineers, I., 2014. International Stormwater Best Management Practices (BMP) Database Pollutant Category Summary Statistical Addendum: Solids, Bacteria, Nutrients, and Metals, http://www.bmpdatabase.org/.

Green, W.H., Ampt, G., 1911. Studies on Soil Phyics. The Journal of Agricultural Science, 4(01): 1-24.

Groffman, P.M., Law, N.L., Belt, K.T., Band, L.E., Fisher, G.T., 2004. Nitrogen fluxes and retention in urban watershed ecosystems. Ecosystems, 7(4): 393-403.

Guo, J., 2008. Volume-Based Imperviousness for Storm Water Designs. Journal of Irrigation and Drainage Engineering, 134(2): 193-196.

Hale, R., Turnbull, L., Earl, S., Childers, D., Grimm, N., 2015. Stormwater Infrastructure Controls Runoff and Dissolved Material Export from Arid Urban Watersheds. Ecosystems, 18(1): 62-75.

Hatt, B.E., Fletcher, T.D., Walsh, C.J., Taylor, S.L., 2004. The Influence of Urban Density and Drainage Infrastructure on the Concentrations and Loads of Pollutants in Small Streams. Environ Manage, 34(1): 112-124.

Hornberger, G.M., Spear, R.C., 1981. Approach to the preliminary analysis of environmental systems. Journal Name: J. Environ. Manage.; (United States); Journal Volume: 12:1: Medium: X; Size: Pages: 7-18.

Hunt, W., Smith, J., Jadlocki, S., Hathaway, J., Eubanks, P., 2008. Pollutant Removal and Peak Flow Mitigation by a Bioretention Cell in Urban Charlotte, N.C. J Environ Eng-ASCE, 134(5): 403-408.

Kaushal, S., Belt, K., 2012. The urban watershed continuum: evolving spatial and temporal dimensions. Urban Ecosystems, 15(2): 409-435.

Kearney, M.A., Zhu, W., Graney, J., 2013. Inorganic nitrogen dynamics in an urban constructed wetland under base-flow and storm-flow conditions. Ecol Eng, 60: 183-191.

Koch, B.J., Febria, C.M., Gevrey, M., Wainger, L.A., Palmer, M.A., 2014. Nitrogen Removal by Stormwater Management Structures: A Data Synthesis. J Am Water Resour As, 50(6): 1594-1607.

Landsberg, J.J., Waring, R.H., 1997. A generalised model of forest productivity using simplified concepts of radiation-use efficiency, carbon balance and partitioning. Forest Ecology and Management, 95(3): 209-228.

Lee, J.G., Heaney, J.P., 2003. Estimation of Urban Imperviousness and its Impacts on Storm Water Systems. Journal of Water Resources Planning and Management, 129(5): 419-426.

Leopold, L.B., 1968. Hydrology for urban land planning: A guidebook on the hydrologic effects of urban land use. USGS Circular 554.

Liu, Y., Bralts, V.F., Engel, B.A., 2015. Evaluating the effectiveness of management practices on hydrology and water quality at watershed scale with a rainfall-runoff model. Science of The Total Environment, 511: 298-308.

Mallin, M.A., Ensign, S.H., Wheeler, T.L., Mayes, D.B., 2002. Pollutant Removal Efficacy of Three Wet Detention Ponds. J. Environ. Qual., 31(2): 654-660.

McCuen, R.H., Knight, Z., Cutter, A.G., 2006. Evaluation of the Nash–Sutcliffe Efficiency Index. Journal of Hydrologic Engineering, 11(6): 597-602.

McKay, M.D., Beckman, R.J., Conover, W.J., 1979. Comparison of Three Methods for Selecting Values of Input Variables in the Analysis of Output from a Computer Code. Technometrics, 21(2): 239-245.

Miles, B., Band, L.E., 2015. Green infrastructure stormwater management at the watershed scale: urban variable source area and watershed capacitance. Hydrol Process, 29(9): 2268-2274.

Monteith, J., 1965. Evaporation and environment, Symposium Society Experimental Biology on The State and Movement of Water in Living Organisms, pp. 205-234.

Nash, J.E., Sutcliffe, J.V., 1970. River flow forecasting through conceptual models part I — A discussion of principles. J Hydrol, 10(3): 282-290.

O'Driscoll, M., Clinton, S., Jefferson, A., Manda, A., McMillan, S., 2010. Urbanization effects on watershed hydrology and in-stream processes in the Southern United States. Water, 2(3): 605-648.

Parton, W. et al., 1996. Generalized model for N2 and N2O production from nitrification and denitrification. Global Biogeochem Cy, 10(3): 401-412.

Paul, M.J., Meyer, J.L., 2001. Streams in the urban landscape. Urban Ecology: 207-231.

Pitt, R., Chen, S., Clark, S., Swenson, J., Ong, C., 2008. Compaction's Impacts on Urban Storm-Water Infiltration. Journal of Irrigation and Drainage Engineering, 134(5): 652-658.

Roesner, L., Bledsoe, B., Brashear, R., 2001. Are best-management-practice criteria really environmentally friendly? Journal of Water Resources Planning and Management, 127(3): 150-154.

Running, S.W., Hunt, E.R., 1993. Generalization of a forest ecosystem process model for other biomes, BIOME-BGC, and an application for global-scale models. Scaling physiological processes: Leaf to globe: 141-158.

Shields, C., Tague, C., 2014. Ecohydrology in semiarid urban ecosystems: Modeling the relationship between connected impervious area and ecosystem productivity. Water Resour Res: n/a-n/a.

Shuster, W.D., Bonta, J., Thurston, H., Warnemuende, E., Smith, D.R., 2005. Impacts of impervious surface on watershed hydrology: A review. Urban Water Journal, 2(4): 263-275.

Soil Survey Staff, 2013. Natural Resources Conservation Service, United States Department of Agriculture. U.S. General Soil Map (STATSGO2). Available online at http://sdmdataaccess.nrcs.usda.gov/. Accessed [09/01/2013].

Tague, C.L., Band, L.E., 2004. RHESSys: regional hydro-ecologic simulation system-an object-oriented approach to spatially distributed modeling of carbon, water, and nutrient cycling. Earth Interactions, 8(19): 1-42.

USDA-NRCS, 2010. Mecklenburg County Soil Survey Report. http://websoilsurvey.nrcs.usda.gov/app/.

Walsh, C.J., Fletcher, T.D., Ladson, A.R., 2005. Stream restoration in urban catchments through redesigning stormwater systems: looking to the catchment to save the stream. J N Am Benthol Soc, 24(3): 690-705.

Walsh, C.J., Kunapo, J., 2009. The importance of upland flow paths in determining urban effects on stream ecosystems. J N Am Benthol Soc, 28(4): 977-990.

White, M.A., Thornton, P.E., Running, S.W., Nemani, R.R., 2000. Parameterization and Sensitivity Analysis of the BIOME–BGC Terrestrial Ecosystem Model: Net Primary Production Controls. Earth Interactions, 4(3): 1-85.

Wigmosta, M.S., Vail, L.W., Lettenmaier, D.P., 1994. A distributed hydrology-vegetation model for complex terrain. Water Resour Res, 30(6): 1665-1679.

Young, P., 1983. The Validity and Credibility of Models for Badly Defined Systems. In: Beck, M.B., van Straten, G. (Eds.), Uncertainty and Forecasting of Water Quality. Springer Berlin Heidelberg, pp. 69-98.

CHAPTER 6. CONCLUSIONS AND IMPLICATIONS

6.1 Study overview

This work tested the hypothesis that "hydrologic and water quality indicators of urban stream behavior will become more damaging as the extent of urban impervious surfaces within watershed increases, but increasing connectivity of these surfaces to SCMs will ameliorate this intensity of this relationship." Characterizing the form and directionality of this relationship will help inform managers seeking to limit the damage that urban runoff inflicts on stream ecosystems. First, variables that characterize hydrology at sixteen urban watersheds in Charlotte, NC, USA were statistically related to a series of numerical metrics that quantify the extent of urban development, extent of SCM mitigation, and the connectivity of urban impervious surfaces to the stream directly. Next, water quality data at the confluence of a stream and SCM outflow channel were compared to determine the effect of SCMs on stream nutrient and carbon concentrations, and how the type and distribution of land use in the watershed modulates the effect of SCM mitigation. Additionally, a computer modeling approach was developed to capture variability in hydrologic and water quality response along a continuum of development and mitigation by SCMs. This was achieved through the development, calibration, validation and assessment of uncertainty of a new SCM model routine that simulates hydrologic and ecological processes within an individual SCMs. Finally, the SCM

routines were incorporated into an existing fully-distributed, process-based model to determine how connecting impervious surfaces to SCMs changes stream hydrology and water quality at the watershed scale.

6.2 Major Findings and Management Implications

Documented below are the major findings of this research effort, and the implications that these findings have for stormwater management.

6.2.1 Watershed metric total impervious (TI) controls event scale hydrologic response

The empirical analysis of hydrologic variables revealed that, at the event scale, the watershed metric TI was the best predictor of all hydrologic variables tested including rainfall runoff ratios, peak discharge, watershed capacity to store small rain events, and the response rate of discharge to additional precipitation once the storage had been exceeded. The strength of TI, which does not contain any information about mitigation with SCM, to predict hydrologic behavior indicates that SCMs implemented at the levels observed may not be influencing hydrologic behavior. Therefore, TI is the watershed characteristic that policy makers should use to manage watersheds to mitigate impacts to streams.

6.2.2 SCMs and tree canopy coverage are strongest controls on annual scale hydrology

Hydrologic variables at annual time scales, including total water yield and record flashiness, were best predicted by watershed metrics other than TI. The fraction of tree coverage in the watersheds was best correlated to total water yield, which was attributed

to transpiration of soil water between rain events by deep rooted plants. Therefore, management strategies that include planting trees could reduce total stormwater and pollutant loads. Hydrologic record flashiness, measured as the time the discharge spent above the annual mean, was best related to impervious area unmitigated by SCMs. This implies that SCMs, while not able to mitigate the peak discharge during rain events, may be able to elevate and extend hydrograph recession. This has ecosystem impacts as mitigating urban impervious surfaces with SCMs can change the disturbance regimes to support stream invertebrate habitat.

6.2.3 Type of urban land use control stream nutrient and carbon concentrations

Concentrations of two nitrogen species, TDN and NO_x-N, were significantly lower at sites with greater forested coverage compared to those with less forest coverage. Therefore, as with the result of total water yield, planting trees may be a way to reduce N loading to the streams. PO_4-P concentrations were higher at recently developed residential watersheds compared to those with older development. Evidence suggests that fertilizer applied to the residential lawns in the newly developed watersheds may be the cause for the increased PO_4-P concentrations. Using P-free fertilizers or campaigns to education the resident on good fertilization practices may be effective ways to reduce sources of PO_4-P to these watersheds, and ultimately the amount of PO_4-P in the streams.

6.2.4 SCM outflow changes stream concentrations

SCMs changed stream water quality throughout storms, although the direction of this transformation depended on the spatial distribution of urban surfaces throughout the

watershed. In two watersheds with older, more uniform urban land cover, SCMs reduced in-stream nutrient and carbon concentrations immediately downstream of a stream-SCM confluence. However, in the two developing suburban watersheds where the addition of SCMs coincided with the addition of new urban surfaces, SCMs outflow increased stream concentrations. This implies that, even if individual SCMs decrease watershed-derived nutrients, SCMs are not returning streams to their predevelopment conditions in terms of water quality.

6.2.5 SCM processes adequately simulated retention and removal of inorganic N

New model routines that simulate hydrological and ecological processes in SCMs were developed. The hydrologic processes were able to replicate the distribution of observed water outflow volume and event outflow duration in a monitored SCM in Charlotte, NC without calibration. Through calibration of parameters that control simulation of algae growth, the water quality routines were able to match the distributions of observed event mean concentrations of NO_3 and NH_4 in outflow. This model is of great value because it has been installed into a widely applied, watershed-scale hydro ecological model called RHESSys and can be used to test the effect of different spatially-explicit SCM implementation scenarios on hydrology and water quality. Additionally, the model is process-based which allows users to test how SCM performance changes under varying environmental conditions and individual SCM designs.

6.2.6 Variability of N removal in SCMs due to environmental and design factors

When simulating the behavior of a single SCM, the newly-developed routines were able to account for some of the variability of N retention and removal performance reported in the literature. First, removal of both NO_3 and NH_4 increased with increasing temperature, which has implications for the success of SCMs in different regions and under climate change scenarios. Second, increased N loading did not affect NH_4 removal. However, it did lead to a decline in the removal efficiency of NO_3, which is likely due to the preference that algae communities in SCMs have for assimilating NH_4 instead of NO_3. The implications are that SCM may be more effective at removing NH_4 than NO_3 in N-replete watersheds. Additionally, increased inflow volumes lead to a decrease in mass removal efficiency of both NO_3 and NH_4 suggesting that SCM performance may be limited during wetter years or if further development causes increased runoff. The depth of permanently pooled water in SCMs also controlled inorganic N removal efficiency with deeper pools removing a greater fraction of inorganic N. When possible, SCMs should be designed with greater volumes, as higher volumes SCMs are more capable of capturing more stormwater runoff from the watershed, storing more water between events and diluting N-rich inflow.

6.2.7 Mitigation of impervious surfaces leads to linear reductions in runoff and nitrogen

Simulating changes to a watershed metric that quantifies the percent of area covered by an impervious surface unmitigated by SCMs (named unmitigated impervious, or UI) resulted in changes to hydrology and water quality. As UI increased from 3% to 15%,

which indicates less influence of SCMs, runoff ratios and annual loads of NO_3 and total dissolved nitrogen (TN) increased by 26% (21-32%), 14% (3-26%) and 13% (2-25%), respectively. The shape of the relationships between these three response variables and UI was linear at this range of UI, which may indicate that mitigating additional impervious surfaces with SCMs will lead to proportional reductions in runoff and loads of these two water quality parameters. However, annual NH_4 increased with more SCM mitigation but the relative magnitude of NH_4 loads compared to the other two N species was very small such that total N loads still decreased.

6.3 Recommendations for future research

6.3.1 Expand range of watershed metrics and repeat analysis

The sites chosen for the empirical analysis have analytical limitations. For the hydrological analysis, the 16 sites used covered a broad range of both urban development (TI from 4-54%) and SCM mitigation (mitigated area from 1-89%). However, the distribution of these two watershed metrics was highly skewed towards the low end of mitigation, which could reduce the power of the statistical tests used. To improve this, more watersheds could be added to the analysis. Some potential limitations to this suggestion are that it can only be done by installing more stream gages in the analysis region, or by incorporating sites in other regions which would introduce variability from differing climates.

Similarly, the watershed-scale model experiments systematically varied the level of impervious surface mitigation across a broad, and uniformly distributed range, but only

one level of TI was considered based on the baseline conditions of an existing watershed in the study area. The experiments should be repeated so that both TI and subsequent mitigation vary across the entire range of expected values. The result will be not a two dimensional plot of response vs. UI as in this study, but rather a three dimensional plot with both TI and UI/TI as the independent axis. This will characterize how mitigation changes response in the stream at varying levels of urban development. Some potential issues include objectively adding impervious surfaces in a way that represents typical urban development as well as placing and parameterizing SCMs that may be designed to mitigate these new impervious surfaces. One potential solution to these issue could be to find a fully developed, fully mitigated watershed and gradually remove impervious surfaces and/or SCMs to create different combinations of TI and UI/TI.

6.3.2 Expand duration of analysis to account for climactic variability

In this study, all analyses were limited to one year of climatic forcing due to data constraints. If the experiments were repeated across a longer time series, this could add depth to the analysis because the climatic controls could be identified. Additionally, a longer time series is important because SCMs are designed to mitigate flows during low frequency events, sometimes including the 50 and 100 year floods. A longer time series would likely capture some of these less frequent events. Some potential limitations to expanding the duration of the empirical analysis are addressing land use change through time and finding longer records of data. For the modeling, expanding the time series

would be simpler as land use is controlled explicitly by the model, and only climate data, which typically has a longer record than hydrologic data, are needed to force the model.

6.3.3 Sample water quality a higher spatial resolution

While the water quality sampling strategy was effective for characterizing changes around the confluence of aa stream and outflow from an SCM, a more spatially distributed sampling protocol would be better suited to quantify the effect of SCMs on stream water quality. Specifically, a time series of SCM inflow and SCM outflow volume and concentrations would be useful for quantifying the mass of nutrient retained by the SCM and exported to the stream during storm events of varying frequency and intensity. This dataset would also improve the calibration and validation approaches during model develop. The limitations to this high spatial resolution sampling are logistical concerns associated with sampling SCM inlets and outlets, which are often poorly suited for monitoring.

6.3.4 Empirically quantify state variables and fluxes of C, N and P within SCMs

The approach to calibration of the SCM water quality routines here was based on aggregated event mean concentrations of two inorganic N species. A more rigorous, empirical analysis of the processes that are occurring in the SCM are necessary for complete model validation. A short list of processes that should be quantified include in-situ nitrification, denitrification, and mass uptake of N and P by both algal and plants. A time series of the standing stock of chl-A in the SCM would also be extremely valuable for calibration and validation, as the new model routines are designed to simulate algae

dynamics. Additionally, tracer tests that identify mixing behavior of SCMs could help determine if modeling SCMs of this size as completely mixed is appropriate, or if they should be spatially discretized. In addition to validating and calibrating the model, quantifying these processes and their environmental controls would add a wealth of understanding of C, N and P cycling in SCMs that could directly inform SCM functioning and design.

6.3.5 Add vegetation to SCM model routines

For wet pond SCMs, vegetation only occupies a small band around the perimeter of the pond. However, some SCMs, like wetlands, are vegetated throughout the entire SCM area. Vegetation in SCMs may increase ET rates, lower rates of algae growth by reducing light and nutrient availability, immobilize carbon and nitrogen for longer time periods, and dramatically change seasonal nutrient and carbon dynamics associated with litterfall. Modeling the effects of this vegetation on the water balance, nutrient cycling, and light availability would be extremely useful for comparing SCM designs and the response of the entire watershed to SCM mitigation.

APPENDICES

Appendix A SCM Hydrologic model

The SCM water mass balance is shown in (Eq. 4.1). The water balance has losses due to evaporation, surface outflow, and infiltration. Sources of water to the pond are surface inflow and precipitation. Evaporation, surface inflow from the watershed, and precipitation interception iare modeled by existing routines in RHESSys. Outflow (Q_{out}) from the SCM to the downslope patches is the sum of outflow through each of the outlet structures weirs and orifices:

A.1 Q_{out}

$$Q_{out} = \sum Q_{t,n} \quad \text{(Eq. A.1)}$$

Where: Q_{out} = outflow through the outlet structure [m hr^{-1}]
t = outlet type [m/d]; o = orifice, r = riser, s= spillway
n = number of each type of outlet

A.1.1 Orifice Outflow ($Q_{o,n}$)

Orifices are assumed to be circular, and are therefore parameterized with a diameter. If the pond level is below the bottom of the orifice, there is no discharge. Discharge from a partially submerged orifice is "proportional to the three halves power of depth, and fitting the expression to the office result at full depth" (Malcom, 1989). Discharge caused by a retained pool of water that submerges the orifice entire is modeled by the orifice equation.

$$if\ (H_{o,n} \geq H)$$
$$Q_{o,n} = 0 \quad \text{(Eq. A.2.1)}$$

$$if\ (H + D_{o,n} > H > H_{o,n})$$

$$Q_{o,n} = \left[0.633\ C_{o,n} * (\ H - H_{o,n})^{3/2}\right] * t_s \qquad \text{(Eq. A.2.2)}$$

$if\ (\ H >\ H + \ D_n\ )$

$$Q_{o,n} = \left[C_{o,n} * (4\pi D_o^2)\sqrt{2g\left(H - H_{o,n}\right)}\right] * t_s \qquad \text{(Eq. A.2.3)}$$

Where: H = height of water in SCM [m]
$H_{o,n}$ = height of orifice n [m]
$D_{o,n}$ = diameter of orifice n [m]
$C_{o,n}$ = coefficient of discharge for orifice n [unitless]
g = gravitational acceleration [$m^2\ s^{-1}$]
t_s = time step unit converter [converts $m^3\ s^{-1}$ to m min^{-1}]

A.1.2 Riser Outflow ($Q_{r,n}$)

Riser discharge is modeled as both sharp-crested weir and a submerged orifice, proportional to the depth to the three-halves and one-half power, respectively. The minimum discharge from these two hydraulic alternatives is chosen. The weir is assumed to have a length equal to the perimeter of the inlet structure, either the circumference of a circular weir or perimeter of a rectangle. In either case, the orifice discharge is assumed to be a rectangle.

$if\ (\ H_{r,n}\ \geq\ H\ )$

$$Q_{r,n} = 0 \qquad \text{(Eq. A.3.1)}$$

$if\ (\ H_{r,n} <\ H\ )$

$$Q_{r,n} = \min\left[\left(C_{r,n,w} * L_{r,n} * \left(H - H_{r,n}\right)^{3/2}\right),\left(C_{r,n,o} * (\tfrac{Lr}{4})^2\sqrt{2g\left(H - H_{r,n}\right)}\right)\right] * t_s \qquad \text{(Eq. A.3.2)}$$

Where: $C_{r,w}$ = coefficient of discharge for riser n as a weir [3.0 for sharp-crested, unitless]
$L_{r,n}$ = perimeter of riser n [m]
$H_{r,n}$ = height of riser n [m]
$C_{r,o}$ = coefficient of discharge for riser n as a orifice [unitless]

A.1.4 Spillway Outflow (Q_s)

Discharge over the spillway is modeled as a broad-crested weir. The equation has the same form of that a sharp crested, with a different coefficient of discharge.

$if\ (\ H_s\ \geq\ H\ )$

$$Q_s = 0 \qquad \text{(Eq. A.4.1)}$$

$if\ (\ \mathrm{s} <\ H\ )$

$$Q_r = \min\left[C_s * L_s * (H - H_s)^{3/2}\right] * t_s \qquad \text{(Eq. A.4.2)}$$

Where: C_s = coefficient of discharge spillway [3.33 for broad-crested, unitless]
L_s = length of spillway [m]
H_s = height of spillway [m]

Appendix B SCM water temperature model

To simulate SCM water temperature, we use the empirical model of Stefan and Preud'homme (1993) that relates stream temperature to air temperature.

$$T = \beta_{0,temp} + \beta_{1,temp} * \left(\frac{T_{max} - T_{min}}{2}\right) \quad \text{(Eq. B.1)}$$

Where: T = average daily water temperature [°C]
$\beta_{0,temp}$ = zero-order coefficient of linear model [5.08 °C of water]
$\beta_{1,temp}$ = first-order coefficient of linear model [0.752 °C of water / °C of air]
T_{max} = maximum daily air temperature [°C]
T_{min} = minimum daily air temperature [°C]

Appendix C Algae growth model

The governing mass balance of algal chlorophyll a is given above in Equation 4.2, and the primary fluxes are growth, death, respiration, settling and advection into the SCM, advection out of the SCM. Suggested parameter ranges for the algae growth model are either given in Table 4-3 or where the variable is defined in the test below.

C.1 Growth Rate:

$$k_g' = k_g * GROW_{temp} * GROW_{light} * GROW_{nut} \quad \text{(Eq. C.1)}$$

Where: k_g' = effective first order growth rate [d^{-1}]
k_g = base first order growth rate [d^{-1}]
$GROW_{temp}$ = scalar based on temperature [unitless]
$GROW_{light}$ = scalar based on light availability [unitless]
$GROW_{nut}$ = scalar based on nutrient [unitless]

C.1.1 $GROW_{TEMP}$: Arrhenius Equation

To simulate the dependence of growth rate on temperature, we use an Arrhenius "Theta" model. This is chosen because we are modeling all algae species as one unit, and we assume that the aggregate population will not be limited at high temperatures found in algae biomass harvesting facilities (Chapra, 2008).

$$GROW_{temp} = \theta_g^{\,T-baseT_g} \quad \text{(Eq. C.2)}$$

Where: $baseT_g$ = temperature used as base condition [20 °C]
Θ_g = Arrhenius constant at specified $baseT_g$
T = water temperature [°C]

C.1.2 $GROW_{light}$: Depth and Time integrated, optimum light condition

The form of the effect of light on growth at any given light intensity symbolized as F(I), is inhibited at light levels and symbolized as (Steele, 1962):

$$F(I) = \frac{I}{I_s} e^{-\frac{I}{I_s}+1} \quad \text{(Eq. C.3)}$$

Where: F(I) = fraction of base growth rate due to light effects [unitless]
I = instantaneous incoming radiation [kJ m^{-2} d^{-1}]
I_s = ecologically optimum radiation level [kJ m^{-2} d^{-1}]

Since the SCM biogeochemistry operators at a daily time step, the diurnal pattern of incoming radiation is modeled in RHESSys as just an average of a half-sinusoid, represented here as I_a. This incident light level (I_a) degrades with depth (z) through the pond's water column following the Beer-Lambert law:

$$I(z) = I_a e^{-k_e z} \quad \text{(Eq. C.4)}$$

Where: I_a = incoming average daily radiation at the surface of the pond [kJ m^{-2} d^{-1}]
k_e = decay rate of light in algae-free water column [m^{-1}]
z = depth from pond surface [m]

The decay rate represents an algae-free condition. However, as the concentration of a increases, so does the decay rate following the empirical equation of Riley (1956):

$$k_e = k'_e + \left(\beta_{0,light} * a\right) + \left(\beta_{1,light} * a^{2/3}\right) \quad \text{(Eq. C.5)}$$

Where: k'_e = decay rate of light in algae-free water column [0.2 m^{-1}]
$\beta_{0,light}$ = first-order coefficient of linear model [0.0088 m mg-chlA^{-1} m^{-3}]
$\beta_{1,light}$= two-thrids-order coefficient of linear model [0.054 m (mg-chlA/m^3)$^{-2/3}$]

Applying this decay (Eq. C.4) to the Steele model (Eq. C.5) and integrating over the pond's depth, from depth 0 to depth H, and the course of a day produces the $GROW_{light}$ scalar. This equation looks like:

$$GROW_{light} = \frac{2.718f}{k_e H}\left(e^{-\frac{I_a}{I_S}e^{-k_e * H}} - e^{-\frac{I_a}{I_S}e^{-k_e * H_0}}\right) \quad \text{(Eq. C.6)}$$

Where: f = photo period, or fraction of the day where the pond is sun-lit [hr/hr]
H_0 = depth of incident radiation [m]
1.718 = numeric value of e

C.1.3 $GROW_{nut}$: Michaeles-Menten saturation of both nitrogen and phosphorous

Growth rate inhibition due to nutrient limitation is governed by both the concentration of total inorganic P and inorganic N (NO_3 + NH_4). Both nutrients are governed by a Michaeles-Menten saturation function, and whichever nutrient exercises a stronger growth rate limitation will be used to retard growth rate. Since RHESSys does not simulate P dynamics, the concentration of inorganic P in the pond is fed into the model either as a single parameter value or as a time series input.

$$\text{GROW}_{nut} = \min\left(\frac{n}{k_{sn}+n}, \frac{p}{k_{sp}+p}\right) \quad \text{(Eq. C.7)}$$

Where: n = total inorganic N concentration (NO_3 + NH_4) [k m^{-3}]
p = total inorganic P concentration [kg m^{-3}]
k_{sn} = half-saturation constant for nitrogen [kg m^{-3}]
k_{sp} = half-saturation constant for nitrogen [kg m^{-3}]

C.2 Respiration and Death

Algal respiration and depth is model as a simple function of temperature, following the same model form at the Arrhenius growth model in for $GROW_{temp}$ (Eq. C.2). Algal

respiration releases inorganic carbon to the atmosphere and NH_4 to the water column, and death release DOC and DON to the water column,

$$k_r' = k_r \theta_r^{T-baseT_r} \quad \text{(Eq. C.8)}$$

Where: k_r' = effective first order respiration rate [d^{-1}]
k_r = first order respiration rate at base temperature [d^{-1}]
$baseT_r$ = temperature used as base condition [20 °C]
Θ_r = Arrhenius constant at specified $baseT_r$
T = water temperature [°C]

$$k_d' = k_d \theta_d^{T-baseT_d} \quad \text{(Eq. C.9)}$$

Where: k_d' = effective first order death rate [d^{-1}]
k_d = first order death rate at base temperature [d^{-1}]
$baseT_d$ = temperature used as base condition [20 °C]
Θ_d = Arrhenius constant at specified $baseT_d$
T = water temperature [°C]

Appendix D Elemental mass balances in water column

The growth, death, and respiration of algae effect the mass of balance of DOC, DON, NO_3 and NH_4 in the pond.

D.1 NH_4:

Ammonium is lost from the water column through algal uptake. Respiration releases ammonium from organic nitrogen N stores in proportion to the chl-a lost to respiration. Advection into the and out of the pond also affects the mass balance.

$$\frac{dNH4}{dt} = (-k'_g a * r_{an} * P_{ap}) + (k'_r a * r_{an}) - \left(\frac{Q_{out}}{V} * NH4\right) + (NH4_{in}) \qquad \text{(Eq. D.1)}$$

Where: NH4 = pond mass of ammonium [kg]
P_{ap} = fractional preference of NH4 uptake from total inorganic N [%]
$NH4_{in}$= inflow of NH_4 into the pond [kg hr^{-1}]

The preferential uptake of ammonium vs. nitrate is governed by the equation:

$$P_{ap} = \frac{NH4*NO3}{(k_{pn}+NH4)(k_{pn}+NO3)} + \frac{NH4*k_{pn}}{(NH4+NO3)(k_{pn}+NO3)} \qquad \text{(Eq. D.2)}$$

Where: k_{pn} = half-saturation preference concentration for ammonium [kg-N m^{-3}]

D.2 NO_3:

Nitrate is taken up by algae during growth and is advected into and out of the SCM with water.

$$\frac{dNO3}{dt} = -k'_g a * r_{an} * (1 - P_{ap}) - \left(\frac{Q_{out}}{V} * NO3\right) + (NO3_{in}) \qquad \text{(Eq. D.3)}$$

Where: NO3 = pond mass of nitrate [kg]
$NO3_{in}$ = inflow of nitrate into the pond [kg hr^{-1}]

D.3 DOC:

DOC is released to the pond upon algae death, parameterized by a fixed ratio. DOC is also be advected into and out of the pond.

$$\frac{dDOC}{dt} = r_{ac} * k'_d * a - \left(\frac{Q_{out}}{V} * DOC\right) + (DOC_{in}) \quad \text{(Eq. D.4)}$$

Where: DOC = mass of DOC in pond [kg-N]
r_{ac} = algal ratio of chl-a to carbon [0.01 kg chl-A kg-C^{-1}]
DON_{in} = inflow of DON from the watershed model into the SCM [kg-C hr^{-1}]

D.2 DON:

As with DOC, DON is released to the SCM upon algae death, and can enter and exit with water advection.

$$\frac{dDON}{dt} = r_{an} * k'_d * a - \left(\frac{Q_{out}}{V} * DON\right) + (DON_{in}) \quad \text{(Eq. D.5)}$$

Where: DON = mass of DON in pond [kg-N]
r_{an} = algal ratio of chl-a to nitrogen [0.2 kg-chl-A kg-N^{-1}]
DOC_{in} = inflow of DOC from the watershed model into the SCM [kg-N hr^{-1}]

VITA

VITA

Colin Bell was born in Rochester, NY. He earned a B.S. in Forest Engineering at the State University of New York College of Environmental Science and Forestry in Syracuse, NY. His undergraduate advisor connected him with Dr. Sara McMillan, then at the University of North Carolina at Charlotte, with whom he earned a M.S.E in Civil and Environmental Engineering. This document partially completes Colin's PhD in the Department of Agricultural and Biological Engineering at Purdue University.